E.O. Paton Electric Welding Institute of the National Academy of Sciences of Ukraine

International Scientific-Technical and Production Journal

The Paton WELDING JOURNAL

Issue 08 2019

Published Monthly Since 2000

English translation of the monthly «Avtomaticheskaya Svarka» (Automatic Welding) journal published in Russian since 1948

Founders
E.O. Paton Electric Welding Institute, NASU
International Association «Welding»

Publisher
International Association «Welding»

Translators
A.A. Fomin, O.S. Kurochko, I.N. Kutianova
Editor
N.G. Khomenko
Electron galley
D.I. Sereda, T.Yu. Snegiryova

Address
E.O. Paton Electric Welding Institute,
International Association «Welding»
11 Kazimir Malevich Str. (former Bozhenko Str.),
03150, Kyiv, Ukraine
Tel.: (38044) 200 60 16, 200 82 77
Fax: (38044) 200 82 77, 200 81 45
E-mail: journal@paton.kiev.ua
www.patonpublishinghouse.com

State Registration Certificate
KV 4790 of 09.01.2001
ISSN 0957-798X
DOI: http://dx.doi.org/10.15407/tpwj

Subscriptions
$384, 12 issues per year,
air postage and packaging included.
Back issues available.

CONTENTS

https://doi.org/10.15407/tpwj2019.08.01

STRESS-STRAIN STATE OF WELDED AND BRAZED ASSEMBLIES OF DISSIMILAR MATERIALS WITH SOFT INTERLAYER AT TEMPERATURE-FORCE LOADING

V.V. KVASNYTSKYI[1], **M.V. MATVIIENKO**[2], **E.A. BUTURLYA**[2], **V.F. KVASNYTSKYI**[2] and **G.V. YERMOLAYEV**[2]
[1]National Technical University of Ukraine «Igor Sikorsky Kyiv Polytechnic Institute»
37 Peremohy Prosp., 03056, Kyiv, Ukraine. E-mail: kvas69@ukr.net
[2]Admiral Makarov National University of Shipbuilding
9 Geroiv Ukrainy Prosp., 54025, Mykolaiv, Ukraine

There was researched a stress-strain state (SSS) at temperature-force loading of cylinder assemblies of materials of similar strength, but different by temperature coefficients of linear expansion (TCLE), with soft (lower yield limit than in base metal) interlayer and average temperature coefficient of linear expansion. Fields and distribution diagrams of stresses and plastic deformations of assemblies were analyzed. Investigation of SSS showed that effect of mutual temperature (cooling) and force (compression) loading of assemblies with soft interlayers appears in increase of radial and circumferential stresses in both materials, increase of equivalent ones in the material with high TCLE and the interlayer and axial ones in the joined materials, and, respectively, decrease of equivalent in the material with lower TCLE. Tangential stresses at that remain virtually the same as at purely temperature loading. In change of cooling by heating the materials change their places. The value of maximum plastic deformations in the interlayer material at interface with base material close to external surface at mutual temperature-force loading reaches 2.3 %. At that, axial tension stresses in brittle materials with low TCLE (ceramics, graphite, etc.) during cooling in the assemblies with soft interlayer reduce by value of compression external stresses, i.e. risk of brittle fracture reduces. 7 Ref., 8 Figures.

Keywords: *diffusion welding, brazing, dissimilar materials, soft interlayer, stresses, deformation, computer modelling, mutual temperature and force loading*

The main problems of joining of dissimilar materials are the processes of activation of surfaces being joined and formation of residual stresses [1, 2]. Intermediate interlayers are used to solve these problems. In brazing such an interlayer is a brazed weld. Residual stresses also play important role in working capacity of fabricated assemblies after cooling [3, 4]. Therefore, investigation of such layers is relevant.

The simplest methods of evaluation of stress-strain state (SSS) are the engineering methods of calculation in limits of elasticity, based on hypothesis of flat sections, however, they do not allow considering effect of many factors even for simple assemblies. Methods of mathematical modeling are the most versatile and perspective at current stage of development of computer engineering and programming. Works [5–7] by finite element method using ANSYS computer complex have investigated the processes of SSS formation in dissimilar materials joining including metals with nonmetals. Works [6–7] studied SSS with interlayers at axial and temperature loading, respectively. Since many assemblies are subjected to axial as well as thermal loading, therefore this work investigates SSS at mutual loading taking into account plastic deformations.

Aim of the present paper is to determine effect of soft intermediate interlayers having lower yield limit in comparison with materials being joined on SSS formation in arc diffusion welding and brazing.

Main material of investigations. The investigations were carried out by the computer modeling method using ANSYS software complex. Axial symmetric problems were solved for assemblies of cylinder-cylinder type of 20 mm diameter, total height h = = 21 mm and interlayer thickness s = 1 mm (Figure 1). Considering specifics of assemblies, presence of large gradients of stresses in a narrow zone close to interlayer there was used a gradient division with variable dimensions of finite elements, sizes of which in a joint zone were selected in such a way as they make not less than 10 over interlayer thickness. PLANE 183 type finite elements were used. Joined materials 1 and 2 had similar yield limits, but different temperature coefficients of linear expansion (TCLE = $20\cdot10^{-6}$ and $10\cdot10^{-6}$ 1/deg). The soft interlayer had considerably lower yield limit (σ_y = 38 MPa), than in base metal (σ_y = 250 MPa) and average TCLE ($15\cdot10^{-6}$ 1/deg). Elasticity modulus and Poisson's coefficients of all materials were taken similar and equal to $2\cdot10^5$ MPa and 0.3, respectively. This allows outlining the effect of particularly plastic constituent of deformation on assembly SSS. Taken properties of materials at given loading provided plastic deformation of the interlayer only. Joined materials at that were elastically deformed over the whole volume that allows using obtained results to joints of brittle materials.

Loading was performed using mutual compression by 40 MPa force and decrease of assembly temperature (after joint formation) per 100°. Obtained at such loading results are true at change of cooling by heating (in welding with thermal cycling), but materials 1 and 2, having different TCLE, change their places at that. Modeling results were compared with similar assemblies at various types of loading (only force and only temperature). Fields and distribution diagrams of all constituents of stresses and plastic deformations of assemblies were analyzed.

Analysis of modeling results showed that SSS nature in whole corresponds to general principles of mechanics and regularities set earlier in [5–7]. Effects of temperature and force loading are algebraically summed, as a result of what the fields of radial and circumferential stresses remain virtually the same as at purely temperature loading. Axial compression stresses in material 1 rise and tensile ones in material 2 reduce by value of compression load. Tangential stresses noticeably rise at the interface of «soft» interlayer with material 1 and decrease at interface with material 2 in comparison with purely temperature loading. In this case it is obviously demonstrated the algebraic summing of the effects from the difference of TCLE and plastic deformation of interlayer and significantly higher level of stresses at temperature loading in comparison with force one.

The field of equivalent stresses changes equivalently. The latter at mutual loading noticeably rises in material 1 and reduces in material 2 in comparison with purely temperature loading.

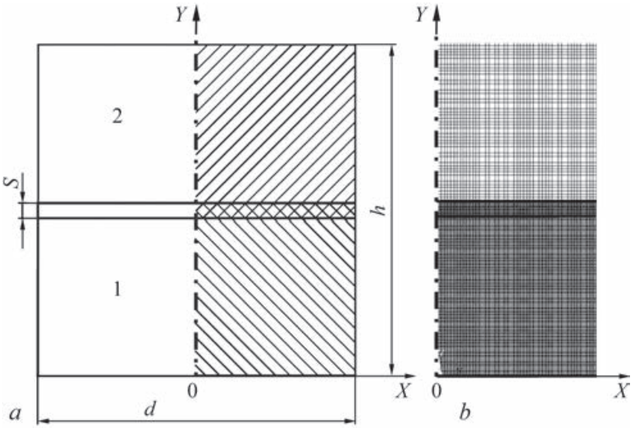

Figure 1. Physical (*a*) and FE (*b*) models of assemblies with interlayer (1, 2 — materials being joined)

In accordance with equivalent stresses there is a change of the field of plastic deformations. As in the case of purely temperature loading the maximum of the latter is accumulated close to external surface of assembly, but their distribution over interlayer thickness distinctly change. They are maximum at the interface with material 1 and reduce with distance from it.

Nature and level of distribution diagrams of radial stresses along the butt in the materials being joined at mutual temperature and force loading match with nature of corresponding distribution diagrams at purely temperature loading (Figure 2). At that the maximum radial stresses in the materials being joined reduce by 15–20 MPa. Circumferential stresses have similar to radial distribution in the materials being joined.

The pattern is completely different in the soft interlayer material. Application of pressure at temperature decrease considerably (in several times) rises plastic deformations from side of material 1 (with higher TCLE) and to lower degree from side of material 2 (with smaller TCLE) at that changing their sign (Figure 3).

The distribution diagrams of axial stresses along assembly generatrix displace to the side of compression by value of axial load of 40 MPa (Figure 4). As a

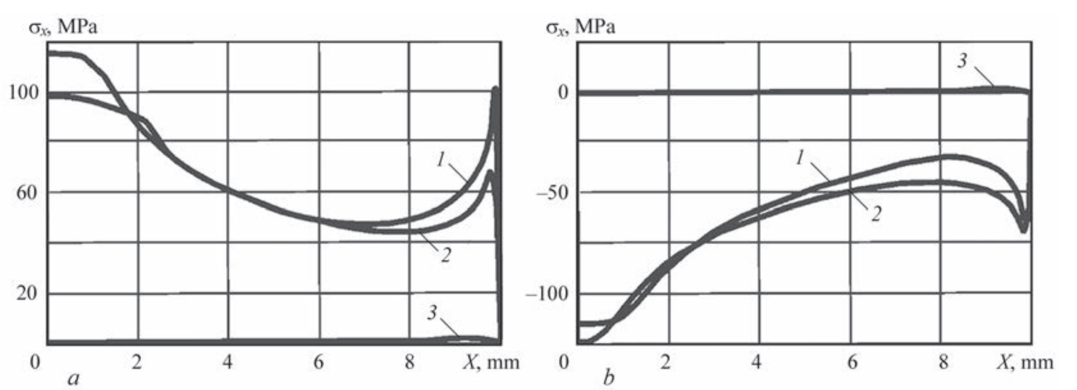

Figure 2. Distribution diagrams of radial stresses in materials 1 (*a*) and 2 (*b*) along butt with «soft» interlayer at temperature-force (*1*), temperature (*2*) and force (*3*) loading

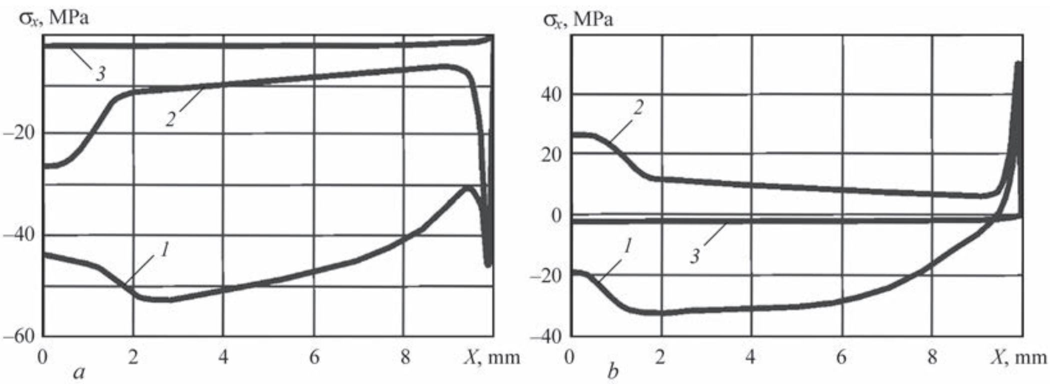

Figure 3. Distribution diagrams of radial stresses in material of «soft» interlayer on butts with material 1 (*a*) and 2 (*b*) at temperature-force (*1*), temperature (*2*) and force (*3*) loading

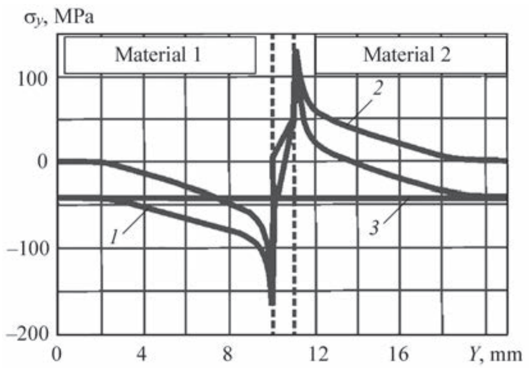

Figure 4. Distribution diagrams of axial stresses on generatrix of assembly with «soft» interlayer at temperature-force (*1*), temperature (*2*) and force (*3*) loading

result tensile stresses in material 2 (with small TCLE) decrease reducing the risk of its brittle fracture.

Tangential stresses being unchangeable on the largest part of the butt increase in the vicinity of external cylinder surface rising from side of material 1 by 10 MPa (Figure 5, *a*) and decreasing by 10 MPa from material 2 side (Figure 5, *b*).

There is a respective change of the distribution diagrams of equivalent stresses. Level of these stresses rises by value of applied pressure 40 MPa in material 1 (Figure 6, *a*) and decreases by 40 MPa in material 2 (Figure 6, *b*). Their distribution in both materials being joined remains close to uniform.

In the material of «soft» interlayer being plastically deformed the value of equivalent stresses in the bigger part of the butt keeps the level of around 40 MPa from material 2 side with smaller TCLE (Figure 7, *b*). From the side of material 1 with larger TCLE the distribution is nonuniform, there is a clearly expressed stagnation zone close to assembly axis, in which equivalent stresses reduce to 10 MPa. In the vicinity of external surface of assemblies they vice-versa rise up to 80 MPa (Figure 7, *a*).

Plastic deformations in the «soft» interlayer material have nonuniform distribution, gradually rising from ones close to 0, in the stagnation zone, up to 1 % and more in the vicinity to the external surface. At that on the interface with material 1 in this zone at mutual loading they are several times higher than at purely temperature loading (Figure 8, *a*). On the interface with material 2, vice versa, distribution is more uniform than at purely temperature loading (Figure 8, *b*), but their level is lower.

Mutual force (compression) and temperature (cooling) loading create more favorable conditions for development of plastic deformations in the «soft» interlayer than purely temperature. Their value and nonuniformity of distribution rise from the side of material 1(with higher TCLE) and they reduce, but distribution becomes more uniform from the side of

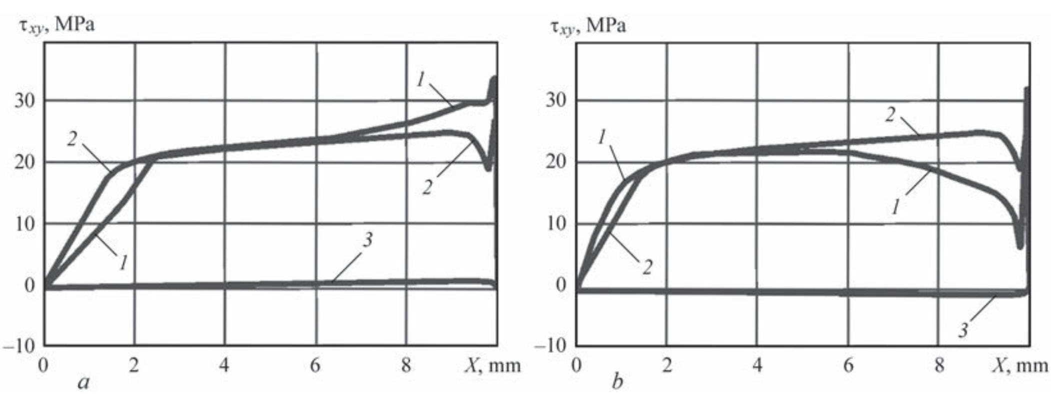

Figure 5. Distribution diagrams of tangential stresses on butts of materials 1 (*a*) and 2 (*b*) with «soft» interlayer at temperature-force (*1*), temperature (*2*) and force *(3*) loading

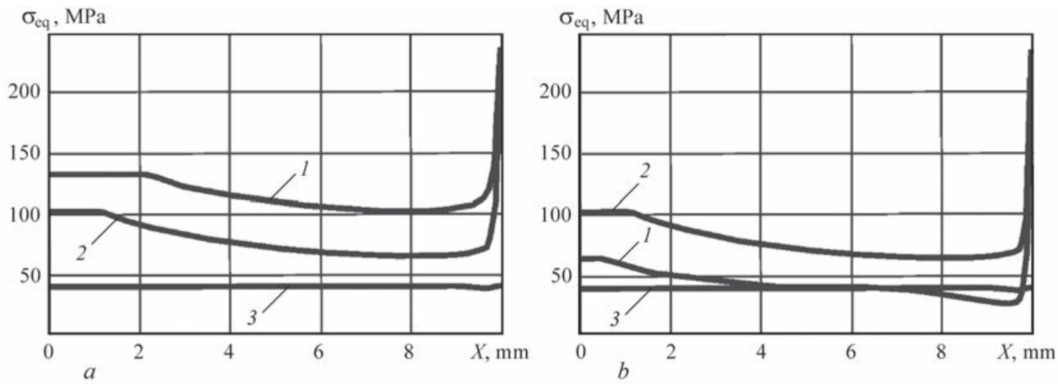

Figure 6. Distribution diagrams of equivalent stresses in joined materials 1 (*a*) and 2 (*b*) on butt with «soft» interlayer at temperature-force (*1*), temperature (*2*) and force (*3*) loading

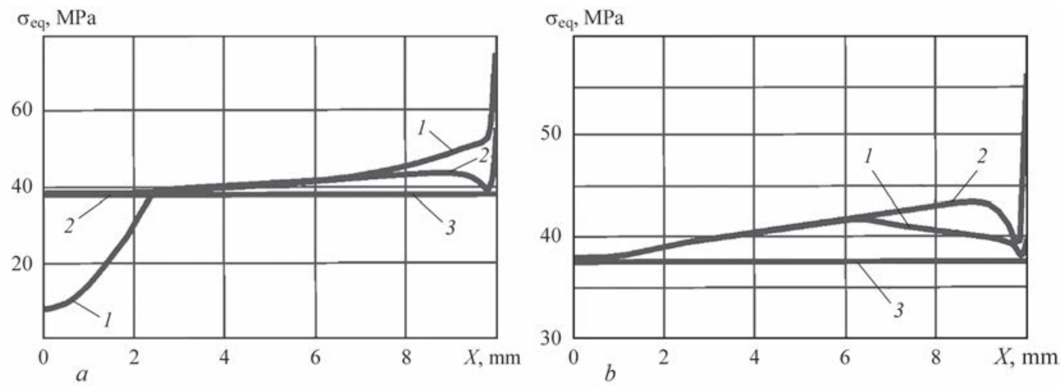

Figure 7. Distribution diagrams of equivalent stresses in material of interlayer on butt with materials 1 (*a*) and 2 (*b*) at temperature-force (*1*), temperature (*2*) and force (*3*) loading

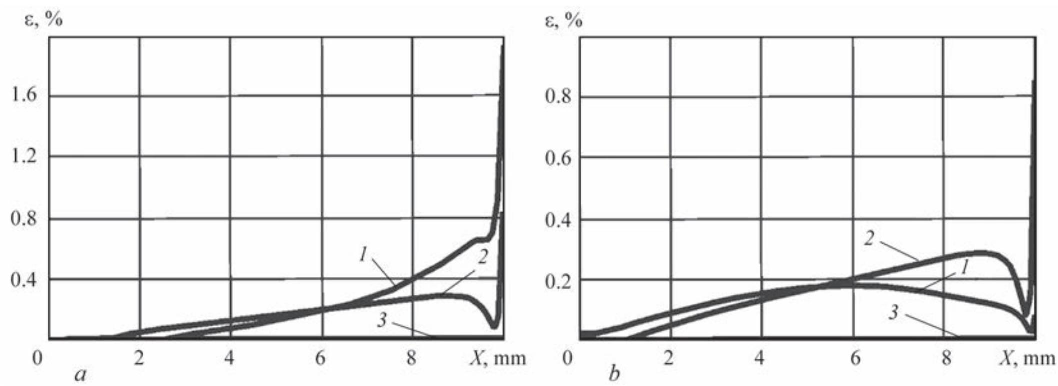

Figure 8. Distribution diagrams of plastic deformations in material of interlayer on butt with materials 1 (*a*) and 2 (*b*) at temperature-force (1), temperature (2) and force (3) loading

material 2 (with lower TCLE). Obviously that the materials change places in alteration of cooling by heating, i.e. thermal cycling under pressure shall promote formation of physical contact and activation of processes of joint formation.

Analysis of the results of SSS investigation showed that effect of mutual temperature and force loading of assemblies with soft interlayers appears at some increase of radial and circumferential stresses in both materials, rise of equivalent ones in material 1 and interlayer and axial in materials being joined and, respectively, decrease of equivalent ones in material 2, tangential stresses at that remain virtually the same as in purely temperature loading.

The value of maximum plastic deformations in the interlayer material on the interface with base materials in the vicinity of external surface at temperature-force loading significantly rises and makes around 2.3 %.

Conclusions

1. At mutual loading by compression and cooling (cooling under pressure) the axial tensile stresses in the brittle materials with low TCLE (ceramics, graphite, etc.), responsible for their fracture in cooling after welding

(brazing) in the assemblies with «soft» interlayer, reduce by the value of compression load. It means that risk of brittle fracture in the assemblies with «soft» interlayer reduces in cooling under pressure.

2. Tangential and equivalent stresses in the butt zone (on interface), determining formation of metallic (physical) contact and activation of process of joint formation in diffusion welding, at mutual loading by compression and cooling of assemblies with soft interlayer noticeably rise in material with higher TCLE in cooling and material with lower TCLE in heating. At that, distribution of equivalent stresses is close to uniform. Thus, thermal cycling under pressure shall promote formation of physical contact and activation of processes of formation of joint in assemblies with «soft» interlayer.

3. Plastic deformations in the material of «soft» interlayer on the interface with material having lower TCLE at mutual loading on cooling stage are more uniformly distributed, but their level is lower than in purely temperature loading. At mutual compression and heating the same takes place on the interface with material having higher TCLE. It can be assumed that welding with thermal cycling under pressure provides in the assemblies with «soft» interlayer more uniform distribution of plastic deformations in the interlayer.

1. Lobanov, L.M., Kvasnytskyi, V.V. et al. (2016) *Stresses and strains in welding and brazing: Manual*. Ed. by L.M. Lobanov. Mukolaiv, NUK [in Ukrainian].
2. Kvasnytskyi, V.V., Yermolayev, H.V., Matviienko, M.V. (2017) *Mechanics of joints in diffusion welding, brazing and spraying of dissimilar materials under elasticity conditions*. Ed. by H.V.Yermolayev. Nikolaev, NUK [in Russian].
3. Makhnenko, V.I. (2006) *Service life of welded joints and assemblies of modern structures*. Kiev, Naukova Dumka [in Russian].
4. Makhnenko, V.I., Kvasnitsky, V.F. (2006) Stress-strain state of assemblies of cylindrical shape in diffusion bonding. *The Paton Welding J*., **2**, 2–7.
5. Ermolaev, G.V., Martynenko, V.A., Olekseenko, S.V. et al. (2017) Effect of the rigid interlayer thickness on the stress-strain state of metal-graphite assemblies under thermal loading. *Strength of Materials*, **49**, 422–428.
6. Kvasnytskyi, V.V., Kvasnytskyi, V.F., Dong Chunlin et al. (2018) Stressed state of welded and brazed assemblies from similar materials with a soft interlayer under axial loading. *The Paton Welding J*., **4**, 6–10.
7. Kvasnytskyi, V.V., Kvasnytskyi, V.F., Matviienko, M.V. et al. (2019) Stress-strain state of welded and brazed assemblies from dissimilar materials with soft interlayer at thermal loading. *Ibid*., **5**, 13–17.

Received 08.05.2019

https://doi.org/10.15407/tpwj2019.08.02

STRUCTURE AND PROPERTIES OF WEAR-RESISTANT MATERIALS BASED ON Co–Mo–Cr–Si–B ALLOYING SYSTEM

A.M. KOSTIN and **V.A. MARTYNENKO**
Admiral Makarov National University of Shipbuilding
9 Heroiv Ukrainy Prosp., 54000, Mykolaiv, Ukraine. E-mail: volodymyr.martynenko@nuos.edu.ua

The aim of the work was to study the structure and properties of Co–Mo–Cr–Si–B alloying system for the case of its application as a wear-resistant material for hardening the contact surfaces of blades of ship gas turbine engines. The studies were performed with application of the methods of high-temperature differential thermal analysis, electron microscopy, X-Ray micro and X-Ray structural analyses. Hardness and microhardness of phase components were measured, adhesion activity of experimental alloys was investigated using the sessile drop method. It is shown that experimental compositions have a balanced structure based on solid solution of cobalt alloyed with molybdenum and chromium, with hardening by complex silicides, borides and carbides, have acceptable mechanical properties and melting temperature below the temperature of irreversible softening of high-temperature nickel alloys, and are characterized by high adhesive activity, which creates favourable prerequisites for their use in ship gas turbine construction. 10 Ref., 1 Table, 4 Figures.

Keywords: *high-temperature nickel alloys, wear-resistant materials, structure phase composition, hardness, melting temperature, adhesive activity*

An important problem in marine engineering is the need to increase the effectiveness, reliability and service life of gas turbine engines. These parameters are primarily determined by the intensity of wearing of contact surfaces of blades, which are in the most severe operating conditions. In this connection, the materials and technologies of hardening the contact surfaces require development of new advanced solutions.

At present, there exists a rather wide selection of wear-resistant materials, which can be deposited on the contact surfaces with melting or without melting of the base material [1]. In this case, the decisive criteria of adaptability-to-fabrication of wear-resistant materials are their melting temperature and possible methods of deposition. Under the conditions of specific production, the above criteria can have mutually exclusive action that essentially complicates selection of optimum compositions and technologies [2].

In ship gas turbine construction high-temperature nickel alloys of ChS88U-VI, ChS70U-VI and other types are used for manufacturing the turbine blades. These alloys are hardened by disperse precipitates of γ'-phase $Ni_3(Al, Ti)$ which is prone to coagulation during contact interaction at high temperatures that creates favourable conditions for increase of wearing intensity, also due to intensification of the processes of oxidation of the surface layer, which is depleted in alloying elements.

These alloys are practically unweldable by the traditional methods of fusion welding, so that their heating temperature should not exceed 1210–1220 °C at deposition of wear-resistant material. Otherwise, an irreversible lowering of base metal strength is observed, caused by degradation of γ'-phase and cracking in the deposition area [1]. In this connection, the alloy which hardens the contact surface, at deposition in the liquid state should have the melting temperature not higher than 1210–1220 °C. At higher intrinsic melting temperature it can be joined to the base, for instance, by brazing. However, the turbine blade design does not always allow application of this effective method.

Thus, it is convenient to classify wear-resistant materials for ship gas turbines into two groups by their melting temperature: below and above 1210–1220 °C.

An extremely complicated problem is development of alloys, which belong to the first group, have the required level of wear resistance at working temperatures (up to 900 °C) and can stand short-term thermal loads at up to 1150 °C temperature «pulses» that is close to the conditions of γ'-phase dissolution in the base metal.

The known alloys of the first group include, for instance, KBNKhL-2 composition, which has the melting temperature at the level of 1070–1090 °C that does not allow the alloy to stand short-term heating up to temperatures of 1150 °C [3].

All the other known nickel- and cobalt-based alloys can be included into the second group, for instance VZhL-2, VKNA-2M [4], V3K-r [5], Stellite 12

[6], Kh30N50Yu5T2 [7], Kh25N10V8 [4], KhTN-61 [8], KhTN-62 [9], Tribaloy T-800, T 400, T 401 alloys [10], etc. The above-listed alloys have melting temperature above 1220 °C which makes their application extremely difficult at deposition on contact surfaces of blades of ship gas turbine engines by surfacing.

The main technological process, which is used for deposition of wear-resistant materials in enterprises of SC GTRPC «Zorya»–«Mashproekt», is the method of oxy-acetylene flame spraying without base metal melting. Additional fluxing of the surface by PV-200 flux is used, in order to increase the adhesive activity of the process. The surfacing process is accompanied by an insignificant dissolution of base metal to the depth of up to 0.1 mm that guarantees formation of a common transition zone, which is responsible for the bond strength. Thus, physicochemical and metallurgical processes, which run during the surfacing process, have a lot of common features with that of brazing. In this case, adhesion activity of surfacing materials is extremely important.

In this connection, the objective of our work was development of a high-temperature material with the required level of wear resistance at working temperatures (up to 900 °C), with melting temperature below 1210–1220 °C, which would have satisfactory adhesion activity for ship high-temperature nickel alloys and could stand the temperature and dynamic conditions of their operation, that is an urgent problem.

The National University of Shipbuilding together with SC GTRPC «Zorya»–«Mashproekt» developed promising wear-resistant high-temperature materials KMKh and KMKhS which satisfy the above requirements [2].

KMKh and KMKhS alloys were developed on the base of Co–Mo–Cr–Si classical system with additional alloying by boron and chromium carbide [2]. Alloy matrix is a solid solution of cobalt (β-modification) alloyed by molybdenum and chromium, which readily withstands contact and thermal loads up to temperatures of 1000 °C, inclusive. Simultaneous addition of silicon and boron allows at the melting stage lowering the alloy temperature to the required level and at the same time significantly increasing their adhesion activity. After melt solidification, boron and silicon actively form a uniformly distributed, thermodynamically stable highly-dispersed hardening phase, which consists of complex silicides and borides (CoB, Mo_2B, MoSi, CoSi) that imparts the required wear resistance level to the alloys. X-Ray structural analysis was performed in DRON-3 diffractometer. Additional presence of chromium carbide (Cr_2C_6) in KMKhS alloy somewhat lowers its melting temperature compared to KMKh alloy and stabilizes its structure and properties.

Test alloys were produced by induction melting in vacuum of the order of 10^{-2} Pa with subsequent annealing at the temperature of 1100 °C for 1 h. The characteristic electronic structure of the alloys is shown in Figure 1. Both the alloys demonstrate the regular two-phase structure, the density and uniformity of which increases at transition from KMKh alloy to KMKhS alloy. The hardness of KMKh alloy is equal to approximately *HV*10 – 710–715, that of alloy KMKhS is *HV*10 – 735–740. Average microhardness $H\mu_{50}$ of phase components of alloy KMKh is equal to 4771 MPa (Figure 1, region 1) and 2365 MPa (region 2), and for alloy KMKhS it is 661 MPa (region 3) and 3213 MPa (region 4), respectively.

Distribution of concentrations of alloying elements in phase components of test alloys was determined using scanning electron microscope-microanalyzer REMMA 102-02. The results are given in the Table. Analysis of obtained results of distribution of alloying elements in phase compositions showed that the base of cobalt-based alloys, up to 67 wt.% for KMKh alloy and 59 wt.% for KMKhS alloy, additionally contains from 4 up to 11 % molybdenum and from 25 up to 26 % chromium, with slight alloying with silicon of up to 2.5 wt.%. The hardening phase, contrarily, simultaneously with lowering of base level of cobalt alloying to 50 wt.% and of chromium, to 16 wt.%, also contains an increased concentration of molybdenum, up to 33 wt.% and of silicon, up to 9 wt.%, that pro-

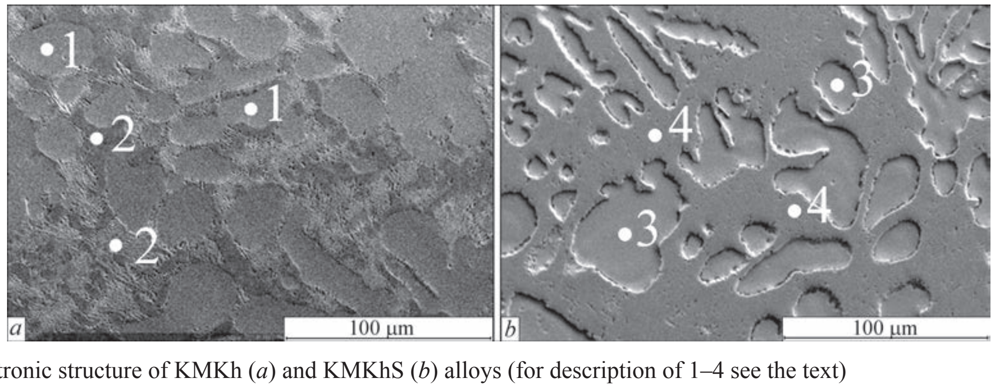

Figure 1. Electronic structure of KMKh (*a*) and KMKhS (*b*) alloys (for description of 1–4 see the text)

Alloying element concentration in phase components of test alloys in keeping with Figure 1

Region number	Alloying element				
	Co	Mo	Cr	Si	Ni
1	50.78–46.03 47.62 (48.41)	33.60–26.37 31.3 (29.99)	16.60–12.25 13.83 (14.43)	7.75–6.25 7.24 (7.0)	–
2	68.25–63.73 67.01 (65.99)	8.37–4.55 5.49 (6.46)	26.11–24.98 25.69 (25.55)	2.11–1.52 1.81 (1.82)	–
3	46.06–45.33 45.78 (45.70)	32.23–29.79 30.70 (31.01)	14.01–12.22 13.24 (13.12)	8.78–8.55 8.70 (8.67)	1.81–1.45 1.58 (1.63)
4	59.06–56.41 57.7 (57.74)	9.15–11.96 10.61 (10.56)	26.38–25.67 26.18 (26.03)	2.98–2.64 2.81 (2.81)	3.06–2.35 2.71 (2.71)

Note. Numerator — max and min value, wt.%, denominator mean value, wt.% (at.%).

motes formation of complex-alloyed hardening phase (CoB, Mo_2B, MoSi, CoSi). The base of the alloys and hardening phases contain the same chemical elements as those in the alloy composition, in different proportions, that ensures their good structural compatibility and smooth change of physical properties at transition through the interphase. Boron and carbon concentration was not determined in the work, in connection with limited capabilities of the used equipment.

Alloy melting temperature was determined by the method of high-temperature differential thermal analysis. Characteristic thermograms of melting and crystallization of alloys KMKh and KMKhS are given in Figure 2. Data of thermal analysis (DSC) are indicative of the fact that at preservation of an optimum ratio of silicon and boron in the alloys, KMKh and KMKhS alloys have only one thermal effect in the heating and cooling curves. The above effect determines the solidus temperature for KMKh alloy on the level of 1185–1190 and 1165–1170 °C for KMKhS alloy. At deviation from the recommended ratio, the stability of phase composition is disturbed, and there is the possibility of phase reaction running with formation of nonequilibrium phases. It results in appearance of additional effects on the thermal curves that leads to increase or lowering of the alloy melting temperature and formation of a wider interval of crystallization that is undesirable.

Adhesion activity of KMKh and KMKhS alloys was studied by the sessile drop method at melting in

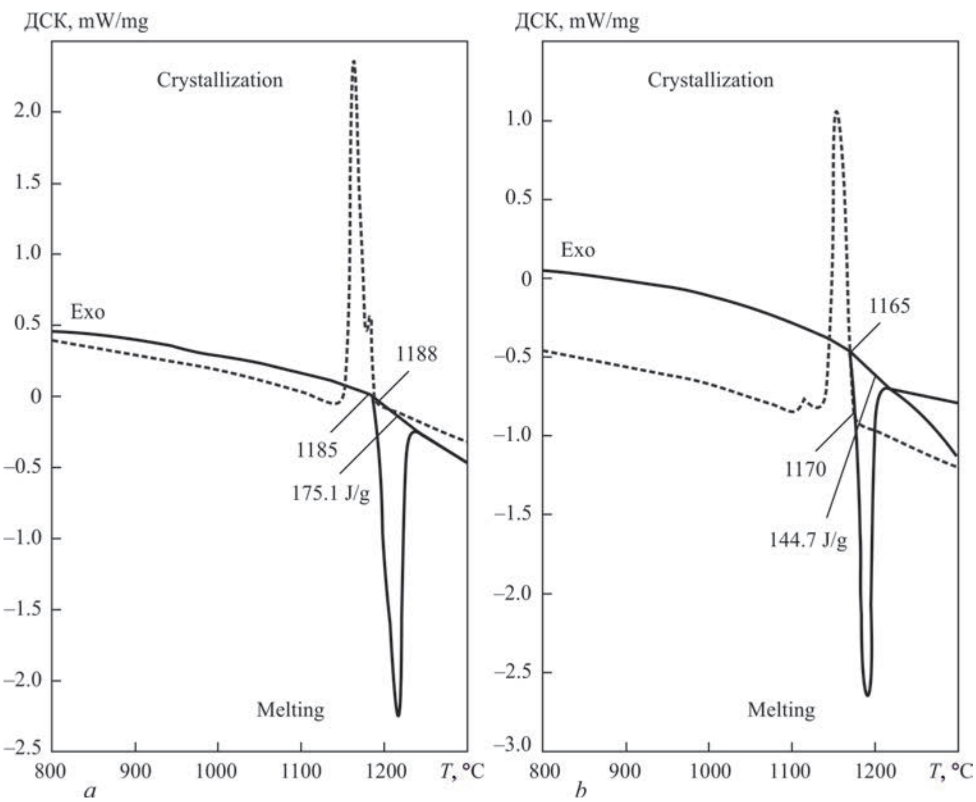

Figure 2. Differential scanning calorimetry of samples of KMKh (*a*) and KMKhS (*b*) alloys

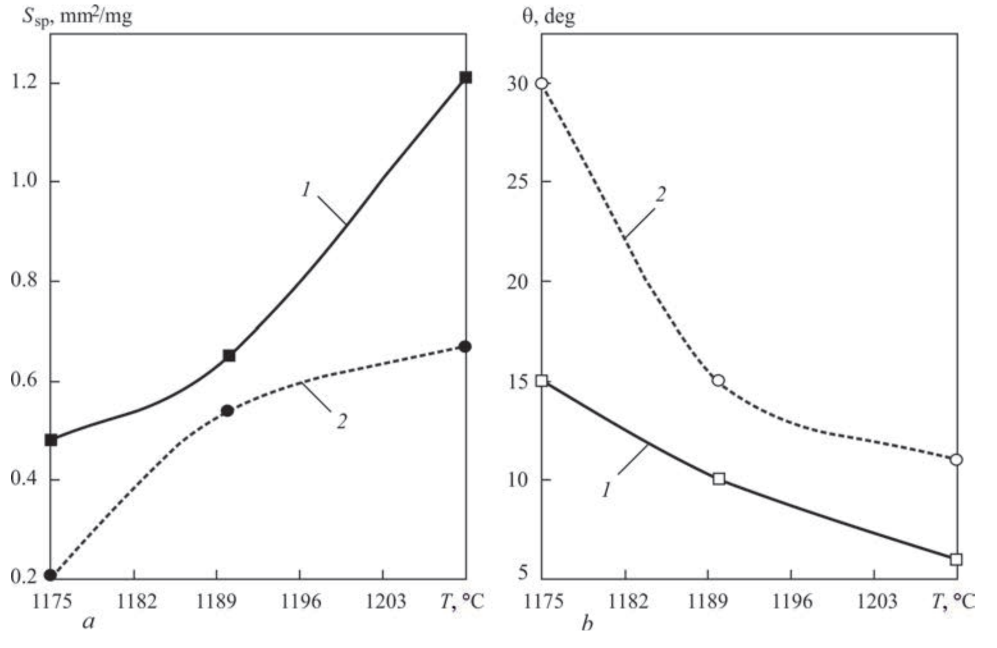

Figure 3. Dependence of specific spreading area S_{sp} (*a*) and wetting angles θ (*b*) of KMKhS (*1*) and KMKh (*2*) alloys on temperature

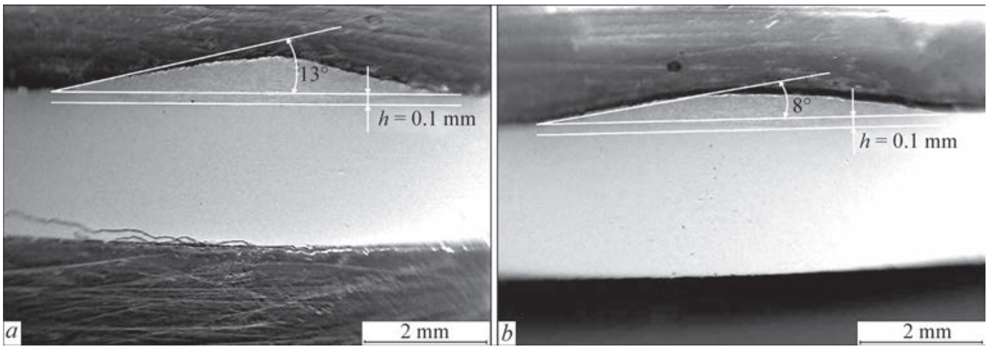

Figure 4. Characteristic macrostructure of the zone of interaction of KMKh (*a*) and KMKhS (*b*) alloys with VZh 98 alloy (T = 1210 °C)

the vacuum of the order of 10^{-2} Pa on the substrate of standard high-temperature nickel alloy VZh 98. The time of soaking at temperatures from 1175 to 1210 °C was 3 min. Measurements of specific area of spreading and angles of wetting for the above experimental conditions are shown in Figure 3. Characteristic macrostructure of the zone of interaction of KMKh and KMKhS alloys with high-temperature alloy VZh-98 is shown in Figure 4.

Analysis of the obtained results showed that at heating temperatures of 1175–1185 °C both the alloys have insufficiently stable wetting and spreading characteristics, the scatter of measured values being more than 15 %. Wetting angles exceed 12° for KMKhS alloy and 20° for KMKh alloy that is insufficient in terms of adaptability to fabrication.

Starting from the temperature of 1190 °C, both the alloys demonstrate high adhesion activity in the specified working temperature range of surfacing (1190–1210 °C). The most stable steady characteristics of wetting and spreading for both the test alloys are fixed in the temperature range of 1190–1195 °C. Wetting angles are within the range of 13–15° for KMKh alloy and 8–10° for KMKhS alloy. Specific spreading areas exceed 0.5 mm²/mg for both the alloys, that is more than sufficient in terms of adaptability-to-fabrication, and creates favourable prerequisites for their industrial application. Good adhesion with the substrate material is observed in the entire temperature range without formation of brittle intermetallic components. Here, the dissolution depth remains minimum right up to the temperature of 1210 °C and does not exceed 0.1 mm (see Figure 4) that guarantees preservation of the deposited metal properties and minimizes its effect on the base metal. More over, the melting temperature of both the alloys increases the critical heating temperature of turbine blades to 1150 °C during possible short-term overspeeding in operation, and does not exceed the limit admissible short-term heating temperature of high-temperature nickel alloys of ChS88U-VI type (1210–1220 °C) that is a mandatory requirement to the properties of new adhesion-active surfacing materials.

Conclusions

1. Structure of KMKh and KMKhS alloys consists of solid solution of cobalt (β-modification) alloyed with molybdenum and chromium with hardening by complex silicides and borides (CoB, Mo_2B, MoSi, CoSi), KMKhS alloy additionally contains chromium carbide (Cr_2C_6).

2. Melting temperature determined by the method of differential thermal analysis, is equal to 1185–1190 °C for KMKh alloy, and 1165–1170 °C for KMKhS alloy.

3. KMKh and KMKhS alloys are characterized by high adhesion activity relative to high-temperature alloy VZh 98. Steady characteristics of wetting and spreading are fixed at temperatures above 1190–1195 °C. For KMKh alloy the wetting angles are equal to 13–15°, for KMKhS — 8–10°. Specific spreading areas exceed 0.5 mm^2/mg.

1. Farafonov, D.P., Migunov, V.P., Alyoshina, R.Sh. (2016) Study of tribological characteristics of materials used for strengthening of flange platforms of GTE blades. *Aviats. Mater. and Technol.*, S1(**43**), 24–30 [in Russian].
2. Kostin, A.M., Martynenko, V.A., Maly, A.B. et al. (2017) Adhesion-active high-temperature wear-resistant surfacing consumables KMKh and KMKhS. *The Paton Welding J.*, **1**, 58–61.
3. Altukhov, A.A., Gavrilov, O.V. (2004) Application of high-temperature material KBNKhL-2 for surfacing of gas turbine parts. *Svarshchik*, **2**, 22–23 [in Russian].
4. Farafonov, D.P., Bazyleva, O.A., Rogalev, A.M. (2016) Alloys for strengthening of flange platforms of GTE blades. *Trudy VIAM*, 9(**45**), 53–60 [in Russian].
5. Pejtchev, G.I., Zamkovoj, V.E., Andrejchenko, N.V. (2009) Comparative characteristics of wear-resistant alloys for strengthening of flange platforms of gas turbine engine blades. *Vestnik Dvigatelestroyeniya*, **2**, 123–125 [in Russian].
6. Som, A.I., Ishchenko, V.Yu., Maly, A.B. (2004) Plasma-powder surfacing with stellite of pipe clamps. *Svarshchik*, **2**, 18–19 [in Russian].
7. Kostin, A.M., Martynenko, V.A., Butenko, A.Yu. (2014) Comparative high-temperature wear-resistance of alloy ChS88UVI and stellite Kh30N50Yu5T2. *Zbirnyk Nauk. Prats NUK*, 454(**4**), 55–59. Mykolaiv [in Russian].
8. Dmitrieva, G.P. et al. (2015) Structure and properties of wear-resistant alloy based on cobalt with niobium carbide. *Metallofizika i Novejshie Tekhnologii*. 37(**7**), 973–986 [in Russian].
9. Cherepova, T.S. et al. (2014) Wear-resistant alloy for protection of contact surfaces of aircraft engine blades from oxidation at high temperatures. *Nauka ta Innovatsii*, 10(**4**), 22–31 [in Ukrainian].
10. Yao, M.X., Wu, J.B.C., Liu, R. (2005) Microstructural characteristics and corrosion resistance in molten Zn-Al bath of Co–Mo–Cr–Si alloys. *Mater. Sci. & Engin. A*, **407**, 299–305.

Received 04.06.2019

https://doi.org/10.15407/tpwj2019.08.03

INVESTIGATION OF INTERACTION OF Ni_3Al-BASED ALLOY WITH INTERLAYERS OF DIFFERENT ALLOYING SYSTEMS FOR TLP-BONDING

V.V. KVASNYTSKYI[1], **G.F. MYALNITSA**[2], **M.V. MATVIIENKO**[3], **E.A. BUTURLYA**[4] and **DONG CHUNLIN**[5]

[1]National Technical University of Ukraine «Igor Sikorsky Kyiv Polytechnic Institute»
37 Peremohy Prosp., 03056, Kyiv, Ukraine. E-mail: kvas69@ukr.net

[2]SE «Scientific-Production Gas Turbine Construction Complex «Zorya»–«Mashproekt»
42a Oktyabrskyi Prosp., 54018, Mykolaiv, Ukraine

[3]Kherson Branch of Admiral Makarov National University of Shipbuilding
44 Ushakova Prosp., 73022, Kherson, Ukraine

[4]Admiral Makarov National University of Shipbuilding
9 Heroiv Ukrainy Prosp., 54025, Mykolaiv, Ukraine

[5]Guangdong Provincial Key Laboratory of Advanced Welding Technology,
Guangdong Welding Institute (China-Ukraine E.O. Paton Institute of Welding), Guangzhou, 510650, China

Fusion welding of cast high-temperature nickel alloys with high content of strengthening disperse phases is problematic. Even more serious problem is welding of intermetallic-based materials. Therefore, different methods of brazing are widely used for such materials joining. TLP-bonding (Transient Liquid Phase Bonding) is a term which has the most often application abroad. Considering that brazing filler materials have lower melting temperature than base metal, the concentration of depressants (reducing brazing filler metal melting temperature) in a brazed weld shall be reduced to the minimum in order to increase working temperature of brazed joints in brazing process. The depressants of high-temperature brazing filler metals are divided on several groups. Interaction of Ni_3Al-based alloy with brazing filler metals containing silicon, boron, zirconium and hafnium was investigated in the work. SBM-3 brazing filler metal of Ni–Cr–Co–Al–Ti–Ta–Re–W–Mo–Hf–B system was developed based on investigations results. 17 Ref. , 7 Figures.

Keywords: *brazing, nickel alloys, strengthening phase, depressants, brazing filler metal development, melting temperature*

The efficiency of gas turbines significantly depends on the temperature of working gas. Therefore, for the manufacture of guides and working blades, materials with higher heat resistance are developed. Such are the new alloys based on intermetallics, in particular, based on the intermetallic Ni_3A1. The promising methods of their joining are welding in the solid state, for example, friction welding, diffusion welding in vacuum with fused or nonfused interlayers or brazing [1, 2]. Brazing is a more universal method of joining, but its main problem is providing strength properties of brazed joints, which are close to those of the base metal. Good results are provided by TLP-bonding technology.

Ni_3A1intermetallic-based alloy is a structural material for gas turbines of a new generation [3, 4]. Ni_3A1 phase has a face-centered cubic lattice, in which chromium, molybdenum and tungsten are limitedly soluble, and the solubility of elements in this series decreases. The metals like titanium, tantalum and niobium dissolve in the γ'-phase, substituting aluminum and strengthening it. Cobalt has a high solubility in nickel, substituting nickel in the γ-solid solution. The ordered structure of the γ'-phase provides its high stability and operation of the alloy up to 1200 °C. The intermetallic, alloyed with small amounts of tantalum and chromium, has a high resistance in oxidizing environment at the temperatures up to 1100–1200 °C.

When joining different structures based on intermetallic Ni_3A1, operating at high temperatures and increasing the efficiency of gas turbines, joining technologies are required having both similar and dissimilar combinations with other high-temperature alloys. The solution to this problem is certainly relevant.

Problem statement. Aircraft materials science is successfully developed and intermetallic materials based on Ni_3A1have been known since the end of the last century [5, 6]. Investigations of methods of their joining began to be actively carried out only recently, and for the first time the possibility of applying existing brazing filler metals for brazing of high-temperature nickel alloys was considered in the works. These brazing filler metals can be divided into three groups [2]:

1) nickel-based alloyed brazing filler metals using silicon and boron as depressants, which in most cases are introduced together to reduce brazing temperature and concentration of each of them;

2) brazing filler metals based on alloyed nickel with the use of elements of the IV and V groups of the Periodic Table as depressants;

3) brazing filler metals of the system Ni–Pd.

In Ukraine and abroad, brazing filler metals of the first group, for example, VPr11, VPr11-40N, BNi1, BNi2, BNi5, VPr42, NS12, NS12A, STEMET 1301, STEMET 1311 are the most widely known. Complex alloyed brazing filler metals containing silicon and boron are VPr24, VPr27 and oth.

In works [7–9], complex alloyed brazing filler metals VPr36, VPr37 and VPr44 were investigated for brazing of high-temperature nickel alloys ZhS32, ZhS36 and EP975 alloy with VKNA-4U alloy based on the intermetallic Ni_3A1. The results obtained are little described, but the mentioned brazing filler metal systems show the possibility of increasing the high-temperature strength of brazed joints of alloys based on the intermetallic Ni_3A1.

The aim of the work is to study the interaction of the alloy based on the intermetallic Ni_3A1 with brazing filler metals of different systems and to increase the strength of joints, produced by TLP-Bonding technology, to the level of 70–80 % of the strength of the base metal.

Materials and procedure of investigations. For investigations, an experimental high alloy based on intermetallic $Ni_3A1$with the following content of basic elements (wt.%) was melted: 0.085 C; 6.6 Cr; 11.63 Co; 4.67 W; 1.49 Mo; 5.61 Si; 7.44 Ta; 1.6 Hf; 2.0 Ti; Ni is the rest. Microstructure of the alloy is shown in Figure 1. In the initial heat-treated state, the alloy has a uniform $\gamma + \gamma'$ structure with a high share of γ'-phase (68–72 vol.%).

The sizes and shape of specimens for investigations and mechanical tests were determined according to the accepted standard procedures (ISO 783–89) and the data given in work [10].

The base of the studied brazing filler metals was nickel alloyed with the same elements as the base material of the system Ni–Co–Cr–A1–Ti–Ta–W–Mo. For this purpose, the available computer programs for calculating the content of phases and critical temperatures were used. To reduce the melting temperature, as a depressant, boron and silicon and similarly zirconium and hafnium were together or separately introduced to the alloy.

The wetting quality of the high-temperature alloy was evaluated by wetting angle at different temperatures. The spreading of brazing filler metal was determined by specific spreading area. After that, the specimens were cut at the center of a drop of brazing filler metal and wetting angle was determined from a photo of macrosection.

To investigate the flow of brazing filler metal into the gap, wedge-shaped specimens with the sizes of 20×12×3 mm (lower) and 20×6×3 mm (upper) were used, which were exposed one on the other along the length with a zero gap on a one side and a gap of 0.3 or 0.6 mm on the other.

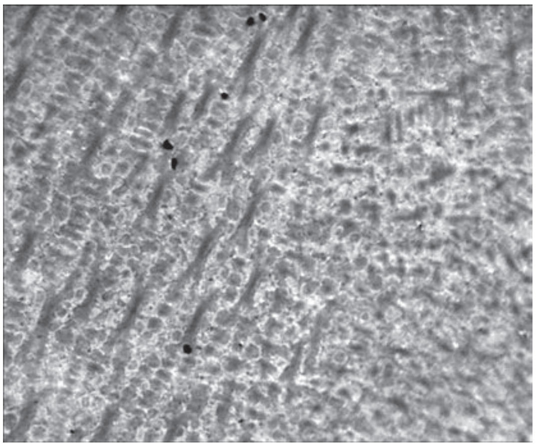

Figure 1. Microstructure (×45) of melted alloy based on Ni_3Al (magnific. by 1.5 times)

The formation of joints of butt welds was investigated on cylindrical specimens with a diameter of 13 mm and a length of 35 mm.

Structural investigations were carried out using optical metallography and scanning electron microscopy. The chemical composition was determined by local X-ray spectrum microanalysis by individual points and by area. The structure of high-temperature alloys was detected by chemical etching in a solution consisting of 10 g of chlorine iron, 30 ml of hydrochloric acid and 120 ml of alcohol or Marble's reagent: 100 ml of HCl, 20 g of $CuSO_4$, 100 ml of H_2O with addition of H_2SO_4 (0–20 ml). Murakami's reagent was used to differentiate between carbides and σ-phase: 10 g of red blood salt, 10 g of potassium hydroxide or 7 g of sodium hydroxide.

Differential thermal analysis was carried out in thermal analyzer HTDTA-8M with simultaneous measurement of temperature of the investigated specimen and the reference under heating and cooling in electric resistance furnace. The rate of heating and cooling was automatically maintained constant.

Investigations on determination of melting and crystallization temperatures were carried out in the atmosphere of high-purity helium. The rate of heating and cooling was 0.8 °C/s. Specimens with the mass of 1 g were placed in the crucibles of yttrium oxide Y_2O_3. The temperatures of phase transformations were determined using a calibration curve constructed on the melting points Al, Cu, Fe, and Pt. The cooling curves were used to qualitatively control the number of phase transitions and to determine the temperatures of the start of crystallization. The error of the results was ±7 °C.

Determination of mechanical characteristics was carried out during static short-term and long-term tensile tests of cylindrical specimens.

At the first stage, as applied to the melted alloy based on Ni_3A1, according to the results of the analysis of sources [7–9], for investigations and correction of composition brazing filler metal VPr36 was selected. To reduce the temperature of brazing, correction of the composition of brazing filler metal VPr36 was also carried out by the authors of works [11, 12], who introduced silicon into brazing filler metals for this purpose, using brazing filler metal NS12, containing 12 % of Si. For alloy based on Ni_3A1, a higher melting point of brazing filler metal is required, and to increase heat resistance of joints, the silicon content in the base metal is strictly limited. Therefore, silicon was not used in our investigations. In addition, in brazing filler metal it was necessary to use alloying by analogy with high-temperature alloys of a new generation, which was taken into account in this work.

When choosing depressants, the investigations were taken into account considered in work [13], in which the prospective use of such depressants as zirconium and hafnium in brazing filler metals was established.

Therefore, at the second stage of investigations in brazing filler metals for brazing intermetallic alloy, zirconium and hafnium were used as depressants. These elements form unlimited solutions between themselves and replace each other in the intermetallics of nickel in any ratios. The temperature of brazing using brazing filler metals with hafnium was 1225–1230 °C, and using brazing filler metals with zirconium was 1200–1210 °C.

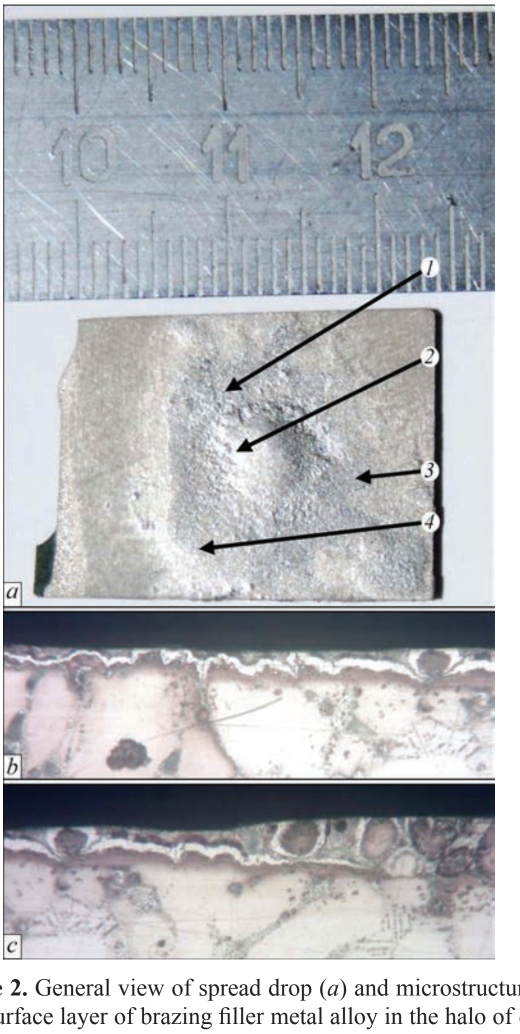

Figure 2. General view of spread drop (*a*) and microstructure of near-surface layer of brazing filler metal alloy in the halo of drop (*b*) and closer to its center (*c*) brazing filler metal with zirconium (see description *1–4* in the text)

The spreading of brazing filler metal with zirconium over the intermellic alloy is shown in Figure 2, where it is seen that spreading area of brazing filler metal consists of the central zone of brazing filler metal at the points *1* and *2*, the peripheral zone at the point *3* and the halo of a drop at the point *4*. The chemical composition of the metal in these zones is significantly different. In the central zone, the composition varies in height of the drop, but contains elements of the base of brazing filler metal. Further, in the peripheral zone and in the halo of a drop, the concentration of zirconium grows and an eutectic layer appears, which repeats micro roughness of the surface and envelops separate particles of brazing filler metal. With the introduction of 2.5 % of Zr in certain areas of the surface, its concentration increases to 11–12 wt.%. When introducing 5.0 % of Zr into brazing filler metal, in some areas the concentration of zirconium reaches 21 %, the concentration of niobium (up to 30 %) and tungsten (up to 14 %) sharply increase, the concentration of nickel (21–25 %), aluminum and titanium decreases, which testifies the formation of intermetallics.

An analogue of zirconium is hafnium, which, unlike zirconium, has a low diffusion mobility of atoms. Both elements have a low solubility in nickel and similar state diagrams with nickel. A low solubility of hafnium and zirconium in nickel along with the formation of eutectics broaden the temperature range of melting and crystallization of brazing filler metals, which is bad for alloys based on Ni_3A1intended for operation at temperatures up to 1200 °C. Brazing filler metals with zirconium and hafnium have a good wetting of the alloy based on Ni_3A1 at a vacuum of 10^{-3} Pa, as well as an uneven distribution in the brazed weld. The wetting angles, depending on the composition of brazing filler metal and temperature, vary from 13 to 5 degrees. Taking into account a high affinity of zirconium and hafnium to oxygen during brazing, it is necessary to strictly control the pressure in the working vacuum chamber (not more than $3\cdot10^{-3}$ Pa) and the leakage value, not more than $3\cdot10^{-5}$ $Pa\cdot m^2\cdot s^{-1}$.

Brazing filler metals with zirconium for brazing the alloy ZhS6U were also used in work [14]. Two brazing filler metals of the system Ni–Co–Cr–Ti–Nb–A1–(Me)–Zr, containing 1 and 2 % of Zr were investigated. Their temperatures are: solidus — 1101 and liquidus 1231 °C with 2 % of Zr and respectively 1141 and 1259 °C with 1 % of Zr. For application brazing filler metal with 1 % of Zr is recommended. As to the brazing temperature, brazing filler metal is not suitable for brazing alloy based on Ni_3A1. Brazing filler metals with zirconium and hafnium are well studied in works [15–18] as-applied to high-temperature nickel alloys with a brazing temperature up to 1210 °C. An increase in brazing temperature can lead to a degradation of the structure of the base metal.

At the third stage, brazing filler metal with the use of boron as a depressant was investigated. These brazing filler metals are the most studied and widespread in industry. During the development of brazing filler metal two problems were solved: the choice of the base of brazing filler metal and the determination of the necessary concentration of boron to provide the necessary liquidus and solidus temperatures. Brazing filler metals with boron traditionally have a high manufacturability.

When choosing a base of brazing filler metal, general provisions of the development of high-temperature alloys were used based on the influence of each of the alloying elements, including alloys of a new generation, on mechanical properties, formation of strengthening phases as well as brittle phases, heat resistance, liquidus, solidus, solvus temperatures, temperature of evolution and number of phases, their composition and other. At the same time, aircraft materials, in particular, intermetallic Ni_3A1 and alloys for marine gas turbines, operating at lower temperatures, but under conditions of high-temperature salt corrosion (HSC), were considered. The operating conditions of marine turbines significantly affect the chromium content in alloys, reducing their heat resistance.

The found ways to increase heat resistance and resistance against HSC allowed creating alloys for marine turbines of a new generation with an increase in their operating temperature by 50–60 °C [19]. Accordingly, it is necessary to increase heat resistance of joints, as well as brazing temperature. To do that, it is necessary to create new brazing filler metals, using the same principles of alloying, which are used to create alloys.

Many other problems are common to aircraft and ship gas turbine building, which allows using the same calculation methods and computer programs. When choosing the base of brazing filler metals, calculations were also used, but with the same base systems of brazing filler metals, the concentrations of a number of elements in them are significantly different. For example, the resistance of alloys against the formation of σ-phase depends on the group of elements, including chromium. Therefore, at a high chromium content, it is necessary to reduce the concentrations of other elements, strengthening a solid solution, at the same number of electronic vacancies and for this purpose the alloy was doped with elements, which are the most effective strengtheners. Such alloying is used in high-temperature alloys of a new generation.

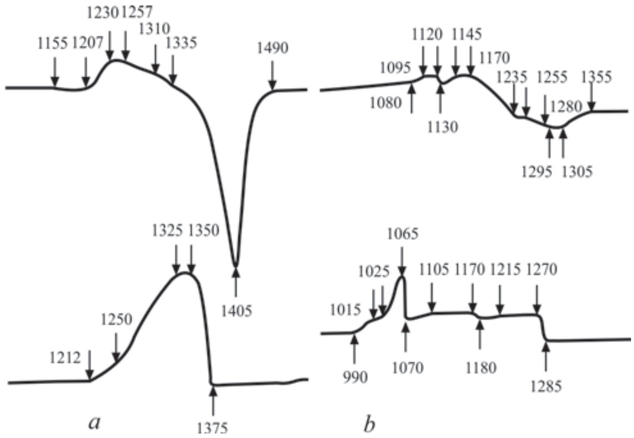

Figure 3. HTDTA curves for base of brazing filler metal (*a*) and after introduction of boron (*b*)

To calculate the second problem (choice of boron concentration), it is necessary to have a regression equation of the effect of boron on the liquidus and solidus temperature of the brazing filler metal base. There is not enough statistical data to do that. Therefore, the problem was solved experimentally. Several alloys were melted (brazing filler metal base), to which boron was added at three different concentrations. The produced specimens were subjected to HTDTA, investigations on wetting and spreading of brazing filler metal. In Figure 3, *a* the thermogram of one of the melted alloys is shown (brazing filler metal base), and in Figure 3, *b* — HTDTA results after addition of boron.

The spreading of one of the brazing filler metals in the alloy based on Ni_3A1 is shown in Figure 4.

Depending on the base of brazing filler metal and boron concentration, the wetting angle and specific spreading areas are changed. The main role is played by brazing temperature. All melted brazing filler metals wet the alloy well, but the temperature range of brazing filler metal application was determined by the wetting angle of not more than 10°. The optimum angle is 3–5°. The specific area of spreading during the

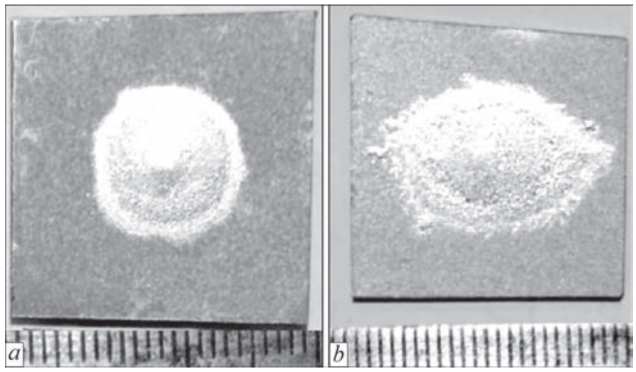

Figure 4. Spreading of batch weight of 100 mg of powder of brazing filler metal SBM-3 on alloy Ni_3A1 at temperatures of 1250 (*a*) and 1265 °C (*b*)

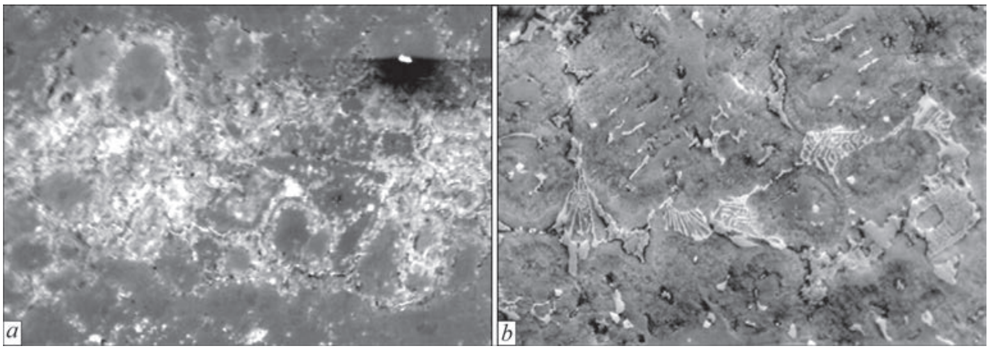

Figure 5. Microstructure of weld metal in brazing of wedge specimen with a gap of 361 (*a*) and 297 μm (*b*)

temperature of investigations of 1250–1265 °C was 1.7–2.0 mm^2/mg.

The formation of a brazed joint was estimated by the structure of the weld, its chemical composition (by area and phase), as well as by the maximum and minimum gaps, which are filled without defects at a temperature of brazing. This can be determined most accurately by brazing wedge-shaped specimens with a change in the gap from zero to 0.6 mm. The depth of dissolution of the base metal was also determined on such specimens. Regardless of the chemical composition of brazing filler metal, with an increase in the temperature of brazing the depth of dissolution of base metal increases, and it is as larger as wider the gap and the higher the boron concentration. The change in the concentration of boron also changes the number and composition of phases: γ, γ′, M_xC_y, M_3B. When analyzing by areas, the composition of the alloy varies little. The combined volume fraction of the carbide and boride phases increases already with increasing boron concentration from 1.0 to 1.2 wt.%, and the content of chromium, molybdenum and tungsten is almost half decreased.

The microstructure of the weld metal, brazed with a filler metal containing 2.5 % of Re, is shown in Figure 5.

According to the results of the analysis of the structure and chemical composition of melted specimens, brazing filler metal SBM-3 was developed, the microstructure of joints of which is shown in Figure 6.

Analyzing the results of investigations of phases and chemical composition of joints of the alloy based on Ni_3A1, produced by TLP-bonding method with brazing filler metal SBM-3, it should be noted that the matrix of brazing filler metal has a composition close to that of the base metal, plus individual elements, which is not in the base metal, but they are introduced into brazing filler metal. The structural composition of the weld metal and base metal are close. The joints structure has no continuous eutectic interlayers, carbide, boride or carboboride precipitations.

Brazed joints pass heat treatment, including high-temperature homogenization and staged cooling. The mode of heat treatment of the alloy includes heating up to 1180 °C with the exposure of 2 h → heating to 1265 °C with the exposure of 2 h and air cooling, heating up to 1050 °C with the exposure of 4 h and air cooling. After heat treatment, the boride eutectic is absent due to the formation of highly-dispersed borides and carboborides, which are characterized by the presence of active carbide and boride formers, which are clearly determined on the spectra during local X-ray spectral analysis. All such inclusions have a low aluminum content.

Mechanical tests of joints were carried out at operating temperatures with the determination of short-term and long-term strength on the basis of 50 and 100 h of tests. The test for the short-term strength of

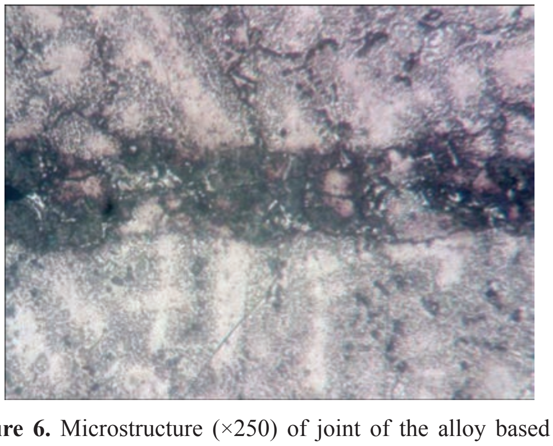

Figure 6. Microstructure (×250) of joint of the alloy based on intermetallics Ni_3A1 in brazing with a constant gap of 0.08 mm by brazing filler metal SBM-3

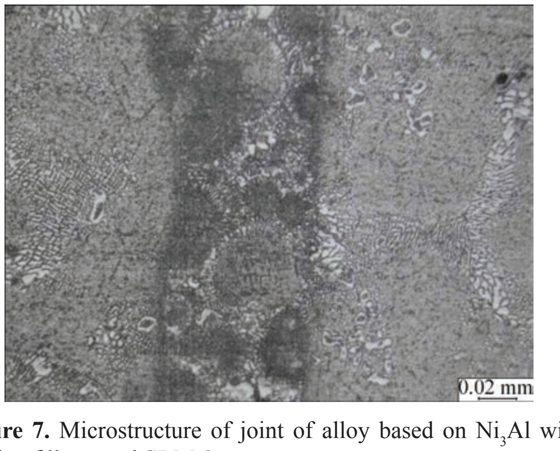

Figure 7. Microstructure of joint of alloy based on Ni_3Al with brazing filler metal SBM-3

the polycrystalline base metal at 900 °C showed a mean value: σ_t = 830 MPa, $\sigma_{0.2}$ = 720 MPa; at 1000 °C σ_t = 530 MPa; $\sigma_{0.2}$ = 460 MPa. The strength of joints was at the same level. The fracture of the specimen occurred on the base metal. The microstructure of a joint in the butt zone is shown in Figure 7.

The long-term strength of joints of Ni_3A1based alloy at a temperature of 900 °C on the basis of tests of 100 h amounted to σ^{900}_{100} = 280 MPa, which is equal to 81.9 % of the strength of base metal, based on 50 h of σ^{900}_{50} = 320 MPa, which is 85.6 % of the strength of base metal.

On the basis of the carried out investigations, brazing filler metal SBM-3M for brazing of high-temperature nickel alloys of marine gas turbines was also developed, a significant difference of which from brazing filler metal SBM-3 is a higher chromium content. Both brazing fillers metals are developed on the base of Ni–Co–Cr–A1–Ti–Ta–Re–W–Mo–B system.

Conclusions

1. The work proposes new approaches to the choice of alloying elements of brazing filler metals base, providing a solid solution and dispersion strengthening. In particular, the introduction of tantalum and rhenium into brazing filler metals, which are used for alloying of high-temperature alloys of turbines of a new generation and have a higher efficiency in increasing heat resistance and heat strength and reducing the concentration of molybdenum and tungsten or replacing them.

2. At a brazing temperature of 1250 °C, the wetting angles of high-temperature alloy based on Ni_3A1 intermetallics by brazing filler metal SBM-3 do not exceed 7°, as to the chemical composition and structure, the weld metal is close to the base metal, short-term strength at 900 °C is at the level of the base metal, and the long-term strength of TLP-joints on the basis of 50 and 100 h of tests is not lower than 80 % of the base metal.

3. The results of the work showed that the created brazing filler metal SBM-3 and the TLP-bonding technology correspond to the aims of investigations.

4. According to the results of work for experimental industrial use, brazing filler metals of Ni–Co–Cr–A1–Ti–Ta–Re–W–Mo–B system were melted with Hf and without it.

1. Krivtsun, I.V., Kvasnytskyi, V.V., Maksymov, S.Yu., Yermolayev H.V. (2017) *Special methods of welding: Manual*. Ed. by B.E. Paton. Mykolaiv, NUK [in Ukrainian].
2. *Yermolayev H.V.,* Kvasnytskyi, V.V., Kvasnytskyi, V.F. et al. (2015) *Brazing of materials: Manual*. Ed. by V.F. Khorunov, V.F. Kvasnytskyi. Mykolaiv, NUK [in Ukrainian].
3. Kablov, E.N. (2012) Strategic tendencies in development of materials and technologies of their processing for period up to 2030. *Aviats. Materialy i Tekhnologii*, **5**, 24–30 [in Russian].
4. Kablov, E.N., Ospennikova, O.G., Bazyleva, O.A. (2011) Materials for high-loaded parts of gas turbine engines. *Vestnik MGTU. Seriya Mashinostroenie*, **9**, 13–19 [in Russian].
5. Buntushkin, V.P., Kablov, E.N., Kachanov, E.B., Shalin, R.E. (1994) High-temperature structural materials based on intermetallic Ni_3Al. In: *Aircraft materials at the turn of the XX-XXI centuries: Sci.-Techn. Transact. Moscow*, VIAM [in Russian].
6. Buntushkin, V.P., Kablov, E.N., Bazyleva, O.A., Morozova, G.I. (1999) Alloys based on nickel aluminides. *Metallovedenie i Termich. Obrab. Metallov*, **1**, 32–34 [in Russian].
7. Lukin, V.I., Rylnikov, V.S., Afanasiev-Khodykin, A.N. (2012) Peculiariries of brazing single-crystal castings and alloy ZhS32. *Svarochn. Proizvodstvo*, **5**, 24–30 [in Russian].
8. Lukin, V.I., Rylnikov, V.S., Afanasiev-Khodykin, A.N. (2010) Peculiaries of producing of ZhS36 alloy brazed joint. *Tekhnol. Mashinostroeniya*, **5**, 21–35 [in Russian].
9. Lukin, V.I., Rylnikov, V.S., Afanasiev-Khodykin, A.N., Timofeeva, O.B. (2013) Peculiarities of diffusion brazing technology of high-temperature alloy EP 975 and cast single-crystal intermetallic alloy VKNA-4U applying to structure «Blisk». *Svarochn. Proizvodstvo*, **7**, 19–25 [in Russian].
10. *Xiong* Yue, Fengmei Liu, Hexing Chen, et al. (2018) Effect of Bonding Temperature on Microstructure Evolution during TLP Bonding of a Ni_3Al based Superalloy IC10. *ICCEMS 2018, MATEC Web of Conferences 206, 03004*.
11. Malashenko, I.S., Kurenkova, V.V., Belyavin, A.F., Trokhimchenko, V.V. (2006) Short-term strength and microstructure of brazed joints of alloy VZhL12U produced using boron-containing brazing alloy with addition of silicon. *Sovrem. Elektrometall*., **4**, 23–38 [in Russian].
12. Malashenko, I.S., Mazurak, V.E., Kushnareva, T.N. et al. (2014) Vacuum brazing of cast nickel alloy ZhS6U with composite brazing alloys on VPr-36 base. Pt 1. *Ibid*., **4**, 49–58 [in Russian].
13. Kvasnytsky, V.F., Kostin, A.M., Kvasnitsky, V.V. (2002) Influence of elements-depressants on properties of nickel brazing filler metals and high-temperature alloys. *Adgeziya Rasplavov i Pajka Materialov*, **35**, 129–139 [in Russian].
14. Maksymova, S.V., Voronov, V.V., Kovalchuk, P.V. (2017) Brazing filler metal without boron and silicon for brazing of heat-resistant nickel alloy. *The Paton Welding J*., **8**, 12–17.
15. Kvasnitskiy, V.V., Timchenko, V.L., Ivanchenko, V.G., Khorunov, V.F. (1998) The investigation of Ni(Nialloy)–Hf–Cr system for heat-proof nickel alloy brazing. *DVS-Berichte: Band 192, Duesseldorf:DVS – VERL*, 262–264.
16. Kvasnitskiy, V.V., Timchenko, V.L., Ivanchenko, V.G., Khorunov, V.F. (1998) Die Untersuchung des System Ni(Niliq)–Hf–Zr– fuer das Loten warmfester Nickellegierungen. *Ibid*., 257–259 [in German].
17. Kvasnitskiy, V.V. (1998) Composite filler metal brazing of heat-proof nickel alloys. *Ibid*., 260–262.
18. Khorunov, V.F., Ivanchenko, V.G., Kvasnitskiy, V.V. (1998) Investigation of systems Ni–Cr–Zr and Ni–Cr–Hf alloys. *Ibid*., 59–61.
19. Myalnytsa, G.P., Maksyuta, I.I., Kvasnitska, Yu.G., Mykhnyan, O.V. (2013) Selection of alloying complex of new corrosion-resistant alloy for nozzle blades of GTE. *Metaloznavstro ta Obrobka Metaliv*, **2**, 29–34 [in Ukrainian].

Received 14.06.2019

https://doi.org/10.15407/tpwj2019.08.04

APPLICATION OF PULSED IMPACT IN CONSUMABLE ELECTRODE GAS-SHIELDED ARC WELDING (Review)

V.A. LEBEDEV[1], **S.V. DRAGAN**[2], **G.V. ZHUK**[1], **S.V. NOVIKOV**[1] and **I.V. SIMUTENKOV**[2]
[1]E.O. Paton Electric Welding Institute of the NAS of Ukraine
11 Kazimir Malevich Str., 03150, Kyiv, Ukraine. E-mail: office@paton.kiev.ua
[2]Admiral Makarov National University of Shipbuilding
9 Heroiv Ukrainy Prosp., 54025, Mykolaiv, Ukraine. E-mail: welding@nuos.edu.ua

The paper presents the main technical means and methods of pulsed control of the process of consumable electrode gas-shielded arc welding, developed over the recent years at PWI and Admiral Makarov National University of Shipbuilding. A lot of attention is given to methods using systems of pulsed impact on the processes of electrode metal transfer, weld formation and deposited metal structure. Good prospects for application of systems with pulsed dozed feed of electrode wire are shown, and results of effective control of welding and surfacing processes are given. Methods of arc welding with pulsed feed of shielding gas and with two-jet gas shielding are considered, and problems are indicated, which prevent extensive application of these processes. The paper gives the results of some studies of the influence of external electromagnetic impact on electrode metal transfer, weld formation and crystallization, and presents some examples of effective application of this method of welding process control. Analysis of the methods of mechanical impact on the welding process using different oscillator systems was performed. The possibility is shown of combined control of electrode metal transfer, deposited bead formation and its metal structure, depending on the scheme of oscillation application and oscillation process parameters. The good prospects for this method application for surfacing operations are pointed out. 34 Ref., 2 Tables, 12 Figures.

Keywords: *welded joint, properties, control, technical means, analysis, application*

Welding and related technologies are continuously, actively and comprehensively developing. Theoretical and technological prerequisites, engineering developments for manufacturing new products are created in the traditional fields of welding production, as well as mastering other spheres of application, which were earlier considered inaccessible for a broad range of tasks, for instance, wet underwater welding [1].

A weld, or deposited layer are the result, which is achieved using mechanized or automated equipment for arc welding and surfacing. Operating (service) properties of welded, reconditioned or strengthened items (structures) depend on the structure of the deposited metal and heat-affected zone, weld surface shape, geometrical parameters of the penetration zone [2].

There exist quite a large number of techniques and methods for influencing the characteristics of the welded joint or deposited layer, including technological, technical characteristics and those related to electrode materials and shielding media. Here, we should also take into account the influence of the material being welded, conditions and media, in which the arc process is conducted.

The objective of this work is analysis and prospects for application of technical means, which are part of welding equipment systems, as well as auxiliary systems.

Developments of PWI and Adm. Makarov NUS are considered for analysis of the main technical means, used for pulsed control of parameters of the weld and deposited layer. The diversity of technical means is generalized and shown in Figure 1.

Inverter-type pulsed welding current sources became widely accepted in welding and surfacing equipment for any purpose, implementing the electric arc process using consumable electrode. The shape of output voltage pulses and their frequency depend on the problems being solved. These are mainly the problems of control of electrode metal transfer, including creation of conditions for optimum transition of molten metal drops into the liquid pool.

Widely accepted are the processes with control algorithms, where different variants of feedbacks are used [3]. As an example, let us note the process of electrode metal drop transfer at continuous feeding of electrode wire, in which the source voltage is stabilized at the stage of drop formation, and a current pulse is supplied at the stage of breaking of the neck of the drop between the electrode and the pool (Figure 2) [4].

Pulsed impact of welding current source allows to:

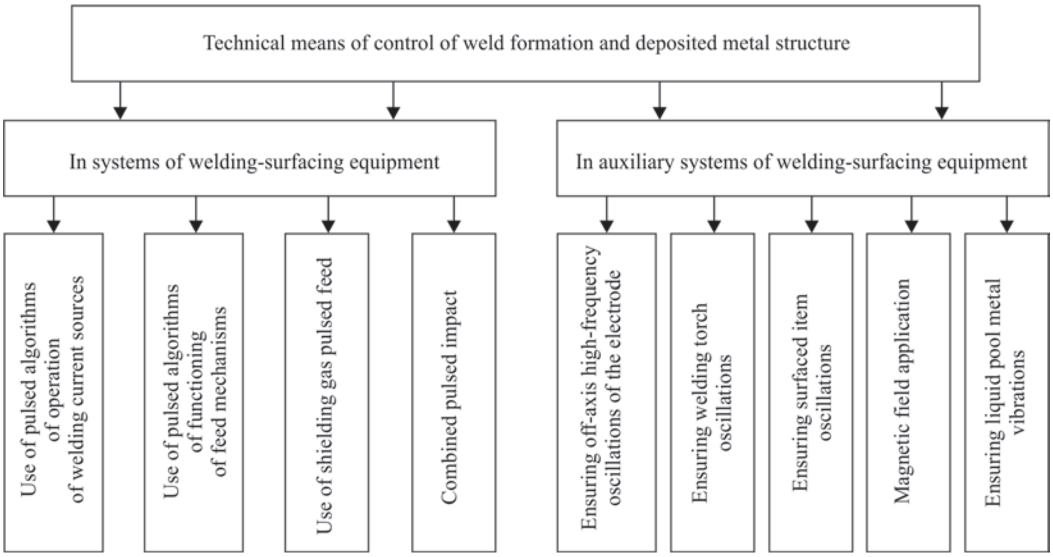

Figure 1. Technical means of influencing the properties of the weld or deposited layer

● control electrode metal transfer through drop separation and its transportation into the weld pool as the main impact of current pulse of the arc process;

● create vibrational oscillations of molten metal pool as concurrent impact of electrodynamic forces.

Controllable transfer of electrode metal can be also obtained using pulsed feed of electrode wire. This approach is becoming more and more widely accepted that is largely determined by the capabilities for improvement of technical means and technological developments in this direction. Different designs of mechanical gearless converters of rotational movement of drive electric motor shaft into pulses of movement of wire movers can be noted [5]. Such engineering solutions allow assigning the preselected mode of electrode wire feed by the movement step and pulse duty cycle. However, the application of such designs is limited. Pulsed feed devices with quasi-wave converters are an exception [6]. As a rule, quite inexpensive d.c. commutator motors are used as drive electric motors in such devices.

Pulsed feed systems with application of brushless electric motors, namely step and valve, have been developed and their development is carried on. Their operational parameters are determined by software, based on digital control systems. Use of such electric motors implies a gearless design of wire feed mechanism that improves system response. Batch-produced sets are mainly used as electric drives with step electric motors. Such sets were used with success in the automatic machine for wet underwater welding [7] and in other types of equipment [8].

Electric drives with valve electric motors and digital control were developed in Ukraine specially for various-purpose welding equipment [9], but they became the most common in systems of electrode wire feed for implementing pulsed movement with controlled characteristics, for instance, wet welding in aqueous environment. The possibilities of pulsed feed influencing bead formation are illustrated by examples of flux-cored wire surfacing in water (Figure 3). Here, the number of nonmetallic inclusions is increased, and mechanical properties of the deposited layers are improved.

Modern valve electric drives ensure up to 50–60 Hz frequency of pulsed feed of electrode wire with controllable parameters (step, amplitude, relative pulse duty cycle) and possibility of movement reverse in feed pulse cycle. Moreover, the signal of feedback by arc process parameters can be entered into the valve electric drive regulator. A drive with current or voltage feedback, realizing dosed feed of electrode wire can be used as an example [10, 11]. Changing the parameters of dosed feed of electrode wire allows controlling the weld shape at unchanged parameters of welding or surfacing mode (average current, voltage and arc movement speed).

One of the basic effects at pulsed feed of electrode wire is also the possibility of producing a disoriented structure of the deposited metal. Detailed metallo-

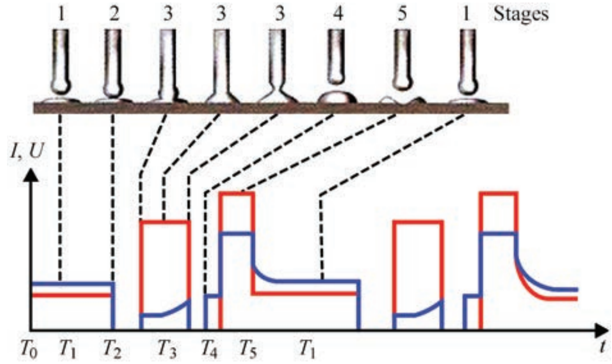

Figure 2. Algorithm of operation of control system of pulsed welding current source

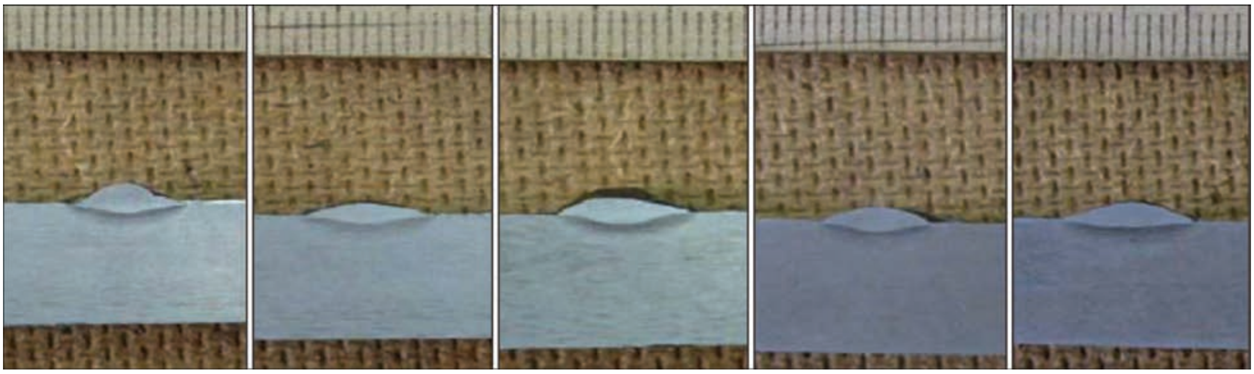

Figure 3. Microsections of beads, deposited with controlled pulses of electrode wire feed

graphic studies of samples, deposited under the same conditions and with the same energy parameters of the process, but using different methods of electrode wire feed, are indicative of significant changes in the deposited metal structure, and reduction of the quantity of nonmetallic inclusions [12].

We should also note the greater stability of the process of metal transfer at application of systems with dosed wire feed. In the oscillograms of the surfacing process performed with dosed wire feed (Figure 4), a clear regularity of the controlled electrode metal transfer is observed that eventually leads to metal structure improvement. Lowering of the degree of alloying elements burn out is observed at the same time. Welds and deposited layers produced by arc welding, also have improved mechanical properties, for instance, strength, wear resistance and toughness [13].

Results of welding (surfacing) with 1.0 mm electrode wire of 0.9 mm thick plates from an aluminium alloy can provide evidence of the effectiveness of application of dosed feed of electrode wire (Figure 5) [14]. In terms of quality indices, these joints practically do not differ from welds produced by nonconsumable electrode argon-arc welding, but as regards the efficiency the process with dosed feed of electrode wire exceeds argon-arc welding 1.5–2.0 times.

Pulsed feed of shielding gas and two-jet gas shielding are relatively new processes of controlling the arc welding process.

During the shielding gas feed pulse, the velocity of gas outflow from the nozzle increases, gas-dynamic pressure on the drop at the electrode wire tip rises, and finer drops move into the pool, but at greater frequency [15]. Here, as a result of reduction of the time of drop transfer into the liquid pool, the intensity of alloying element burning out changes.

Among the different variants of pulsed feed of shielding gases, the main ones are the following two: with feeding one type of gas and with alternative feeding of several types of gases, the second variant being more effective. In [16] it is shown that alternative feeding of argon and helium results in a new technological process, in which the effect of pulsed impact on the weld pool arises due to pulsed change of pressure in the arc gap (because of different density and ionization potential of argon and helium). This promotes producing metal of the weld and deposited layer with fine-grained metal structure with high values of metal ductility and strength.

The appearance of welds (surface shape, ripple) depends not only on the type of shielding gas, but also on pulsed feed frequency. Gas feeding with pulse fre-

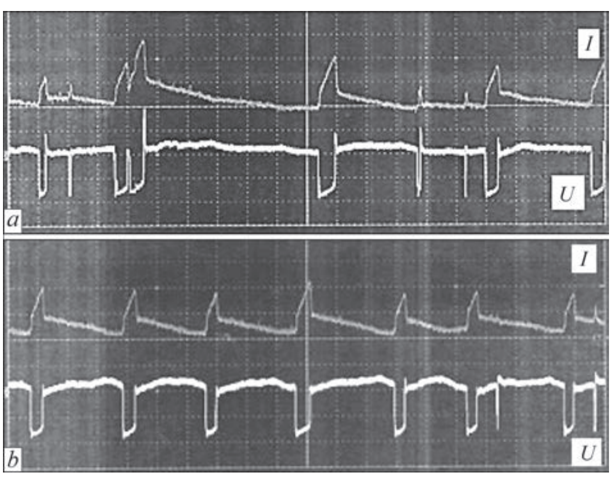

Figure 4. Oscillograms of surfacing process with electrode wire feed: *a* — discontinuous; *b* — dosed

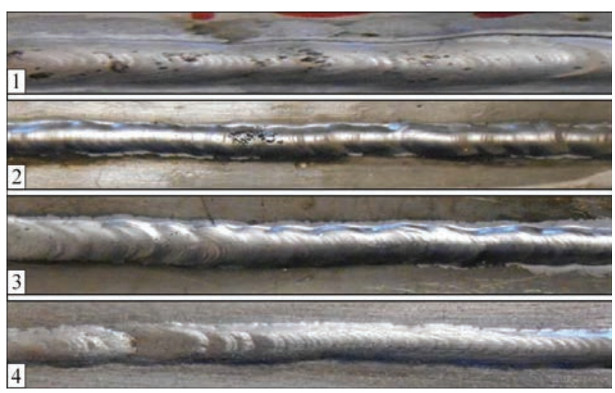

Figure 5. Appearance of beads, obtained with dosed feed of electrode wire, on sheet metal structures: 1 — surfacing with semi-automatic machine; 2, 3 — butt welding with semi-automatic machine; 4 — surfacing with automatic welding machine

quency of up to 20 Hz has a predominant effect on weld geometry [17–19].

Despite the obvious advantages of arc welding and surfacing with pulsed feed of shielding gas, wide acceptance of the method, in our opinion, is prevented by inertia of the shielding gas feed system. Here, placing the gas valve even directly at the nozzle cannot provide an effective solution of the problem. It should be also taken into account that with increase of the pulsed feed frequency, it is more difficult to ensure shielding gas feeding in individual portions without mixing.

The process of welding with two-jet gas shielding is interesting from the view point of its effect on the weld and improvement of shielding gas feed system [20]. With such a welding process, the shielding gas jet is enclosed in an outer jet, which stabilizes the inner jet, lowers its turbulence, limits air suction into the arcing zone and protects the near-weld zone. Increased gas-dynamic pressure of the inner gas jet promotes cooling of the molten electrode metal drop at its movement from the electrode tip and lowers alloying elements loss. More intensive mixing of the main and electrode metal takes place in the weld pool.

Developments of welding equipment systems with combined effects on the welding process, formation of the welded joint and deposited layer are of great interest. Engineering capabilities of application of the method of controlling electrode metal transfer at simultaneous impact of welding current source and pulsed feed mechanism with different operating algorithms on electrode wire melting were studied in [21]. Pulsed-feed mechanism with one-sided grips and electric magnets allowing synchronization of wire feed pulses with mains frequency were used for experimental studies [22].

It is found that the current pulse should always precede the pulsed movement of electrode wire. At optimum synchronization parameters controllable transfer of electrode metal is achieved in welding with short-circuiting of the arc gap, and in a number of cases controllable transfer without the short-circuiting phase with less than 3 % electrode metal losses, is possible. Use of pulsed feed allows control of welded joint formation (Figure 6).

On the whole, the advantages of application of a combined pulsed impact of welding current source and electrode wire feed mechanism are as follows:

● range of stable welding modes, possibility of controlling the geometrical characteristics of the welded joint and deposited layer are expanded;

● high level of control of electrode metal transfer is achieved, both in welding with short-circuiting and without it;

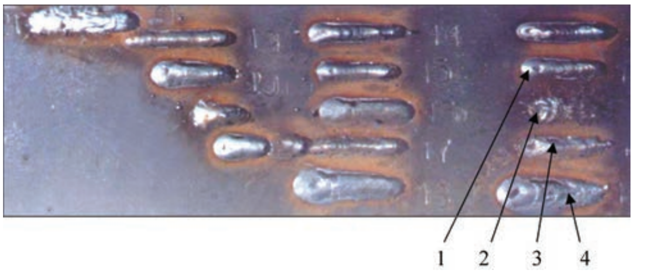

Figure 6. Beads deposited at different parameters of the process of control of electrode metal transfer due to combined effect of pulses of current source and electrode wire feed mechanism (*1–4* — ineffective pulse synchronization)

● operational conditions of pulsed feed mechanisms are facilitated, as there is no need to form pulses with high values of accelerations of wire movement in the pulse;

● problems of weld metal structuring are solved at a rather high level with reduction of crystal dimensions and respective increase of mechanical properties of the item being welded or surfaced;

● electrode metal drop stays in the zone of impact of high temperatures for a shorter time, and alloying element loss is lowered, accordingly.

The problem of combined impact on metal transfer was solved at the E.O.Paton Electric Welding Institute at development of a new method of arc mechanized and automatic welding with dosed feed of electrode wire. Here, arc feedbacks are used for feeding the current pulse from the power source at any time at the stage of impact of electrode wire feed pulse. This is a promising direction, which can be accepted in welding and surfacing of various steels and aluminium alloys, and with application of both solid and flux-cored wires.

Research work is carried on in the direction related to a combined pulsed impact from welding current source and system of shielding gas pulsed feed. Some research results [18] contain materials on two welding processes: with alternating feed of several kinds of shielding gases and pulsed-arc process with pulsed feed of shielding gas.

Combined impact on the welding process by the second method ensures formation of the weld with a high quality of the surface and has a positive influence on weld metal structure, improving its mechanical properties.

Considering the inertia of the gas feed system, complexity of selection of gas equipment, as well as certain problems in ensuring synchronization of operation of the welding current source and shielding gas feed system can be regarded as the common drawbacks of the above ingenious welding methods with a combination of pulsed impact of shielding gas and welding current source.

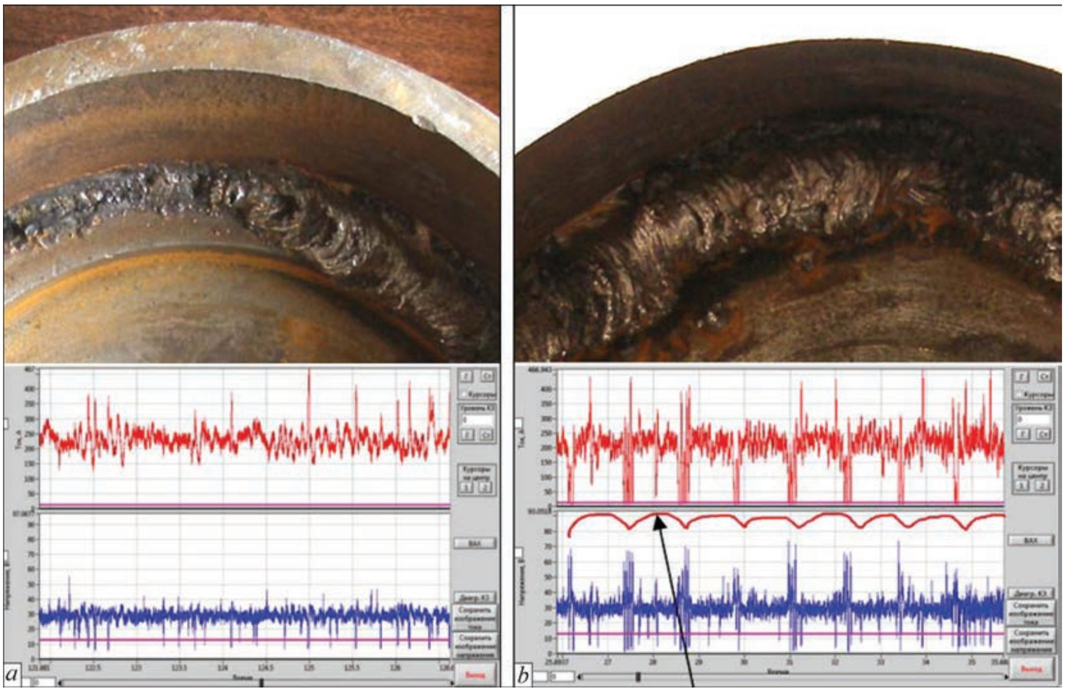

Figure 7. Appearance of welds and oscillograms of current and voltage in welding-in plugs: *a* — regular process; *b* — torch oscillations (arrow shows current supply oscillation)

Next, we will consider promising developments on control of formation of the welded joint and deposited layer, using technical means, which, as a rule, are not included into the list of the main systems of welding-surfacing equipment, but are used for a considerable increase of their effectiveness. In particular, we should note the fact that different methods of influencing the weld pool formation using technical means, realizing various pulsed or oscillatory impact, differ by the frequency spectrum of their effective impact, as part of them influences the overall volume of molten metal, and another part acts locally.

Oscillations of the torch of automated welding equipment are performed, mainly, in order to fill wide grooves or increase the deposited metal width [23]. The frequency of these oscillations is usually equal to 0.2–2.0 Hz, and it is limited by inertia properties of the torch oscillatory system. The concomitant result of operation of torch oscillators is their impact on the structure of weld metal and deposited layer. It is found that transverse oscillations of the arc allow reducing the dendritic heterogeneity of weld metal and width of heat-affected zone that promotes improvement of mechanical properties of the weld and deposited layer [24]. Transverse oscillations of the torch movement can be realized by two main methods, namely swinging of the torch or parallel displacements of the carriage with the welding torch attached to it. In the first case, the electrode wire extension is changed that also influences formation of the welded joint or deposited bead.

An example of original and effective application of torch oscillations to solve the problem of welding over a larger gap is development of a device for welding-in plugs inside a pipe of 157 mm diameter with 10 mm wall thickness by wet method in a liquid medium at more than 200 m depth, performed by PWI [25]. Torch oscillations are realized from the electrode wire feed mechanism by special eccentric mechanism, allowing adjustment of oscillation amplitude. Special features and results of welding with application of the developed torch oscillator are illustrated by Figure 7.

In particular, the oscillogram (Figure 7, *b*) clearly shows the arc process current pulses, resulting from the change of electrode extension in the extreme points of oscillations. Such pulses are close to current pulses in welding with mode modulation and have the respective effect on weld characteristics.

Let us briefly consider the known systems of welding process control and formation of welded joint and deposited layer, using the magnetic fields [26]. Quite often the complexity of application of these engineering systems limits their mounting in systems of automatic equipment for welding and surfacing. In a number of cases, however, their use is necessary and has prospects for application in the future.

The effectiveness of controlling the above processes, using external pulsed magnetic fields was proved experimentally [27]. It is found that application of axial pulsed fields allows not only controlling the frequency of transfer and dimensions of electrode metal drops, but also changing the transfer type, for instance, from globular to jet transfer. Losses of electrode wire metal for spattering become smaller with increase of electromagnetic pulse frequency. Con-

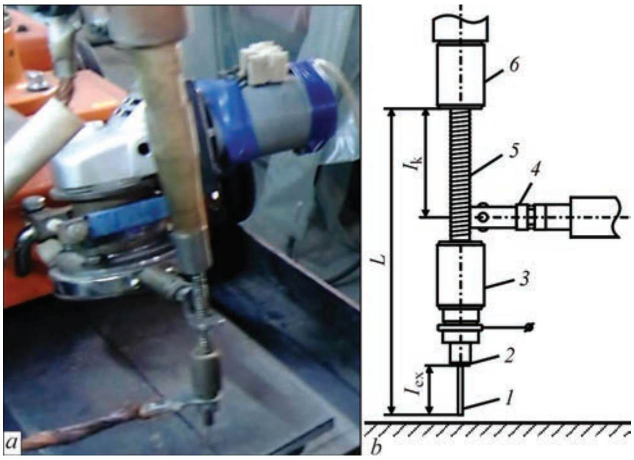

Figure 8. General view (*a*) and scheme of inducing high-frequency oscillations of electrode wire (*b*): *1* — electrode wire; *2* — current supply; *3*, *6* — current supply fastening components; *4* — vibration component of mechanical oscillator; *5* — flexible spiral; *L* — length of mobile (elastically fastened) part of current supply with the electrode; l_k — arm of application of the force from mechanical oscillator; l_{ex} — electrode extension

trolled electromagnetic field, acting on weld pool liquid metal enables changing the weld geometry and thereby serves as a means of increasing the hot cracking resistance of the metal.

In order to obtain the required structure and geometry of the deposited layer at surfacing operations, different methods are used, which are based on adjustment of the heat input into the processed metal and physicochemical impact on the arc and weld pool [13, 28]. Control of the structure ensures the required mechanical characteristics of the deposit metal, and control of penetration dimensions promotes increase of surfacing process efficiency and reducing the fraction of base metal in the deposited layer.

Work associated with development of high-frequency direct (without additional converters) oscillator of electrode wire using new engineering means and original application of a number of physical effects is aimed at solving this range of problems [29, 30]. Mechanical generator of high-frequency electrode oscillations provides a combined impact, at which the conditions of simultaneous control of metal transfer through the arc and of deposited layer geometry at automatic submerged-arc surfacing are realized.

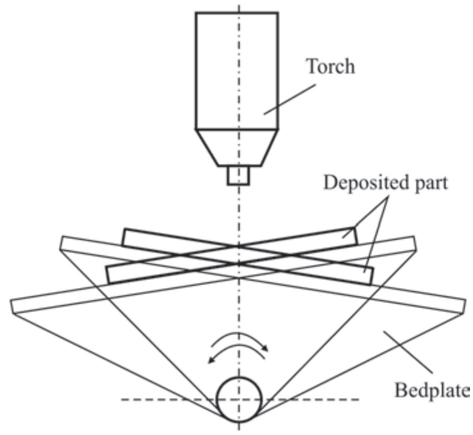

Figure 9. Scheme of weld pool harmonic oscillations

The generator features the capability of creating high-frequency electrode oscillations, consisting of two harmonics with the required values of frequency and amplitude. The harmonics with a higher frequency provides an increase of electrode melting stability, and that with a lower frequency, but greater amplitude, promotes increase of deposited bead width and reduction of base metal penetration depth. Improved design of mechanical oscillator (Figure 8), allows, unlike previous developments, inducing electrode oscillations along or across the deposited bead and adjusting their amplitude, irrespective of the length of electrode extension, required by the technology [31].

Mounting the mechanical oscillator on standard equipment for automatic welding allows achieving the following results, depending on amplitude-frequency characteristics of induced oscillations:

- ensuring microdrop transfer of metal as a result of gravitation-capillary dispersion;
- controlling metal transfer;
- controlling deposited layer geometry due to heat flux dispersion.

Possibilities of combined control of surfacing process characteristics using high-frequency transverse mechanical oscillations of the electrode can be assessed by the results presented in Table 1 [32]. Oscillations with frequencies close to the resonance ones have an especially significant effect.

Considering the good technological results (metal structure, geometrical parameters of deposited lay-

Table 1. Influence of the frequency of electrode oscillations on surfacing characteristics

Oscillation frequency, Hz	0	680 (resonance)	1295	3820 (resonance)	5800
Deposited bead macrosection		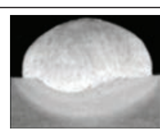	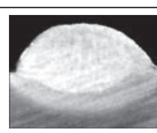	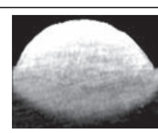	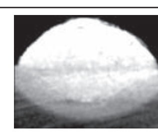
Base metal share in deposited bead	0.36	0.13	0.30	0.22	0.25
Electrode melting coefficient, g/(A·h)	15.0–15,2 15.1	16.5–17.2 16.9	15.1–15.5 15.3	18.0–18.9 18.6	15.8–16.3 161.1

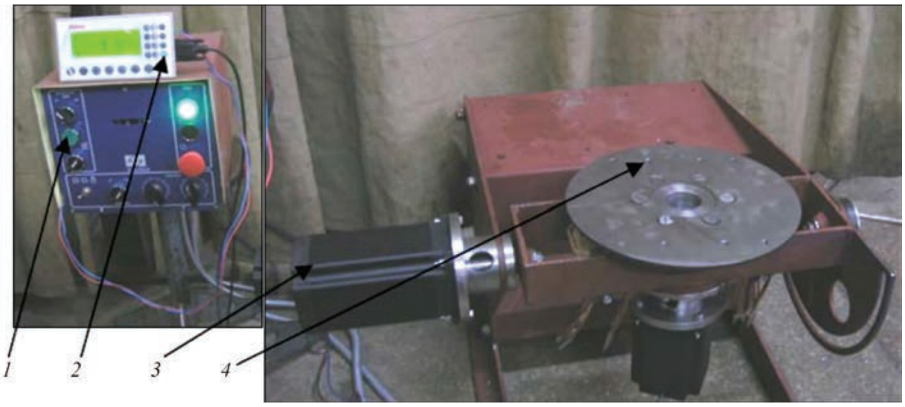

Figure 10. Unit for transverse oscillations of the surfaced item: *1* — control module; *2* — oscillation parameter regulator; *3* — oscillation drive electric motor; *4* — work table

ers), produced at surfacing with high-frequency controlled oscillations of electrode wire, we believe it is expedient to apply them also in other processes using a consumable electrode.

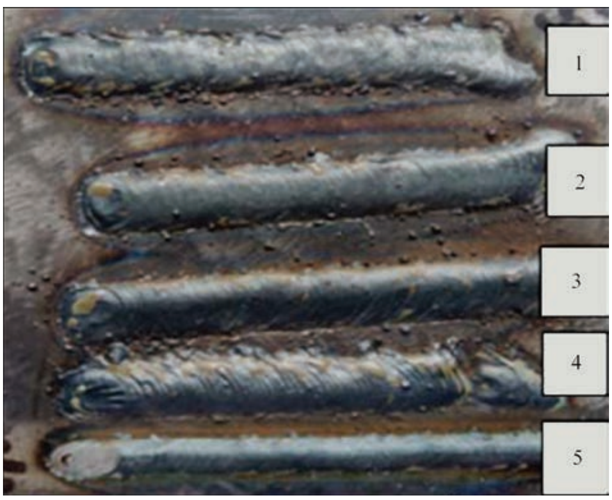

Figure 11. Beads deposited with oscillations of unit work table with frequency, Hz: 1 — 4.67; 2 — 4.0; 3 — 3.0; 4 — 2.0; 5 — without oscillations

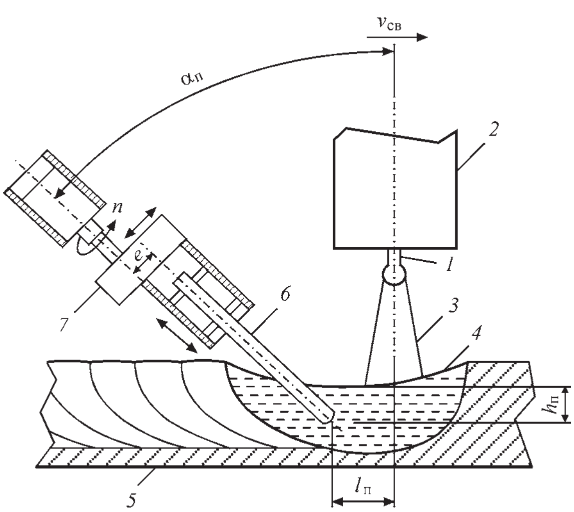

Figure 12. Scheme of welding-surfacing process using mechanical vibrator of the weld pool: *1* — electrode wire; *2* — torch; *3* — welding arc; *4* — weld pool; *5* — item; *6* — vibrator waveguide; *7* — generator; *n* — waveguide rotation frequency; *e* — half-amplitude of waveguide oscillations

PWI is working on application of other oscillatory processes, also at lower frequency. It was noted above that weld pool vibrations lead to a change of the structure of weld metal or deposited layer. Plane or plane-parallel movements of vibrators in the form of vibrating tables of different design are usually applied to excite oscillations of molten metal of the pool.

Based on achievements of modern mechanotronics with computerized control of drive systems, new engineering solutions and techniques are proposed for making an impact on the weld pool with controlled oscillations parameters, such as frequency, amplitude, and shape. Figure 9 gives the scheme of inducing oscillations of the surfaced item, which are transverse relative to the weld, Figure 10 is a fragment of an experimental unit, and Figure 11 shows the deposited bead appearance.

A step motor with gearless transmission of movement directly to the work table was used as the drive for transverse oscillations. The unit was applied to perform experimental verification of the developed mathematical model of the surfacing process with item oscillations [33], which showed satisfactory convergence of results (Table 2).

An essential increase of the deposited bead width at accordingly reduced height as a result of weld pool oscillations is indicative of higher efficiency of this surfacing process, compared to the conventional

Table 2. Results of checking the adequacy of the mathematical model

Experiment number	Oscillation frequency, Hz	Deposited bead width, mm		Error, %
		calculation	experiment	
1	4.67	15.4	14.0	10
2	4.0	13.6	13.0	4.6
3	3.0	12.0	14.0	14.3
4	2.0	11	14.0	21.4
5	0	–	8.0	–

method, performed under the conditions of stationarity of the surfaced item. Moreover, improved structure of the deposited metal provides higher service characteristics of the surface layer [34].

Results of the performed studies give ground to believe that the technology with item oscillations should be developed in the direction of application of other parameters of the oscillatory process. The considered surfacing process can be used at manufacture or repair of parts of agricultural machinery, components of stamping or metal-cutting tools [34], etc.

Recently, a method of welding-surfacing with addition of mechanical oscillations into the weld pool, using an additional vibrator, was proposed (Figure 12).

When performing the welding or surfacing processes, the vibrator waveguide, immersed into the liquid metal of the weld pool behind the arc, moves together with it at speed V_w. The position of the waveguide working end (distance from welding arc l_{im}, immersion depth h_{im}, angle of inclination α_{im}) is determined by weld pool dimensions, and oscillatory process parameters (frequency and amplitude) are set by oscillatory mechanism generator. The effect of mechanical mixing of the weld pool consists in structuring the deposited metal and, as a consequence, in improvement of mechanical properties of the joint or deposited layer.

Conclusions

1. At great diversity of methods and techniques of controlling the welded joint operating properties, correct selection of welding method and modes is the determinant factor to produce a joint with the required mechanical and special characteristics. However, a versatile welding process, which, allowing for various external conditions of conducting the process, ensures absolutely equal strength and quality of the joints, has not been developed yet.

2. The main directions of effective improvement of welded joint quality are rational application of the methods of pulsed and vibrational impact on the welding process, using welding equipment systems proper, as well as auxiliary systems, allowing control of the deposited metal properties.

3. The results of mechanical impact on the characteristics of welded joint or deposited layer can be significantly enhanced by application of different methods of combined impact, selecting the most effective of them, taking into account their cost-effectiveness.

1. Paton, B.E. (2003) Current trends of research and development in the field of welding and strength of structures. *The Paton Welding J.*, **10–11**, 5–11.
2. Makovetskaya, O.K. (2012) Main tendencies at the market of welding technologies in 2008–2011 and forecast of its development (Review). *Ibid.*, **6**, 32–38.
3. Mironov, S. (2003) Inverter power sources for arc welding. Svarochn. Proizvodstvo, **4**, 41–43 [in Russian].
4. Saraev, Yu.N., Bezborodov, V.P., Grigorieva, A.A. et al. (2015) Control of structure and properties of welded joints of critical technical systems by methods of adaptive pulsed arc welding. *Voprosy Materialovedeniya*, **1**, 127–131 [in Russian].
5. Paton, B.E., Lebedev, V.A., Poloskov, S.I., Lendel, I.V. (2013) Application of mechanical pulses for control of processes of automatic and mechanized consumable electrode welding. *Svarka i Diagnostika*, **6**, 16–20 [in Russian].
6. Paton, B.E., Lebedev, V.A., Pichak, V.G., Poloskov, S.I. (2009) Evolution of systems of pulsed wire feed for welding and surfacing. *Ibid.*, **3**, 46–51 [in Russian].
7. Maksimov, S.Yu., Lebedev, V.A., Lendel, I.V. (2015) Sealing of heat exchanger pipes by «wet» welding at depth of 200 m. *Voprosy Materialovedeniya*, **1**, 199–204 [in Russian].
8. Lebedev, V.A., Dragan, S.V., Trunin, K.K. (2016) Automatic submerged-arc welding with pulsed electrode wire feed by step motor. *Svarochn. Proizvodstvo*, **2**, 27–34 [in Russian].
9. Lebedev, V.A., Guly, M.V. (2014) Fast valve electric drive for mechanized arc welding equipment. *Mekhatronika. Avtomatizatsiya. Upravlenie*, **6**, 47–51 [in Russian].
10. Lebedev, V.A., Zhuk, G.V. (2017) Control of electrode metal transfer based on pulse algorithms of systems functioning with dosed electrode wire feed during mechanized arc welding. *Tyazholoe Mashinostroenie*, **6**, 27–32 [in Russian].
11. Lebedev, V.A. (2016) Mechanized synergic welding with pulsed electrode wire feed. *Naukoyomkie Tekhnologii v Mashinostroenii*, **2**, 19–24 [in Russian].
12. Lebedev, V., Reisgen, U., Lendel, I. (2016) Study of technological opportunities of GMA welding and surfacing with pulse electrode wire feed. *Welding in the World, February*, 9–14.
13. Paton, B.E., Lebedev, V.A., Zhuk, G.V., Dragan, S.V. (2017) Mechanical pulse and vibration effects in equipment and technologies of mechanized welding and surfacing. In: *Proc. of 16th Intern. Sci.-Techn. Conf. on Vibrations in Engineering and Technologies (Ukraine, Vinnytsya, 26–27 October 2017)*, 10–16.
14. Lebedev, V.A., Zhuk, G.V. (2017) Solution of problems of mechanized welding of thin sheet aluminium alloys based on application of programmable feed mechanism electric drives. *Montazhnye i Spec. Raboty v Stroitelstve*, **9**, 21–24 [in Russian].
15. Denisov, L.S., Barsukov, I.V., Apolonik, S.A. (1998) Development and analysis of equipment for welding with alternate gas supply. In: *Proc. of Sci. Conf. on Advanced Engineering and Technology of Machine Building, Instrument Making and Welding Production*. Kiev, Vol. 4, 310–313 [in Russian].
16. Tarasov, N.M., Tulin, V.M. (1982) Control of electrode metal transfer by short-time increase of the rate of shielding gas flow. *Svarochn. Proizvodstvo*, **8**, 23–25 [in Russian].
17. Zhernosekov, A.M. (2012) Tendencies in development of control of metal transfer processes in shielding gases (Review). *The Paton Welding J.*, **1**, 29–33.
18. Zhernosekov, A.M., Sidorets, V.N., Shevchuk, S.A. (2013) Combined pulsed action of shielding gases and welding current in consumable electrode welding. *Svarochn. Proizvodstvo*, **12**, 9–13 [in Russian].
19. Kitsch, M. (2006) Metall-Inert Gas Schweissen von Aluminium mitgepulster Schutzgaszufuhr. *Schweissen und Schneiden*, 58(**1**), 19–22 [in German].

20. Chinakhov, D.A. (2009) Effect of double-jet gas shielding on performance of welded joints on GL-E36 shipbuilding steel. *The Paton Welding J*., **9**, 29–32.
21. Paton, B.E., Lebedev, V.A., Mikitin, Ya.I. (2006) Method of combined control of electrode metal transfer process in mechanized arc welding. *Svarochn. Proizvodstvo*, **8**, 27–32 [in Russian].
22. Fedko, V.T., Solodsky, S.A., Kryukov, A.V. (2004) Pulsed welding wire feed with controlled transfer of electrode metal. In: *Proc. of Sci.-Techn. Conf. on Science-Education-Production. Nizhny Tagil*, Vol. 2, 100–103 [in Russian].
23. Makara, A.M., Kushnerenko, B.N. (1967) Transverse arc movements as the factor of improvement of structure and properties of welded joints. *Avtomatich. Svarka*, **1**, 31–35 [in Russian].
24. Boldyrev, A.M. (1976) On mechanism of formation of weld metal structure at low-frequency oscillations in weld pool. *Svarochn. Proizvodstvo*, **2**, 1–3 [in Russian].
25. Lebedev, V.A. (2019) Automatic underwater welding in increased gap. *Remont. Vosstanovlenie. Modernizatsiya*, **3**, 16–20 [in Russian].
26. Sidorenko, P.Yu., Ryzhov, R.N. (2010) Application of pulse electromagnetic effects to control the process of electrode metal transfer in arc welding. *The Paton Welding J*., **6**, 44–45.
27. Ryzhov, R.N. (2007) Influence of pulse electromagnetic actions on formation and solidification of welds. *Ibid*., **2**, 49–50.
28. Lebedev, V.A., Tishchenko, V.A., Loj, S.A. (2019) Technical-technological effects in mechanized surfacing with modulation of modes. In: *Proc. of 19th Int. Sci. and Techn. Seminar on Modern Question of Production and Repair in Industry and Transport (Slovak Republik, Kosice, February 18–23)*, 106–109.
29. Goloborodko, Zh.G., Dragan, S.V., Simutenkov, I.V. (2013) Automatic submerged-arc surfacing of structural steels with transverse high-frequency movements of electrode. *The Paton Welding J*., **6**, 34–37.
30. Simutenkov, I.V., Dragan, S.V., Yaros, Yu.A. (2014) Stability of arc process in automatic submerged-arc surfacing with high-frequency electrode oscillations. *Zb. Nauk. Prats NUK*, **4**, 43–48 [in Russian].
31. Simutenkov, I.V., Yaros, Yu.O., Dragan, S.V., Gal, A.F. (2015) *Device for automatic submerged-arc surfacing*. Ukraine Pat. 10288, Int. Cl. B23K 9/00, No. u 201504821 [in Ukrainian].
32. Dragan, S.V., Simutenkov, I.V., Ignatenkov, O.V. (2012) Procedure for determination of parameters of electrode high-frequency mechanical oscillations in automatic submergedarc surfacing. *Visnyk Derzh. Mashynobudivnoi Akademii*, 3(**28**), 124–129 [in Russian].
33. Lebedev, V.A., Novikov, S.V., Zhuk, G.V. et al. (2018) Mathematical modeling of arc surfacing process with controlled variations of arc gap length. *Tekhnologiya Mashinostroyeniya*, **3**, 56–62 [in Russian].
34. Lebedev, V.A., Solomichuk, T.G., Novykov, S.V. (2019) Study if a welding harmonic oscillation influences on the welded metal hardness and weld bead width. *J. of Eng. Sci*., **6**, 16–21.

Received 21.06.2019

Interview with Yu. A. Nikityuk, Director of SPC VISP

Yuriy Anatolievich, the title of your Company SPC VISP has association for many welders with the title of known enough in the USSR Vsesoyuznogo Instituta Svarochnogo Proizvodstva VISP (All-Union Institute of Welding Engineering), which was liquidated at the beginning of the 1990th and was reorganized into Ukrainian Design-Technological Institute of Welding Engineering (UkrISP). Is there any connection? What are the main directions of activity of your Company?

Yes, there is some connection. As it is well known, VISP and later on UkrISP were the main is the Soviet Union and Ukraine developers of mechanical welding equipment, means of complex mechanization and automation of welding engineering, units for deposition of thermal coatings. In the process of development of market economy UkrISP was unable to adapt to new challenges and was liquidated in 2004. Part of the workers of the Institute started another activity and part of the professional tried to continue work in welding sphere.

These people made a core of our company, which was registered in 2007. As time passed younger specialists having experience of work in other organizations joined our Company.

The main thematic scope of works typical for VISP and UrkISP was preserved. Giving credit to contribution of VISP into development of welding engineering and activity of professionals, many of whom was our teachers, we preserved historical memory about it in the title of Company.

Your company for sufficiently long time has been working under market economy conditions. What are the main constituents of successful activity of SPC VISP today in a difficult period of country existence? What are the problems?

First of all I would like to outline the complex approach to work, which covers the cycle: «designing–manufacture–timely delivery of equipment–adjustment–training of customer specialists–service».

In a unified manner the work is organized in a subdivision of product engineers, mechanical designers, electricians, electronic engineers, programmers and setup men. These are competent specialists and wonderful people, which always assist each other.

Winning a tender for supply of equipment is only possible under condition that the Company has specific history of successful development of competitive products. For example, last year we manufactured and implemented a unique machine for bead deposition at one of the subdivisions of Metinvest Company in Mariupol. This year we have won a tender for development, manufacture and supply at this enterprise of three more serious units. As for problems there are lots of them. One of them is financing of orders. Most of them are fulfilled using bank credits without prepayment of works by customer. And everybody knows what is a lending policy in our country. We risk. The staff problem has become more acute with rise of volumes. No one in the country really tries to find a radical and systematic solution.

Many people say that the industry research institutes almost have disappeared in the country. And what is the main reason? There are no government-wide mechanisms allowing regulation of this problem. Now to talk about renovation of industry research institutes in my opinion is not prospective. From my point of view, the industry research institutes should give way to innovation mobile complex companies having corresponding support of government including due to creation of expert-credit agency.

Yuriy Anatolievich, please, tell about your recent developments. What are the perspectives of development of your Company?

Let me give several examples of works fulfilled by us in the recent years. We have longstanding partnership with enterprises of «Ukrzaliznytsya». We manufactured for them equipment for induction heating of surfaces for their quenching, leveling and fitting. There was also created a series of units for induction surfacing of flat surfaces (friction plates, automatic coupling devices, etc.). A unit for thermal restoration of surfaces of crankshafts was designed and manufactured. There was developed and manufactured a series of automatic machines for hardfacing of different spare parts of railway transport (rolls, tails, center bowls, bolsters, side frames of railway bogies).

For mining and smelting enterprises we have developed surfacing units, technology and equipment for vibration treatment of welded structures for the purpose of reduction of residual stresses.

A unique manipulator of welded structures of 10 tones load-carrying capacity was designed and manufactured for Kremenchug plant «Kreddormash». By feedback from production men, it considerably improved welders' labor conditions of work and increased productivity.

An equipped automatic line, automatic load-transfer devices and dosing devices applicable to manufacture of cartridges of self-rescue devices were delivered into Turkey.

SPC VISP has active cooperation with enterprises of defense complex of the country. As for perspectives of development of SPC VISP we see them in intensification of works on entry into foreign markets with supply of our traditional equipment as well as brand new equipment and technologies, which we develop together with researchers of the E.O. Paton Electric Welding Institute, V. Bakul Institute for Superhard Materials and other institutes of the NAS of Ukraine.

Editorial board of journal

https://doi.org/10.15407/tpwj2019.08.05

PROSPECTS FOR APPLICATION OF ELECTROMAGNETIC FIELDS IN WELDING AND RELATED PROCESSES

L.M. LOBANOV[1], **M.O. PASHCHIN**[1], **O.V. CHERKASHYN**[1], **O.L. MIKHODUI**[1], **I.P. KONDRATENKO**[2] and **O.M. SIZONENKO**[3]

[1]E.O. Paton Electric Welding Institute of the NAS of Ukraine
11 Kazimir Malevich Str., 03150, Kyiv, Ukraine. E-mail: office@paton.kiev.ua
[2]Institute of Electrodynamics of the NAS of Ukraine
56 Peremogy Prosp., 03057, Kyiv, Ukraine. E-mail: ied1@ied.org.ua
[3]Institute of Pulse Processes and Technologies of the NAS of Ukraine
43a Bohoyavlenskyi Prosp., 54018, Mykolayiv, Ukraine. E-mail: office.iip@nas.gov.ua

Development and introduction of new energy-saving technologies meets the modern demands of Ukraine. In the paper background, current state and directions of development of investigations of the influence of electromagnetic fields on mechanical properties and stressed state of metallic materials and welded joints are considered. The possibility of their application for control of the stressed state, evolution of the structure, properties, and extension of the life of welded structures is shown. 49 Ref.

Keywords: *electromagnetic treatment technologies, electromagnetic fields, welded joints, structures, metallic materials, pulsed spark and current discharges, electroplastic effect, stress-strain state, nanodispersed modifiers*

Development of high-tech industries stimulates increase of the requirements to metallic materials, the set of their main and special properties, and methods of their permanent joining.

Considering the current problems of Ukraine, a promising reserve for improving the state of its industry is development and introduction of new energy-saving technologies. Increase of strength, ductility and other mechanical characteristics can be achieved through combined treatment of metallic materials by pulsed electric current (PEC) and electromagnetic field (EMF) of a high intensity during a short period of time. Results of studying the electrophysical processes running in metallic materials under EMF impact give reason to think that the principles of controlling the mechanical properties with EMF application are an alternative to traditional technologies, at the same time having a number of advantages such as energy effectiveness and adaptability to fabrication.

The purpose of the paper is analysis of development, current state and directions of solving the problem of EMF effect on mechanical characteristics and stressed state of metallic materials and welded joints. The question of controlling the structure and mechanical properties of liquid metal with application of EMF in the welding process, that is a separate (and rather urgent) issue of engineering practice [1], is not considered in this work.

Prospects for application of pulsed spark and current discharges for welded joint treatment. Methods of improvement of mechanical characteristics of metals and alloys include different kinds of their PEC and EMF treatment [2]. High-voltage pulsed discharge in liquid is used in industrial technology as a source of dynamic pressure, under the impact of which the treated materials can fail, be formed, and can change their structure and mechanical characteristics. Electrohydropulse treatment (EHPT) consists in the action of mechanical loading on the object, which is initiated by high-voltage pulsed discharge of electric current in the current-conducting medium (water). There are numerous results that confirm the possibility of EHPT application for lowering the residual technological stresses. Investigations of EHPT effect on the stress-strain state of welded joints showed that it reduces tensile stresses in welded structures to 90 % due to activation of dislocation processes. By the effectiveness of lowering the level of residual welding stresses, EHPT is comparable to high-temperature tempering [3].

At the same time, EHPT method has a number of disadvantages, which may include the need to apply technological tanks with water, having a high metal content, which are characterized by a rather complex structure, because of higher rigidity, so as to resist the compression-tension waves, initiated by electrohydraulic effect.

At the same time, EHPT is rational for application in fabrication of large-sized welded products, for instance, cast-welded bed plates. Over the recent years, there was no further development of EHPT in Ukraine that is obvious from absence of publications, and is related to reduction of the volumes of heavy machine-building, but it has good prospects, provided the growth rate of local metal structure fabrication is restored.

Electric spark treatment, widely used in machine-building technology, can be regarded as a technique close to EHPT by the method of its realization (but not by its purpose). At electric spark treatment a PEC discharge is initiated on the surface of the billet that is part of the discharge circuit and is located in the dielectric liquid (kerosene, oil). During this discharge, heat is generated that is consumed for melting, partial evaporation and explosive release of treated metal particles. The similarity between electric spark treatment and EHPT consists in that during their performance the current discharge runs in the liquid medium, and the discharge energy is provided by a capacitive storage. While EHPT realization requires a current-conducting medium, electric spark treatment requires a dielectric one. This method is applied at calibration, piercing holes and dies, cutting and grinding. At the same time, realization of electric erosion processes without application of current-conducting and dielectric environments markedly widens the possibilities of application of electric spark treatment of large-sized metal structures, for instance, for strengthening the cutting surfaces of agricultural machinery parts [4]. The capabilities of this method allow realization of the processes of nanostructuring of the surface layers of structural steels and deposited surfaces, aimed at improvement of their tribological characteristics.

PEC treatment is used for strengthening the surfaces of friction contact, which is determined by interaction of wheel-rail pair [5]. The principle of rail strengthening consists in electric spark deposition of coating of a discrete type with regions, having different characteristics of hardness, impact toughness and friction coefficients. Discrete coating of the rail contact surface was formed with application of electric spark treatment. One of the advantages of a discrete coating is its discontinuity that provides a minimum level of residual stresses, compared to a continuous coating. Coating was deposited by moving an electrode from different metallic materials in the form of a disc over the surface being treated. PEC of specified duration and configuration was initiated between the electrode and the rail that provided a discrete metal transfer from the electrode to the rail. Application of the method ensured high tribological characteristics of both the rail contact surface, and wheel-rail pair [6]. Electric spark structure formation is promising from the viewpoint of its realization in the case of welded joints. Development of electric pulse nanostructuring methods, as well as the implantation proper of nanostructures in the specified regions of welded joint cross-section appears to be a promising method of improvement of metal structure service life.

Investigation of electroplastic effect that is the base for promising technologies of welded joint treatment. Investigations in the field of physics of solids that have been conducted since 1960s, allowed establishing the phenomenon of an abrupt increase of ductility and lowering of metal resistance to deformation, due to simultaneous impact of active mechanical loading and high-density PEC. This phenomenon was called the electroplasticity effect (EPE), and the deformation initiated by EPE — the electroplastic deformation (EPD). EPE opened up new possibilities, both for the technologies of mechanical forming of metals and alloys, including refractory materials [7], and for regulation of their stressed state [8]. In 1925 Heckmann, studying the properties of crystals, expressed the idea about the interrelation between their mechanical, electric and thermal characteristics. As electrons are the main «carriers» of electric properties in metals, and the connection between the atoms is carried out by electrostatic forces, then influencing the energy spectrum of free electrons leads to a change of mechanical properties of metals [9]. The question of acceleration of the dislocation movement under the impact of a directed electron flow was studied, and it was shown that such acceleration can take place provided the electron speed is higher than that of the dislocations. It was found that PEC impact causes a jump, lowering the magnitude of the deforming force, and this phenomenon was observed only in the region of elastic-plastic deformations.

The main purpose of the majority of investigations conducted in 1970–1980s consisted in studying EPE mechanism. This became a stimulus for investigation of the influence of side effects: thermal and mechanical (ponderomotive) action of PEC, as well as the impact of nonuniformity of current density distribution over the sample cross-section (skin-effect) on lowering of metal resistance to deformation.

Here, for the considered materials and PEC parameters in the above-mentioned works the skin-layer thickness exceed the sample diameter, i.e. the skin effect was practically absent.

The results of studying the influence of pinch-effect on EPE realization showed that the latter is determined by intensity H of the magnetic field and magnetic permeability of the material, as well as the sample surface area [10]. H value directly depends on current value and is inversely dependent on sample cross-section. Pressure P develops over the sample surface, as a result of pinch-effect, which is determined by the following expression:

$$P = 0.5\mu_0 H^2, \quad (1)$$

where μ_0 is the absolute magnetic permeability of the material.

Evaluation of the impact of pinch-effect on lowering of sample resistance to deformation showed that its contribution is not more than 0.4–6.0 % of the yield limit of metallic materials. This confirms its small influence on EPD [11].

When PEC flows through the metal, its temperature is increased due to Joule heating. During PEC impact increase of internal energy in the material is determined by pulse duration, current amplitude and magnitude of electric resistance. Thermal energy dissipation in the metal can both lower its resistance to deformation at the moment of PEC impact as a result of thermal strength loss, and cause the change of mechanical characteristics [12].

It should be noted that the main focus of investigations of electric current impact on plastic deformation of metals, was both on establishing the physical essence of the phenomena, and on technological applications of EPE in engineering practice. Investigations of EPE physical model were performed for a large number of metals and alloys of different classes, in different modes of PEC treatment performance, and kinds of loading in a broad temperature range. At present there exist a number of interpretations and descriptions of EPD and EPE mechanisms. The most well-known is the dislocation model of EPE, which is based on electron-dislocation interaction that leads to dislocation disruption from the stoppers and their capture by mobile conduction electrons. However, in [13], another EPE interpretation is proposed. Taken as its base is the gradient-dislocation model, where the chemical potential gradient φ (φ is the minimum energy, required for breaking the electron bonds with crystal lattice atoms) of vacancies in polycrystalline metallic materials is the determinant factor for dislocation movement in pulsed electromagnetic field (PEMF). Dislocation and gradient-dislocation physical models allow clarifying only the increase of ductile properties of metals. A gradient-diffusion physical model was proposed in [14], which provides clarification of the main effects, manifested in metals at PEC treatment. According to this model, at PEC impact due to the concentration of force lines of the electromagnetic field, not only grad φ along the defect boundaries, but also localized fields of thermoelastic stresses form on such structure defects as micropores, cracks and delaminations.

Concurrent heating at PEC treatment of metal samples in the thermoelastic temperature region leads to reduction of the level of initial tensile stresses [15]. At similar heating without PEC application, the level of stresses in the metal after cooling to room temperature returned to its initial level. Here PEC effect (without taking into account the Joule heating) decreased with increase of the duration of an individual pulse, and at multiple PEC treatment material resistance to deformation increased with increase of the number of current discharges. In terms of electron-dislocation interaction, this is attributed to the fact that at one-time PEC impact a single pulse acts on the material, which has considerable dislocation potential. In multiple impact modes the previous pulses take part of the dislocations out of the relaxation processes, and material reaction to PEC impact is weakened. Change of PEC polarity also affects EPE manifestation. In [16] it is shown that at the same amount of electricity and amplitude of PEC, passing through the loaded sample, bipolar pulses cause smaller relaxation (jump) of stresses that unipolar ones. This is caused by that successive PEC of different polarity, while initiating the movement of dislocations in opposite directions, counteract each other. Hence, their resulting impact is smaller, than that with unipolar PEC. PEC impact on metal ductility is manifested in the region of plastic deformation that is accompanied by relieving of the deformation force, whereas EPE is not observed in the elastic deformation region. In [17] a method for determination of part of the energy of electric current pulse which is directly consumed for plastic deformation work was proposed, based on the mechanism of electroplastic deformation. This allows determination of the stress of the start of plastic flow initiated by PEC, for materials of different classes in the temperature range of 293–4.2 K.

At this moment EPE regularities have been studied in greatest detail, in keeping with the requirements of engineering practice for finding the most effective means to increase the ductility of metallic materials, applied in industry. To reduce the thermal impact of PEC and magnetic field, one of the directions of EPE investigations was their performance at cryogenic temperatures [18] that is important in the scientific and applied aspects. The scientific interest is due to the fact that with temperature lowering from 293 K to values, close to the cryogenic ones, PEC impact becomes stronger, as at such temperatures the electron viscosity (because of absence of Joule heat) becomes the main source of lowering of dislocation mobility that leads to changes in mechanical properties of metallic materials [19]. Applied aspect is associated with development of high-energy products, where the superconductivity effect is used (cryoturbogenerators, thermonuclear reactors). PEC specific impact on EPE realization at cryogenic temperatures is manifested in that the magnitude of stress jump under the action of the current discharge increases with lowering of testing temperature, increase of PEC amplitude and its duration. PEC flowing in the region of elastic stresses gives rise to residual deformation at stresses, which, depending on testing temperature, pulse parameters and material class, are 10–35 % smaller than its yield limit. Here, the above changes become greater with lowering of investigation temperature from 293 to 4.2 K, while PEC amplitude is a more potent factor than its duration [20].

Methods of treatment of metallic materials and welded joints by electromagnetic fields. Proceeding from the results of investigations of electromagnetic impact of PEC on mechanical characteristics of metals and alloys, we developed metal treatment technologies. Changing PEC and PEMF duration and energy, it is possible to manufacture products and parts with specified performance, due to activation of a spectrum of dislocation, phase and other physical processes. Impact of PEC and PEMF of different duration and configuration which is realized in different metal treatment technologies, causes structural changes in metals and alloys [21], that affect their characteristics. An increase of wear resistance of cutting tools [22], corrosion resistance [23], lowering of stress concentration in the treated parts and elements of structures, elimination of fatigue cracks, extension of the life of stamped parts from light and special alloys, are noted. It is established that at optimum parameters of electric pulse impacts material ultimate strength, endurance limit and fatigue strength are increased without detracting from its ductile properties [24]. The mentioned metalworking processes are promising for increase of mechanical characteristics and service properties of welded structures, allowing for structural features and stress-strain state of welded joints. This is confirmed by establishing respective research programs in such European research organizations as University of Birmingham (UK), University of Hertfordshire (UK), Imperial College (UK), Katholieke Universiteit Leuven (Belgium), EBF-Dresden (Germany), Fraunhofer-Institut fur Werkstoff- und Strahltechnik IWS (Germany). A lot of attention to research in this area is given in PRC and Japan, for instance: Sichuan University, China University of Geosciences, Army Academy of Armed Forces, Process Institute of Inner Mongolia First Machinery Group, Wuhan University of Technology, Beijing Institute of Technology, Nagoya University.

At operation of metal structures, including welded structures, microcracks initiate and propagate in the metal under the impact of loads. They cause a lowering of metal mechanical properties that leads to product failure. The problem of «healing» such defects is urgent, and now several methods of its realization are known: restoration heat treatment (RHT); mechanothermal treatment (MTT); and diffusion metallization (DM) [7]. These methods have their disadvantages, which include high power consumption, limited application for large-sized metal structures, and long duration of the process. Energy impact on a propagating crack can be realized at its treatment by PEC and PEMF, which can not only slow down crack propagation, but also increase the metal strength in the zone of the defect tip [25]. PEC passage through a part with a marginal crack is accompanied by a microexplosion in its tip, leading to formation of a crater, at 5 to 10 mm distance from which the metal is heated by several tens of degrees. This phenomenon can be used for blunting the crack tip. A method of healing microcracks in 65G steel and armco-iron, using crossed fields of PEC and PEMF, was proposed. Structure refinement at concurrent increase of microhardness relative to the initial material is observed in the zone of restored continuity [26].

At cyclic testing, the impact of PEC and PEMF leads to increase of fatigue resistance of metallic materials, which is related to microcrack healing, evolution of defective structure and phase composition, as well as elimination of the stress raisers. Positive impact of PEC on technological tensile stresses in spray-deposited surfaces of tool steels was established [27]. However, the given results did not have any further development.

Analyzing on the whole the results of EPE investigations at regulation of the stress-strain state of metallic materials, it should be noted that application of electromagnetic impacts was performed, mainly, in the plastic region of loading, in connection with the focus on EPE practical application in forming technologies. Here, the region of elastic deformation of metallic materials at electromagnetic impact remains little studied [28]. At the same time, investigation of the features of elastic stress relaxation in metals and alloys at their electromagnetic treatment is urgent for regulation of stressed state of welded structures. Results of studying the PEC and PEMF impact on controlling the residual welding stresses showed that EPE realization at welded joint treatment is limited by the features of discharge circuit formation, which includes the structure being treated. So, in the majority of cases, the welded structure dimensions do not allow providing the required current density j in the zone of PEC impact. PEC treatment of small-sized welded products is an exception, for instance hardfaced surfaces of cutting tools parts, where the cross-sections allow providing current density values, necessary for EPE realization. Studies were performed of PEMF impact on lowering residual stresses in butt welded joints of an aluminium alloy with application of a system of flat inductors rigidly fixed on the surface of plates, which were treated, and were part of the discharge circuit [29]. Conducted studies showed the possibility in principle of lowering the welding stresses at PEMF impact, although their initial level after treatment was reduced by not more than 30 %. PEMF impact on lowering the residual stresses in welded and surfaced samples of low-carbon steels, which is based on intensification of dynamic effect of magnetostriction [30], ensured lowering of the initial level of stresses to 40 %. Here, the features of fastening the welded joints influence the effectiveness of PEMF impact. Thus, at sample treatment under the conditions of rigid fastening, relaxation of residual welding stresses proceeds more intensively, than under the conditions of free support.

In work [31] investigation of electromagnetic impact on the change of mechanical properties of welded joints of carbon and low-alloyed steels was performed, which demonstrated an essential increase of impact toughness values after treatment of samples of steels of grades 20 and 09G2S at preservation of their ultimate tensile strength characteristics. Explanation of the obtained results is based on the theory of electron-dislocation interaction, as well as magnetoelastic interaction of interdomain boundaries (Bloch walls) with dislocations, that stimulate their movement at magnetization [32]. The ambiguous results of studying PEMF impact on the change of residual welding stresses are shown in [33]. So, residual stresses in samples of steels St2ps(semi-killed) and 20KhMFL in the active zone decrease by 3–25 %, while increasing up to 15 % in the reactive zone. At the same time, PEMF lowers stresses of the second kind to the level that is provided by annealing at the temperature of 1060 °C, and also leads to a more uniform distribution of α-phase through the treated metal volume.

Proceeding from the presented results, evaluation of PEC and PEMF impact on regulation of stress-strain state of welded joints of steels and aluminium alloys, leads to the conclusion that, despite the obvious effect, maximum lowering of the initial level of stresses is not more than 40 %. Development and improvement of energy-effective technologies of electromagnetic impact on welded joints, clad and spray-deposited surfaces, with which stress lowering would be close to 100 %, seems to be promising.

Realization of EPE at direct passage of PEC through metal structure elements is a rather complex task, because of the need to ensure the current density $j \geq 10^3$ A/mm^2 in the cross-sections, the area of which is much greater than 100 mm^2. The difficulty is associated with scattering of current force lines that occurs already at a small distance from the points of connection of the discharge circuit to the part. The scattering factor can be minimized through localizing of the region of current flowing in the treatment zone, and its density j that is required for EPE realization, is achieved through movement of dynamic contact of the current-conducting electrode with the treated surface. This scheme of PEC impact was studied for the novel method of nondestructive testing of stress-strain state of welded joints [34], where it is shown that adding dynamic loading to the electrode during PEC impact improves the reliability of electrode contact with welded joint surface. Here, dynamic loading intensifies dislocation movement and multiplication that determines the degree of plastic deformation of polycrystalline structures under the conditions of PEC impact. The controlling mechanism of the impact of dynamic loading, considered in the physical model of discontinuous metal flow at cryogenic temperatures [7], was extended to the region of temperatures in the range from 273 to 293 K, for the case of magnetic-pulse forming of ferromagnetic materials [35]. It is found that the small jump of stress that is caused by dynamic or thermal loading [36], acts as an initiator or synchronizer of plastic deformation, which is determined by mass breaking of dislocations through barriers over the entire volume of polycrystalline structure, to which active mechanical loading is applied. Here, directed movement of conduction electrons at the moment of PEC impact promotes dislocation advance, increasing the degree of plastic deformation of material, compared to the case of application of purely mechanical loading. Work [37] presents the results of studying the influence of mechanical and electromagnetic effects at summary and divided impact of PEMF and mechanical pressure pulses on mobility of edge dislocations in NaCl and LiF crystals. The dislocation free path l was taken as the characteristic of pulsed impact on their mobility. It is found that the mean free path length $\langle l \rangle$ increases considerably at simultaneous impact of PEMF and mechanical loading pulses, compared to $\langle l \rangle$ values, that are recorded under the action of each of the factors taken separately. Increase of $\langle l \rangle$ under the impact of current is related to increase of the intensity of electromagnetic pumping of the crystal, and superposition of pulsed impacts of different origin initiates rather extended in time relaxation processes in the crystals that affect their stressed state. This physical model is valid also for metal polycrystalline structures that was confirmed in [38], which shows the results of evaluation of the influence of current pulses and mechanical loading σ on plastic deformation rate $\dot{\varepsilon}$ in Zn samples. It is shown that PEC impact at the value of current density j above the threshold one, increases velocity v of dislocations moving in the direction of current action. Increase of $j > 1.0$ kA/mm^2 initiates the above-mentioned process, PEC impact accelerating the dislocation movement due to their interaction with charge carriers (electrons).

The possibility of simultaneous application of electric pulse and mechanical impact for welded structure treatment with the purpose of their service life extension was substantiated proceeding from analysis of previous research [39]. This was the base for development of a new kind of welded joint treatment — electrodynamic treatment (EDT) [40]. At EDT the metal is subjected to bulk electrodynamic impact, which is characterized by simultaneous running of electric pulse and dynamic processes, the first of which causes EPE in the treatment zone, and the second results in formation of waves of stresses with the specified amplitude, plastic deformation and refinement of metal structure. Interaction of stress waves with the static field of residual stresses can initiate relaxation of the latter that may lead to decrease of their values. PEC localization in the deformation zone reduces the factor of scattering of current force lines, thus ensuring achievement of threshold density that is a mandatory condition of EPE realization. Interaction of the components of electrodynamic effect during PEC passage through the metal determines the effectiveness of EDT impact on the residual stresses, structure evolution, accuracy and fatigue life of welded structures from light alloys [41].

Proceeding from the mechanism of electron-dislocation interaction for creation of the conditions for crystallization, which ensures formation of a fine-grained structure, development of the technology of welded joint modifying by nanostructured highly dispersed materials is believed to be promising. This will be the subject of further investigations of advanced methods of structural material treatment.

A mathematical model of EDT process was developed in order to assess the influence of electrophysical and dynamic components of electrodynamic impacts that determine the change of characteristics of residual welding stresses. This allowed optimizing the treatment modes, in order to control the stress-strain state of welded joints of aluminium alloy AMg6 [42–44]. Improvement of the current model will allow calculation of stress-strain state of welded structures under the conditions of concurrent heating of the weld, with different schemes of fastening the structure being treated, and at magnetic field impact.

Considering the results of [8], where it is shown that concurrent heating stimulates stress relaxation at electric pulse treatment of thin steel rods, it is promising to study the effectiveness of EDT of a cooling weld, which is performed during the thermodeformational cycle of welding. Development of hybrid technologies (automatic welding + EDT) will allow lowering the energy intensity of the treatment process, shortening the working time of metal structure fabrication at its improved quality [45].

Among the novel techniques of external impact on the quality of metal products, studies are actively performed of the action of constant magnetic fields (CMF) that are applied to the melt during its solidification, when producing cast billets and parts from nonferromagnetic materials, for instance, aluminium alloys. It is established that CMF action promotes the evolution of material structure, and increase of corrosion resistance. The structure forming mechanism is based on CMF action manifestations, namely refinement of structural components, change of intermetallic phase morphology, increase of their microhardness, change of their dimensions and configuration that corresponds to the processes of solidification at high cooling rates [46]. It should be noted that the liquid metal of the pool in fusion welding under certain conditions, is similar by its properties (at much smaller volume) to cast metal, i.e. is suitable for CMF treatment. Considering the conditions of formation of the pool rear edge, CMF treatment of cooling weld metal is promising, as a method to control the stressed state and structure of the joint metal. This can stimulate development of a promising method of CMF treatment of welded joints during the thermodeformational cycle of welding and can prompt development of hybrid technologies (automatic welding + CMF treatment) for nonferromagnetic metallic materials based on Al, Mg, Fe.

Modification of metals and alloys by doping the melt with nanomodifiers has a marked effect on crystallization, for instance, causes dispersion of the structural components and change of their distribution. Modifying improves the alloy mechanical properties. Quality characteristics of modifiers are the size of individual refractory particles, its chemical purity and price. A certain quantity of modifiers is manufactured by powder metallurgy methods, or with application of ball mills. It is known that the high-voltage electric discharge (HVED) in the dispersed system of metal powder + kerosene allows not only refining the metal particles, but also initiating chemical reactions. At HVED application the possibility of manufacturing highly dispersed nanostructured modifiers and their prices are attractive for their commercial application in metalworking. The technology of dispersion with HVED application is similar, by its acting mechanism, to EHPT method, shown above. It should be noted that scientific principles were developed for HVED treatment in kerosene of mixtures of Al, Ti powders, where dispersion and synthesis of refractory components, in particular TiC, $AlTi_3$, AlTi, Al_2Ti, Al_3Ti, Ti_3AlC, $TiAlC_2$, Ti_3AlC_2, Ti_2AlC and longsdaleite, take place [47, 48]. Alongside foundry, nanomodifying can be applied in the technologies of welding and surfacing by adding nanoparticles of refractory chemical compounds to the weld pool during laser and electroslag welding, and electron beam deposition. At surfacing with high-temperature resistant alloys based on iron, nickel and chromium and carbon steels, which are modified by nanoparticles, resistance of the surfaced tool exposed to cyclic temperature-force impact, is increased. At modifying by nanoparticles, transcrystallization zones in the deposited or welded metal are removed, dendrite dimensions are refined, morphology and topography of the strengthening phases are improved that promotes higher high-temperature strength and fatigue resistance of the alloys [49]. There are certain limitations for nanomodifying of metal at automatic and manual arc welding. The main problem for application of nanocomposites in fusion welding is adding the latter to the weld pool. One of the ways to solve this problem is development of advanced technologies of producing welding and surfacing consumables (electrodes, fluxes, flux-cored wires) with addition of highly-dispersed nanostructured modifiers, produced on the base of energy effective HVED method. This is a new approach to improvement of service characteristics of welded structures that is based on electric pulse processes.

Thus, the experience of many years of investigations of the impact of electromagnetic technologies on metals and alloys proves their applicability for controlling the stressed state, structure evolution, tribological and mechanical characteristics, extension of the service life of welded structures in different sectors of machine-building, metallurgical complex, aerospace and defense industry.

1. Razmyshlyaev, A.D., Ageeva, M.V. (2018) On mechanism of weld metal refining in arc welding under action of magnetic fields (Review). *The Paton Welding J.*, **3**, 25–28.
2. Dubodelov, V.I., Goryuk, M.S. (2018) Application of electromagnetic fields and magnetohydrodynamic phenomena for intensification of effect on metal systems: World and Ukrainian experience. In: *Materials science: Achievements and perspectives*. In: 2 Vol. Vol. 2. Kyiv, Akademperiodyka, 24–50 [in Ukrainian].
3. Opara, V.S., Reznikov, L.Ya., Onatskaya, N.A., Demidenko, L.Yu. (1998) Electrohydropulsed treatment as a universal and effective method for improvement of service characteristics of metal structures with technological stresses. *Tyazholoe Mashinostroenie*, **10**, 7–9 [in Russian].
4. Khromov, V.N., Kuznetsov, I.S., Petrashov, A.S. (2009) Electrospark machining of surfaces of parts for producing wear-resistant volume nanostructural coatings on cutting parts of farming machines. *Vestnik OrelGAU*, **1**, 6–8 [in Russian].
5. Uzlov, I.G. (2003) Advanced processes of production and quality of railway wheels. *Stal*, **5**, 69–72 [in Russian].
6. Volkogon, V.M., Avramchuk, S.K., Strilets, E.V. (2005) Formation of strengthening coatings under action of highpower electric discharge. In: *Proc. of 5th Int. Sci.-Techn. Conf. on Surface Engineering and Renovation of Products (Yalta, 21–24 May, 2005)*, 48–51.
7. Baranov, Yu.V., Troitsky, O.A., Avramov, Yu.S. (2001) *Physical principles of electropulse and electroplastic treatment and new materials*. Moscow, MGIU [in Russian].
8. Stepanov, G.V., Babutsky, A.I., Mameev, I.A. (2004) Non-stanionary stress-strain state in long rod, caused by pulse electric current of high density. *Problemy Prochnosti*, **4**, 60–67 [in Russian].
9. Strizhalo, V.A., Novogrudsky, L.S., Vorobiov, E.V. (2008) *Strength of materials at cryogenic temperatures taking into account the effect of electromagnetic fields*. Kiev, IPS [in Russian].
10. Zuev, L.B., Gromov, V.E., Gurevich, L.I. (1990) Effect of electric current pulses on dislocation mobility in single crystals *Zn. Metallofizika*, 12(**4**), 11–15 [in Russian].
11. Okazaki, K., Kagana, M., Conrad, H. (1979) Evaluation of the contour, of skin, pinch and heating to the electroplastic effect in titanium. *Ibid.*, **13**, 473–500.
12. Braunovic, M. (1986) The effect of electric current on the stress relaxation of aluminium wire conditions. *Strength Metals and Alloys* (ICSMA 7), Oxford, 1, 619–624.
13. Gromov, V.E. (1989) On mechanisms of electroplastic effect in metals. *Izv. Vuzov, Chyorn. Metallurgiya*, **10**, 71–75 [in Russian].
14. Beklemishev, N.N., Koryagin, N.I., Shapiro, G.S. (1984) Effect of local heterogeneous pulsed electromagnetic field on plasticity and strength of conducting materials. *Izv. AN SSSR. Metally*, **4**, 184–187 [in Russian].
15. Stepanov, G.V., Babutsky, A.I., Mameev, I.A., Olisov, A.N. (2006) Analysis of process of tensile stress relaxation under electric current effect. Problemy Prochnosti, 1, 116–127 [in Russian].
16. Troitsky, O.A., Kalymbetov, P.U. (1981) Dependence of electroplastic effect in zinc on duration of separate pulses. *Fizika Metallov i Metallovedenie*, 51(**5**), 1056–1059 [in Russian].
17. Strizhalo, V.A., Novogrudsky, L.S. (1997) Determination of energy of electroplastic deformation of metals. *Problemy Prochnosti*, **4**, 38–43 [in Russian].
18. Strizhalo, V.A., Vorobiov, E.V. (2003) Stepwise deformation of metal under conditions of effect of pulsed magnetic field and cryogenic temperatures. *Ibid.*, **1**, 137–142 [in Russian].
19. Vorobiov, E.V., Anpilogova, T.V. (2007) Instability of deformation and strength of structural alloys under conditions of stress concentration and cryogenic temperatures. *Ibid.*, **2**, 153–156 [in Russian].
20. Dolgin, A.M., Natsik, V.D. (1991) Criteria of instability and kinetics of jumps under unstable low temperature plastic flow. *Acta Univ. Carol. Math. and Phys*., 32(**1**), 77–78.

21. Liping Ma, Wenxiang Zhao, Zhiqiang Liang et al. (2014) An investigation on the mechanical property changing mechanism of high speed steel by pulsed magnetic treatment. *Mater. Sci. & Engin*., **A609**, 16–25.
22. Batainen, O., Klamecki, B., Koepke, B. (2003) Effect of pulsed magnetic treatment on drill wear. *J. Mater. Process. Tech*., **134**, 190–196.
23. Babutsky, A., Chrysanthou, A., Ioannou, J. (2009) Influence of pulsed electric treatment on corrosion of structural metals. *Strength of Materials*, **4**, 387–391.
24. Semashko, N.A., Krupsky, R.F., Kupov, A.V. (2004) Acoustic emission in electropulsed deformation of titanium alloys. *Materialovedenie*, **7**, 29–33 [in Russian].
25. Semakin, E.V., Chirakidze, D.Z., Tsellermayer, V.Ya. (1997) Electric simulation restoration of service life of welded joints: Experiment and model. *Izv. Vuzov, Chyorn. Metallurgiya*, **6**, 48–51 [in Russian].
26. Baranov, Yu.V. (2003) Formation of defects and healing of defects in metallic materials by pulsed electric current. In: *Proc. of Int. Sci.-Pract. Conf. on Effect of Electromagnetic Fields on Plasticity and Strength of Materials (Voronezh)*, 17–12.
27. Jaewoong Jang, Yang Ju, Yasuyki Morita, Yuki Toku (2016) Effect of pulsed electric current on the growth behavior of fatigue crack in Al alloy. In: *Proc. of 21st Europ. Conf. on Fracture, ECF21 (20-24 June 2016, Catania, Italy)*, 2889–2993.
28. Stepanov, G.V., Babutsky, A.I. (2007) Modeling of stress relaxation under effect of pulsed electric current of high density. *Problemy Prochnosti*, **2**, 113–120 [in Russian].
29. Stepanov, G.V., Babutsky, A.I., Mameev, I.A. et al. (2011) Redistribution of residual welding stresses as a result of treatment by pulsed electromagnetic field. *Ibid.*, 123–131 [in Russian].
30. Yanli Song, Lin Hua (2012) Mechanism of residual stress reduction in low alloy steel by a low frequency alternating magnetic treatment. *J. Mater. Sci. Technol*. 28(**9**), 803–808.
31. Tsaryuk, A.K., Skulsky, V.Yu., Moravetsky, S.I.,Sokirko, V.A. (2008) Change of mechanical properties of welded joints of carbon and low-alloy steels under influence of electromagnetic effects. *The Paton Welding J*., **7**, 27–30.
32. Shao Quan, Kang Jiajie, Xing Zhiguo et al. (2019) Effect of pulsed magnetic field treatment on the residual stress of 20Cr2Ni4A steel. *J. of Magnetism and Magnetic Materials*, **476**, 218–224.
33. Tsaryuk, A.K., Skulsky, V.Yu., Moravetsky, S.I., Sokirko, V.A. (2008) Influence of electromagnetic treatment on residual welding stresses in welded joints of carbon and lowalloyed steels. *The Paton Welding J*., **9**, 22–25.
34. Lobanov, L., Pivtorak, V., Pashchin, N. et al. (2014) Application of local current pulses for determination and control of residual stresses. *Advanced Mater. Research*, **996**, 386–391.
35. Gnatov, A.V. (2012) Magnetic pulsed technologies for contact-less dressing of hull components of transport vehicles. *Maukovyi Visnyk KhDMA*, 7(**2**), 108–114 [in Russian].
36. Hodowant, J., Ravichndram, G., Rosakis, P, (2000) Partition of plastic work into heat and stored energy in metal. *Exp. Mech.*, 40(**2**), 113–123.
37. Alshits, V.I., Dariinskaya, E.V., Legenkov, M.A., Morozov, V.A. (1999) Dislocation mobility in NaCl crystals under combined impact of mechanical and electromagnetic pulses, formed by electron beam. *Fizika Tvyordogo Tela*, 41(**11**), 2004–2006 [in Russian].
38. Gromov, V.E., Gurevich, L.I., Kurilov, V.F., Erilova, T.V. (1989) Effect of current pulses on mobility and multiplication of dislocations in Zn. *Problemy Prochnosti*, **10**, 48–53 [in Russian].
39. Lobanov, L.M., Pashchin, N.A., Loginov, V.P, Poklyatsky, A.G. (2010) Effect of electric pulsed treatment on residual forming of thin sheet welded structures (Review). *Ibid*., **3**, 13–17 [in Russian].
40. Lobanov, L.M., Pashchin, N.A., Loginov, V.P., Skulsky, V.Yu. (2005) Effect of electrodynamic treatment on stress-strain state of heat-resistant steels. *Ibid*., **5**, 13–17 [in Russian].
41. Lobanov, L.M., Kondratenko, I.P., Zhiltsov, A.V., Mikhodui, O.L. (2018) Development of post-weld electrodynamic treatment using electric current pulses for control of stressstrain states and improvement of life of welded structures. *Materials Performance and Characterization*, **7**, Issue 4, https://doi.org/10.1520/MPC20170092.
42. Lobanov, L.M., Kondratenko, I.P., Zhiltsov, A.V. et al. (2016) Nonstationary electrophysical processes in systems for reduction of residual stresses in welded joints. *Tekhnichna Elektrodynamika*, **6**, 10–19 [in Ukrainian].
43. Kondratenko, I.P., Zhiltsov, A.V., Pashchin, M.O., Vasyuk, V.V. (2017) Selection of parameters of electromechanical converter of induction type for electrodynamic treatment of welded joints. *Ibid*., **5**, 83–88 [in Ukrainian].
44. Lobanov, L.M., Pashchin, M.O., Mikhoduj, O.L. et al. (2017) Effect of impact action of electrode-indentor on stress-strain state of AMg6 alloy in electrodynamic treatment. *Problemy Prochnosti*, **3**, 30–42 [in Ukrainian].
45. Lobanov, L.M., Pashchin, M.O., Pivtorak, V.A., Volkov, S.S. (2015) *Method of removal of residual stresses and strains of welded joints*. Ukraine Pat. 110273 [in Ukrainian].
46. Dubodelov, V.I., Serednenko, O.V., Zatulovsky, A.S., Serednenko, V.O. (2018) Improvement of properties of aluminium alloys by action of constant magnetic field on melt at the solidification. *Metaloznavstvo ta Obrobka Metaliv*, **4**, 3–8 [in Ukrainian].
47. Sizonenko, O.N., Lipyan, E.V., Torpakov, A.S. (2015) To problem of parameter optimization by high-voltage pulsed treatment. *Naukovi Notatky*, **50**, 203–207 [in Russian].
48. Zajchenko, A.D., Zhdanov, O.O., Torpakov, A.S., Syzonenko, O.M. (2018) Influence of high-dispersed modifier on structure and properties of SM88U nickel alloy. *Metaloznavstvo ta Obrobka Metaliv*, **4**, 55–57 [in Ukrainian].
49. Serhienko, R.A., Verkhovlyuk, A.M. (2018) Treatment of cast alloys by metallic nanoparticles. In: *Materials science: Achievements and perspectives*. In: 2 Vol. Vol. 2. Kyiv, Akademperiodyka, 88–103 [in Ukrainian].

Received 26.02.2019

https://doi.org/10.15407/tpwj2019.08.06

PREDICTION OF PARAMETERS OF FRICTION STIR WELDING PROCESS OF SHEET ALUMINIUM ALLOYS

A.G. POKLYATSKII
E.O. Paton Electric Welding Institute of the NAS of Ukraine
11 Kazimir Malevich Str., 03150, Kyiv, Ukraine. E-mail: office@paton.kiev.ua

Optimum parameters of the modes of friction stir welding of 0.8–3.0 mm thick aluminium alloys widely used in fabrication of welded structures were determined. It is shown that sound formation of welds can be ensured at tool immersion into the metal being welded to the depth of 0.10–0.15 mm due to correct selection of the frequency of tool rotation and welding speed. A relationship is established between the total content of alloying and modifying elements in the aluminium alloy being welded, welding speed and frequency of tool rotation. A range of optimum relationships was determined, showing the length of the tool linear movement along the butt during one rotation, when sound formation of welds of sheet aluminium alloys AMtsN, AD33, AMg2M, 1460, AMg5M, 1201 and AMg6M is provided. Formulas were derived, which express the dependencies in the form of power functions, limiting this range and allowing calculation of the required speeds of tool rotation and displacement for any aluminium alloy, containing 2.2–8.4 % of alloying and modifying elements. Characteristic defects, forming in welds at deviation of the above parameters from the optimum range, are shown. 18 Ref., 5 Figures.

Keywords: *aluminium alloys, friction stir welding, tool rotation speed, welding speed, characteristic defects*

Friction stir welding (FSW), being one of the novel methods for obtaining permanent joints in solid phase, finds wider and wider application in shipbuilding, manufacture of land and air transport, space engineering, etc. [1–4].

Formation of a weld as a result of heating due to friction to plastic state, stirring and plastic deformation of small volume of metal of parts being joined in closed space, provides some advantages of this process in comparison with fusion welding. First of all it allows eliminating the possibility of defect formation in form of hot cracks, pores, macroinclusions of oxide film and such, provoked by melting and crystallization of metal. Besides, welding of aluminium alloys is carried out without application of shielding gas and filler material and allows eliminating ultraviolet radiation, metal fumes and vapors emission. This guarantees high mechanical properties of joints and decrease of level of base metal softening and deformation of welded structures [3, 5–8].

However, as with any method of welding, obtaining of defect-free joints in FSW is possible only at specific parameters of the process. Incorrect selection or their deviation from the optimum values can result in formation of characteristic surface or inner defects in form of flash, lack of fusion or discontinuities [9–11].

It is believed that the main parameters of FSW process, except for structural peculiarities of working surfaces of a tool, are angle of tool tilt relatively to vertical axis, pressing force of tool to the surfaces of parts being joined, value of immersion of tool shoulder and depth of penetration of tool pin into welded metal as well as rotation speed and its linear displacement (welding speed) [5, 9].

The investigations carried by foreign specialists showed that welding shall be carried out with «forward angle», deviating the tool at small angle from vertical axis. At that due to force applied to the tool in vertical plane its shoulder insignificantly immerses into metal being welded and is tightly pressed against it in process of welding. Tip of the tool should provide stirring of metal along the whole thickness of edges being welded in order to eliminate a defect in form of lack of fusion in low part of weld [12–15]. Speeds of rotation and linear displacement of the tool to significant extent determine the volume of plasticized metal in a welding zone and temperature of its heating. They can change in sufficiently wide range depending on thickness of material being welded, its thermal and physical and ductile characteristics as well as trajectory of displacement of plasticized metal determined by structural peculiarities of tool working surfaces [9, 16]. Some researchers determined the optimum relationships between the welding speeds and tool rotation frequencies, expressing length of linear displacement of the tool along the butt per its one revolution, depending on thickness of material being welded or temperature interval of crystallization of aluminium alloys [14, 17].

Aim of the present work is to determine the optimum parameters of modes of friction stir welding widely used in manufacture of welded structures of aluminium alloys of different alloying systems of 0.8–3.0 mm thickness.

Investigation procedure. Friction stir welding of sheets of aluminium alloys AMtsN, AD33, AMg2M, AMg5M, AMg6M, 1201 and 1460 of thickness from 0.8 to 3.0 mm was carried out on a laboratory unit, designed at the E.O. Paton Electric Welding Institute. A special tool with 12 mm diameter shoulder and pin of conical shape [18] was used to obtain butt joints. Length of tool pin was selected in such a way as it was 0.15 mm smaller than the thickness of metal being welded. It was forward angle welding at 2–3° tool tilt relatively to vertical axis. Tool rotation was carried out using replaceable serial asynchronous alternating current motors (U = 380 V) of 4 kW power and shaft rotation frequency N = 1420 and 2880 rpm set on a support. Using the latter the tool fixed on the motor shaft moved in a vertical plane thanks to which necessary immersion of its working parts into the material being welded was provided and value of axial force of its pressing to the parts being joined in process of welding was kept. The sheets being welded were safely fixed on a steel substrate of movable table. At that speed of welding can be varied in v_w = 2–42 m/h limits. Specially set ahead of the tool pressure roll prevented a change in the process of welding of spatial position of edges of thin-sheet material, which is too sensitive to heat effect.

Presence of macrodefects in form of flash and lack of fusion on the surfaces of welded joints was determined using visual inspection. The inner defects were found on cross-sections, preliminary prepared using electrolytic polishing and their additional etching in a solution of perchloric, nitric and hydrofluoric acids, using optical microscope MIM-8M.

Investigation results and their discussion. As a result of carried investigations it was determined that quality formation of welds in friction stir welding of sheet aluminium alloys can be provided by correct selection of depth of tool immersion into metal being welded, frequency of tool rotation and speed of its linear displacement along the butt or welding speed (v_w).

Depth of tool immersion provokes thermodeformational conditions in all zones of welded joint, since simultaneously predetermines a value of tool shoulder immersion and depth of pin penetration into metal being welded. Its reduction (< 0.10 mm) results in decrease of value of shoulder immersion and depth of penetration of tool pin into metal being welded. As a result, pressure under the shoulder working surface and tool pin and value of heat emission in the place of their contact with metal being welded are reduced. Due to this, the necessary volume of plasticized metal for quality weld formation is not provided or required level of its plasticization is not reached in the zone of formation of permanent joint. This can lead to formation of inner defects in form of discontinuities (Figure 1, *a*) or surface defects from weld face in form of lack of fusion (Figure 1, *b*). Besides, as a result of

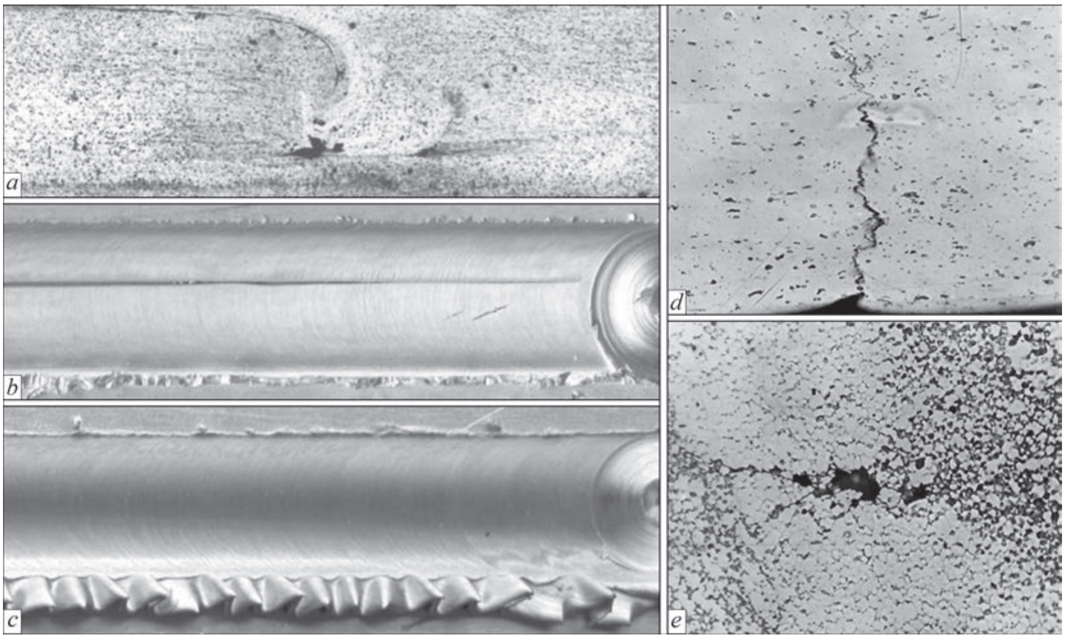

Figure 1. Characteristic defects forming in FSW welds: *a*, *e* — inner discontinuities; *b* — lack of fusion from weld face; *c* — flash on weld face; *d* — lack of fusion in weld root part (*a* — ×15; *b*, *c* — ×2; *d* — ×300; *e* — ×500)

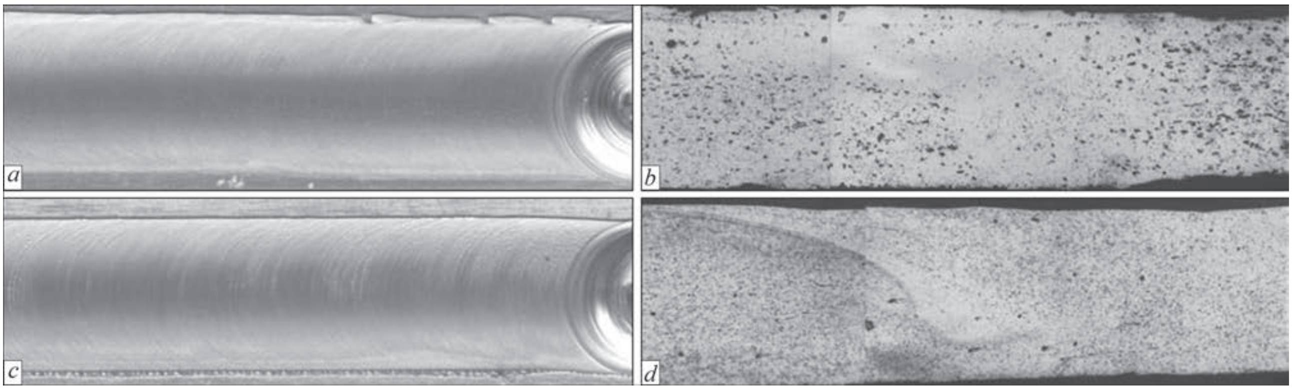

Figure 2. Appearance (*a*, *c* — ×2) and transverse macrosections (*b*, *d* — ×12) of FSW welds of aluminium alloys AMtsN (*a*, *b*) and AMg2M (*c*, *d*) of 2 mm thickness produced at welding speeds 38 and 32 m/h, respectively

decrease of tool penetration depth into the metal being welded and emitted in its friction heat, the defects in form of lack of fusion (Figure 1, *d*) can also appear in the root part of the weld. Quality of welded joints can be deteriorated by excessive (> 0.15 mm) deepening of the tool. Thus, welding of ductile low aluminium alloys (AMtsN, AD33, AMg2M) can provoke formation of surface defects in form of flash (Figure 1, *c*) on the weld face, and in welding of stronger alloys these are inner discontinuities, caused by metal overheating (Figure 1, *e*). Therefore, in order to provide quality formation of welds it is necessary to immerse the tool into metal being welded to 0.10–0.15 mm depth and keep it in such position in process of welding due to axial pressing force.

Conditions of plastic deformation of metal in the zone of formation of permanent joint are determined by temperature of its heating and deformation rate, which depend on frequency of tool rotation and rate of its linear displacement along the butt. Carried experimental investigations proved that quality formation of welds in friction stir welding of different aluminium alloys is provided at different values of these parameters. Thus, at frequency of tool rotation $N = 1420$ rpm ductile low aluminium alloys are successfully welded at sufficiently high welding speeds (Figure 2).

To obtain quality joints on stronger aluminium alloys containing significant amount of alloying and modifying elements it is necessary to reduce welding speed. For example, in the welds of aluminium-lithium alloy 1460 the inner defects in form of cavities, provoked by insufficient volume of plasticized metal in a zone of permanent joint formation, are formed in tool displacement along the weld with more than

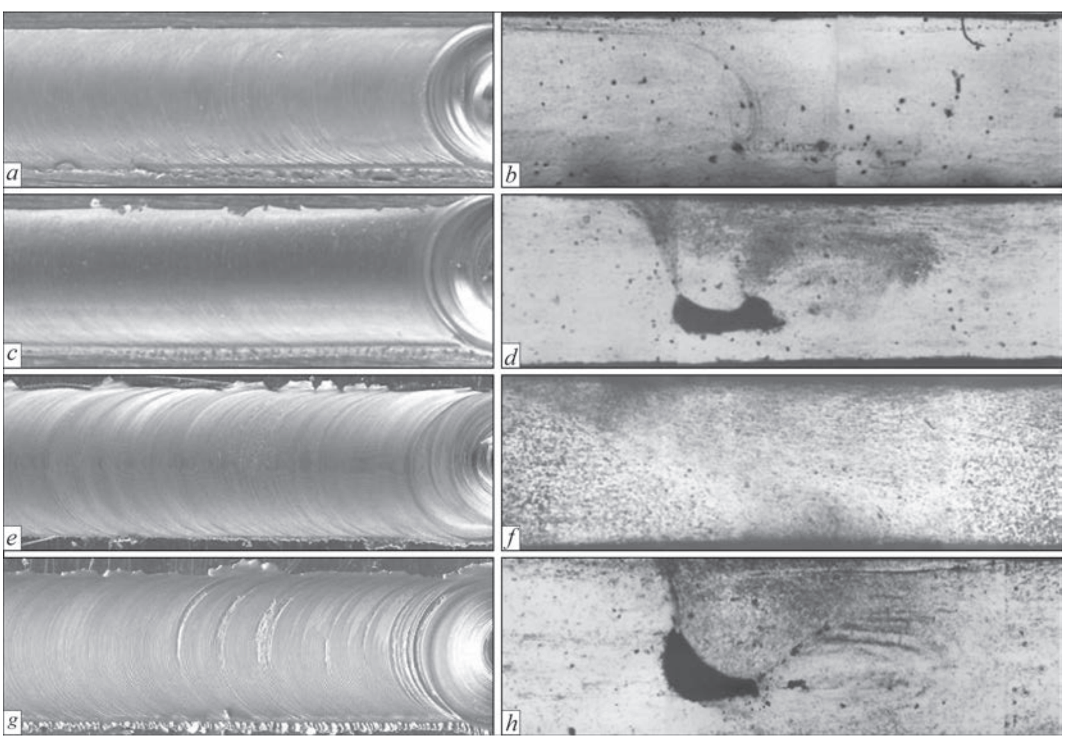

Figure 3. Appearance (*a*, *c*, *e*, *g* — ×2) and transverse macrosections (*b*, *d*, *f*, *h* — ×12) of FSW welds of aluminium alloys 1460 (*a*–*d*) and 1201 (*e*–*h*) of 2 mm thickness produced at welding speeds 8 m/h (*a*, *b*, *e*, *f*), 24 m/h (*c*, *d*) and 18 m/h (*g*, *h*)

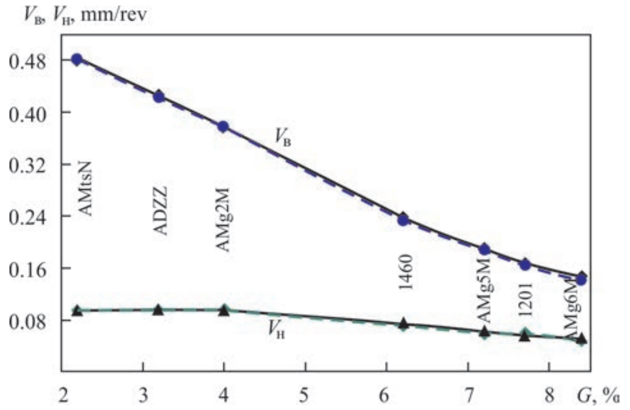

Figure 4. Range of optimum relationships of welding speeds and tool rotation frequencies in FSW of aluminium alloys with different content of alloying and modifying elements and approximated curves limiting it (N = 1420–2880 rpm)

20 m/h speed, and in 1201 alloy welds it makes more than 14 m/h (Figure 3).

Increase of tool rotation frequency to 2880 rpm provokes rise of heat emission in a zone of permanent joint formation that allows 2 times increase of speed of linear displacement of a tool without deterioration of welds' quality. Taking into account relationship between noted parameters of the process, v_w/N relationship was used. It expresses length of linear displacement of the tool along butt per its one revolution. Carried experimental investigations allowed determining the optimum values of this relationship depending on total content of alloying and modifying elements in welded aluminium alloys (Figure 4).

It is determined that in friction stir welding of aluminium alloy AMtsN, containing around 2.2 % of alloying and modifying elements, quality formation of the welds is provided at value of v_w/N relationship in 0.094–0.481 mm/rev limits, i.e. at tool rotation frequency 1420 rpm the welding speed can vary in 8–41 m/h limits. For alloy AD33, in which content of such elements makes around 3.2 %, the range of optimum v_w/N relationships reduces to 0.094–0.423 mm/rev, that at mentioned above frequency of tool rotation allows successfully performing welding on 8–36 m/h speed. Quality formation of welds based on AMg2M alloy, containing higher amount of alloying and modifying elements (4 %) is reached at value of v_w/N relationship in 0.094–0.376 mm/rev limits or at v_w = = 8–32 m/h.

For stronger aluminium alloys, containing considerable amount of alloying and modifying elements, the range of optimum v_w/N relationships, which provide quality weld formation, becomes significantly narrower. Thus, for alloy 1460, which in its content has around 6.2 % of other elements in addition to aluminium, it makes 0.070–0.233 mm/rev, i.e. at tool rotation frequency 1420 rpm the welding speed should be in 6–20 m/h limits and at 2880 rpm it is 12–40 m/h. On alloy AMg5M, containing 7.2 % of alloying and modifying elements, quality formation of welds is provided at v_w/N = 0.058–0.187 mm/rev or at welding speeds 5–16 and 10–32 m/h, when the tool rotation frequency makes 1420 and 2880 rpm, respectively. More doped alloy 1201, containing 7.7 % of other elements in addition to aluminium, is successfully welded at value of linear displacement of the tool per its one revolution in 0.047–0.163 mm limits, that corresponds to 5–14 m/h welding speeds at tool rotation frequency 1420 rpm and 10–28 m/h at 2880 rpm. For alloy AMg6M, containing around 8.4 % of alloying and modifying elements, the optimum v_w/N relationship is in 0.047–0.140 mm/rev range, i.e. welding speed can vary in 4–12 m/h limits at tool rotation frequency 1420 rpm or 8–24 m/h at 2880 rpm.

Obtained empirical curves, limiting the range of optimum relationships between the length of linear displacement of tool per its one revolution and total content of alloying and modifying elements in the alloy, were approximated by power functions. For the curve, limiting upper boundary of this range such a function will be expressed by the following formula:

$$V_B(G) = V_{B0}[1.46–0.08G/G_0 – – 0.541(G/G_0)^2 + 0.16(G/G_0)^3], \quad (1)$$

where $V_B(G)$ is the maximum allowable value of linear displacement of the tool per its one revolution, which provides quality formation of welds, mm/rev; V_{B0} = 0.376 mm/rev is the maximum allowable value of linear displacement of tool per its one revolution for alloy AMg2M; G_0 = 4 % is the total content of alloying and modifying elements in aluminium alloy AMg2M; G is the total content of alloying and modifying elements in welded aluminium alloy, % (2.2–8.4 % range).

For the curve, limiting lower boundary of indicated range, the approximated dependence can be expressed by such formula:

$$V_H(G) = V_{H0}[0.64 + 1.12G/G_0 – – 0.972(G/G_0)^2 + 0.197(G/G_0)^3], \quad (2)$$

where $V_H(G)$ is the minimum allowable value of linear displacement of the tool per its one revolution, which provides quality formation of welds, mm/rev; V_{H0} = 0.094 mm/rev is the minimum allowable value of linear displacement of the tool per its one revolution for alloy AMg2M.

The curves presented on the diagram (see Figure 4) by solid lines, obtained using approximated formula dependencies virtually match with dashed curves plotted based on the results of experimental investigations. Therefore, in friction stir welding of aluminium alloys containing total amount of alloying and modifying elements within 2.2–8.4 % limits the range of optimum relationships between the speeds of linear displacements and tool rotation frequency, which provide quality weld formation, can be determined using formulae given above.

Increase or decrease of the set optimum v_w/N relationships for aluminium alloys containing specific amount of alloying and modifying elements results in formation of defects in the welds. Exceeding the set maximum allowable speed of tool displacement per its one revolution by 10–20 % leads to appearance in the welds of inner discontinuities (see Figure 1, *a*) caused by insufficient plasticization of metal in the welding zone. Its further increase provokes formation of surface defects in form of lacks of fusion (see Figure 1, *b*) from the weld face.

Decrease of v_w/N relationship below the set minimum allowable value in welding of ductile aluminium alloys with small content of alloying and modifying elements (AMtsN, AD33, AMg2M) results in formation of defects in form of flash (see Figure 1, *c*) from the weld face. In welding of the rest of alloys decrease of minimum allowable speed of tool displacement per its one revolution by 10–20 % provokes appearance of areas of overheated metal on weld face (Figure 5). And its further reduction promotes in the welds formation of inner discontinuities caused by metal overheating (see Figure 1, *e*).

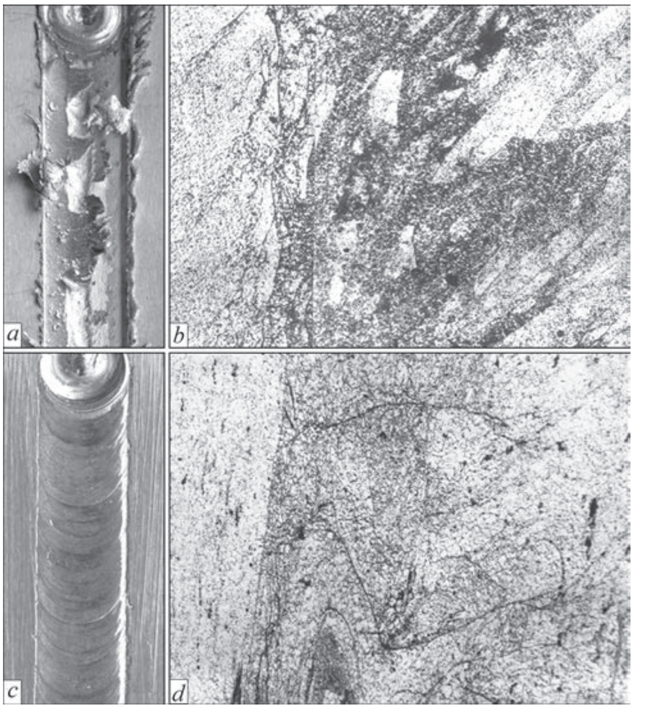

Figure 5. Appearance (*a*, *c* — ×2) and microstructure (*b*, *d* — ×125) of face of FSW welds of 1420 alloy of 1.8 mm thickness; *a*, *b* — overheated weld; *c*, *d* — normal

Conclusions

1. Quality weld formation in friction stir welding of sheet (0.8–3.0 mm) aluminium alloys of different doping systems can be provided at tool immersion into metal being welded by 0.10–0.15 mm depth due to proper selection of tool rotation frequency and welding speed.

2. Ductile low aluminium alloys are successfully welded at sufficiently high welding speeds. At $N = 1420$ rpm tool rotation frequency the speed of its linear displacement for alloy AMtsN can vary in 8–41 m/h limits, for AD33 alloy it is 8–36 m/h and for AMg2M alloy — 8–32 m/h. Welding speed shall be reduced to obtain quality joints on stronger aluminium alloys containing significant amount of alloying and modifying elements.

3. Range of the optimum relationships of welding speeds and tool rotation frequencies in friction stir welding of aluminium alloys depends of total content in them of alloying and modifying elements. At 2.2 % of their total content in alloy (AMtsN alloy) the value of tool linear displacement per its one revolution can change in sufficiently wide limits from 0.094 to 0.423 mm. For stronger high alloys the range of its change narrows to 0.047–0.163 mm at 7.7 % content (1201 alloy) of such elements in alloy being welded and to 0.047–0.140 mm at their content of 8.4 % (AMg6M alloy). Deviation of indicated parameters from the optimum range results in formation of typical inner and surface defects, caused by insufficient plasticization or overheating of material being welded.

4. The curves limiting the range of optimum relationships of welding speeds and tool rotation frequencies, plotted based on the results of experimental investigations and approximated by formula dependencies in form of power functions, allow calculation of necessary rotation and displacement speeds of tool for any aluminium alloy containing 2.2–8.4 % of alloying and modifying elements.

1. Lahti, K. (2003) FSW — possibilities in shipbuilding. *Svetsaren*, **1**, 6–8.
2. Kuriyama, T. (2008) Advantages of aluminium alloy rolling stocks and transition of carbody structures. *J. of Light Metal Welding and Construction*, **9**, 418–421.
3. Arbegast, W.J. (2006) Friction stir welding after a decade of development. *Welding J.*, **3**, 28–35.
4. Ding, J., Carter, R., Lawless, K. et al. (2006) Friction stir welding flies high at NASA. *Ibid.*, **3**, 54–59.

5. Okamura, H., Aota, K., Ezumi, M. (2000) Friction Stir welding of aluminium alloy and application to structure. *J. of Japan Institute of Light Metals*, **4**, 166–172.
6. Defalco, J. (2006) Friction stir welding vs. fusion welding. *Welding J.*, **3**, 42–44.
7. Lanciotti, A., Vitali, F. (2003) Characterization of friction welded joints in aluminium alloy 6082-T6 plates. *Welding Int.*, **8**, 624–630.
8. Kulekci, M.K. (2003) Mechanické vlastnosti spojov hliníkovej zliatiny AlCu4SiMg vyhotovených trecím zvaraním premiešaním. *Zvaranie–Svařování*, **5-6**, 104–107 [in Slovak].
9. Pietras, A., Zadroga, L., Lomozik, M. (2004) Characteristics of welds formed by pressure welding incorporating stirring of the weld material (FSW). *Welding Int.*, **1**, 5–10.
10. Oosterkamp, A., Oosterkamp, L., Nordeide, A. (2004) «Kissing bond» phenomena in solid-state welds of aluminium alloys. *Welding J.*, **8**, 225–231.
11. Poklyatsky, A.G. (2008) Characteristic defects in FSW of sheet aluminium alloys and main causes for their formation. *The Paton Welding J.*, **6**, 39-43.
12. Shinoda, T. (2002) Effect of tool angle on metal flow phenomenon in friction stir welds. In: *Proc. of 6th Int. Conf. on Trends in Welding Research. Georgia, USA*.
13. Okamura, H., Aota, K., Takai, H. et al. (2003) Point of application for FSW. *Welding Technology*, **5**, 60–69.
14. Colegrove, P.A., Shercliff, H.R. (2003) Experimental and numerical analysis of aluminium alloy 7075-T7351 friction stir welds. *Sci. and Techn. of Welding and Joining*, **5**, 360–368.
15. Enomoto, M. (2003) Friction stir welding: research and industrial applications. *Welding Int.*, **5**, 341–345.
16. Hassan, A.A., Prangnell, P.B., Norman, A.F. et al. (2003) Effect of welding parameters on nugget zone microstructure and properties in high strength aluminium alloy friction stir welds. *Ibid.*, **4**, 257–268.
17. Ryazantsev, V.I., Matsnev, V.N., Konkevich, V.Yu. (2004) Friction stir welding of wrought and cast aluminium alloys. *Aviats. Promyshlennost*, **4**, 33–36 [in Russian].
18. Ishchenko, A.Ya., Poklyatsky, A.G. (2010) *Tool for friction stir welding of aluminium alloys*. Ukraine Pat. 54096. Int. Cl. B23K 20/12, No. u 201005315 [in Ukrainian].

Received 19.05.2019

https://doi.org/10.15407/tpwj2019.08.07

EQUIPMENT AND TECHNOLOGIES OF SAFE GRINDING OF FERROALLOYS OF ELECTRODE PRODUCTION

A.E. MARCHENKO
E.O. Paton Electric Welding Institute of the NAS of Ukraine
11 Kazimir Malevich Str., 03150, Kyiv, Ukraine. E-mail: office@paton.kiev.ua

The preferred types of equipment are considered to provide safe grinding of ferromaterials used in electrode production. The design features of the equipment, their advantages and disadvantages are described. 6 Ref., 8 Figures.

Keywords: *electrode production, ferromaterials, fire and explosion safe grinding, slotted mill, vibration mill, paddle-type grinder, vibroinertial grinder*

When choosing grinding equipment intended for fire and explosion safe grinding of ferroalloys, the preference is given to installations that:

● are characterized by low specific energy consumption for grinding and, consequently, insignificant heating of material during grinding;

● have small sizes of grinding chamber;

● provide a quick withdrawal of the grinded material outside the grinding chamber, preventing its heating, overgrinding and minimizing the change in the energy state of the surface layer of its particles;

● allow not only isolating working space of the grinding chamber from the surrounding atmosphere, but also its connections with loading-unloading units, as well as in the zone of extraction of target fractions.

The experience of electrode-manufacturing enterprises showed that these requirements are met to the greatest extent by:

● modernized slotted ball mill of drum type with peripheral screening of the Institute «Giprometiz»;

● two-chamber rod-type vibration mill of a tube type of the model PALLA-U (KHD HUMBOLDT WEDAG Company);

● conical vibroinertial grinder of the «Mechanobr» Institute (model KID 300);

● vertical paddle-type grinder Pluristadio GR 80 (GUSSEO Company).

Let us consider the design features of the listed grinders, including providing the required degree of fire and explosion safety of the grinding process.

Slotted mill of Giprometiz. In the traditional technology of grinding ferroalloys in shielding gas, a conventional slotted mill with a drum of 700 mm diameter of Giprometiz was used, which was placed in a sealed chamber with a volume of 25.5 m^3. Such an installation has the following disadvantages:

● low efficiency, which is predetermined by the duration of preparatory operations, including also switching the installation to a safe mode of operation;

● complexity of maintenance;

● large volume of the sealed chamber;

● high dustiness of the working space and accumulation of deposits of toxic, pyrophoric and explosive dust in the chamber in the amount exceeding 20 kg per day; when this dust is swept up during cleaning, it can exceed MAC and the lower flammability concentration limit (LFCL).

Based on the results of mathematical modeling and production experiments performed on one of the operating grinding installations of this type, the authors of works [1, 2] modernized the schemes and modes of shielding gas supply, as well as the aspiration system, which provide fire-explosion-safe oxygen concentrations in the active zone (8 %) and the acceptable dust level of aspirated air.

The scheme of the modernized installation is shown in Figure 1.

According to this scheme, there is no need in a special chamber, a standard casing with five inert gas (IG)-nitrogen supplies is enough: into the drum cavity (pointlike supply through the collet through the pipe of 10 mm diameter), into the upper and hopper parts of the casing and also into the over and under sieve area of the shelter of the vibrating screen and the Kibble for the finished powder (by a perforated pipe providing a uniform spatial distribution of IG).

Aspiration shelters are mounted on the end walls of the mill casing. They communicate with the cavi-

*Retrospective review of publications in small editions and sources of non-welding profile.

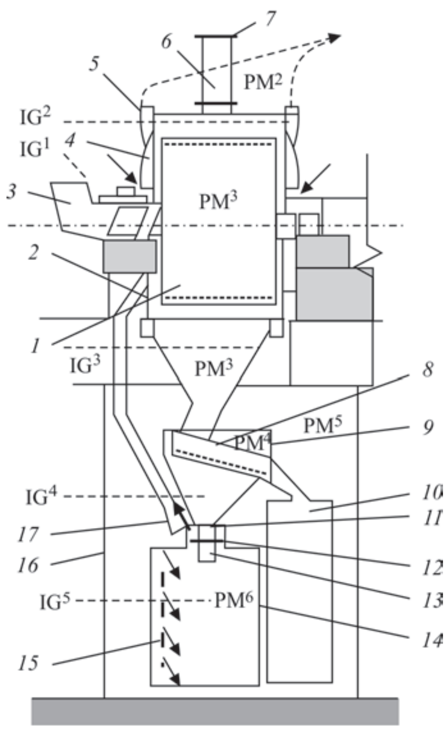

Figure 1. Scheme of installation for fire and explosion safe grinding of ferroalloys on the basis of slotted mill Giprometiz [2]: *1* — mill drum; *2* — mill casing; *3* — supplier; *4* — aspiration shelter; *5* — aspiration branch-pipe; *6* — pipeline for pressure diffusion; *7* — membrane; *8*, *9* — vibrating screen with aspiration shelter; *10* — capacity for over-lattice product; *11* — slotted adjustable diaphragm; *12–14* — slotted adjustable diaphragm, loading branch-pipe and Kibble of the finished product; *15* — device, distributing inert gas in the Kibble; *16* — general chamber of the vibrating screen and the receiving Kibble; *17* — branch-pipe and funnel of the ejection device; IG and PM points for inert gas supply and pressure measurements

ties of the drum and the casing only through leakages in the places of passage of collets, they are open from the bottom and taper up. The air drawn in from the room through the lower openings, washing the collets, entrains dust emissions from the mill at the places of indicated leakages, almost without violating the composition of shielding gas inside the mill casing and the drum and keeping the concentration of suspended particles in the suction pumps at a sufficiently low level. The increasing rate of aspirated air in the narrowing section of external chambers prevents deposition of particles from the stream and their accumulation on the collets surface.

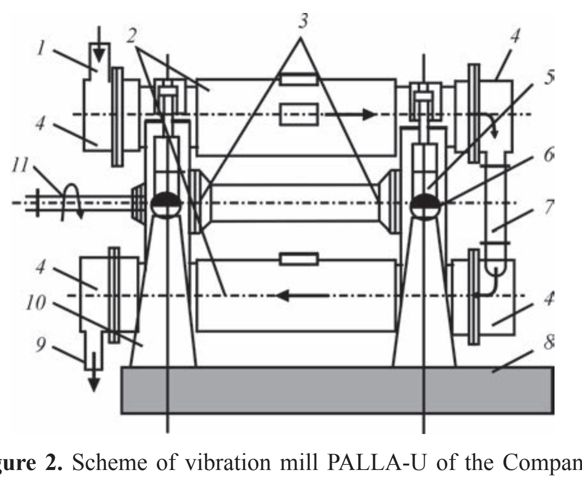

Figure 2. Scheme of vibration mill PALLA-U of the Company KHD HUMBOLDT WEDAG; *1* — loading branch-pipe; *2* — tube mill chambers; *3* — units of unbalanced vibrating exciters; *4* — replaceable end bottoms of mill chambers; *5* — tube bundles; *6* — shock absorbers; *7* — transfer sleeve; *8* — vibration-insulated foundation; *9* — outlet fitting-pipe; *10* — fixed frame; *11* — driven shaft

Aspiration of the loading unit of the Kibble localizes the possible dust emissions here, as well as in the powder classification zone on the vibrating screen.

The selected optimal supplying modes and the ratios of the specific flow rates of nitrogen supplied to the mill cavity and to the cavity between the drum and the casing, aerodynamically connected with the vibrating screen and the Kibble, provide a reliable prevention of inflammations and explosions.

The concentration of dust in the workplace decreased to the level of total background dustiness in the workshop space.

The duration of purging the cavities with nitrogen before starting the mill was reduced from 2.0–2.25 h (designing variant for placing the grinding installation in the sealed chamber with a volume of 25.5 m^3) to 15 min.

Vibration mill of the model PALLA-U is shown in Figure 2.

The installation consists of a movable (grinding) and a fixed part. A fixed part in the form of a rigid metal frame *10* is mounted on a vibration-insulated foundation *8*. A movable part consists of two horizontal, tube grinding chambers *5* located one above the other, reliably connected to each other by means of steel coupling bands. The vibration-excitation units *3* are located in the gap between the mill chambers, strictly vertically equidistant from them. Each of the units represents a short unbalanced shaft on rolling bearings, and they being located in a protective tube, are interconnected by means of an intermediate shaft with cross-bars. Through the driveshaft *11* they are driven by an asynchronous electric motor mounted on a console-mounted platform located on the front-facial side of the installation. A movable part of the installation rests on a fixed frame through elastic elements-shock absorbers *6*. The general view of the mill is shown in Figure 3 [2–4].

At the outlet of the chamber, an end grating of high-strength steel is installed, which as to the sizes and a number of holes is designed for the maximum passage of the finished product.

This allows producing it without a risk of overgrinding, without classification on screening. Depending on the grinded material, 55–65 vol.% of the cavity of each milling chamber is filled with cylinders, which additionally guarantees the prevention of overgrinding.

At a continuous supply of material into the chamber, the friction arising from vibration on the surface of horizontal grinding cylinders allows not only grinding, but also moving the material in the space between them along a spiral path to the exit from the chamber. Efficiency of a mill is controlled by the angle of internal friction at unloading, by standard types and sizes of grinding bodies, coarseness of the supply, properties of the material and a circular movement of the chamber. The degree of grinding depends mainly on the time of retention of particles in the chambers, i.e., on the variant of connecting grinding chambers — in series, as is shown by the arrows in Figure 2, parallel or combined.

On the first mode, the material sequentially passes through the upper, and then through the lower chamber. According to this mode, ferromanganese, ferrotitanium and ferrosilicon are grinded. When working in parallel mode, those materials are grinded which one less strength than ferroalloys. The material is loaded separately into each chamber, and at the output the target product is obtained. The efficiency of the process grows twice, and the achieved degree of grinding is determined by the value of the material grindability factor. In the manufacture of electrodes on this mode, quartz sand, rutile concentrate and marble are grinded. The third mode is designed for the most easily milled materials. They are loaded into the tube chambers through the central hatches, and the grinding products move from the central section to the outlet hatches of each chamber. The degree of grinding is minimal and the efficiency of the process is the highest as compared to serial and parallel modes of operation.

The modes and efficiency of grinding of each new material are selected by conducting preliminary tests, on the results of which the type of grinding bodies (steel balls, cylinders, rods) and the mill operating mode (frequency, vibration amplitude, grinding duration) are determined. In the former Soviet Union, the electrode shops used two-chamber mills PALLA-U to grind not only ferroalloys, but also ore-mineral coating ingredients. At the same time, coarser powders were produced than those when using other types of through drum ball mills, even with peripheral screening.

The cavities of mill chambers are sealed with heat-resistant sealing rings, the branch pipes at the inlet and outlet are connected to the shelters of the loading and receiving units by elastic corrugated transitions.

The mills are equipped with a carbon dioxide generator and a soundproof capsule. Therefore, grinding installations based on the vibration mills PALLA-U

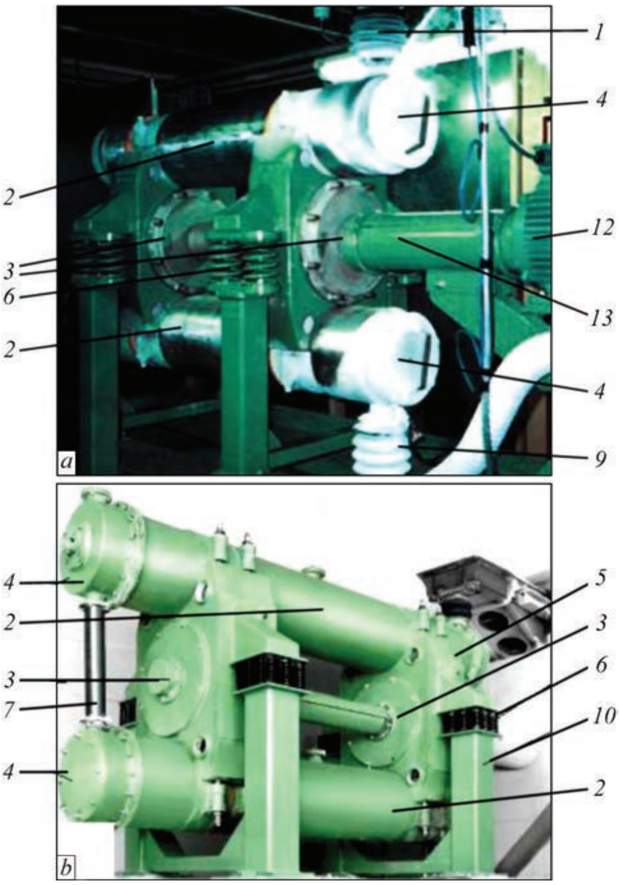

Figure 3. Frontal-facial (*a*) and rear (*b*) apperance of vibration mill PALLA-U: *12* — electric motor; *13* — casing of driving shaft (other designations see in Figure 2)

provide operating conditions for service personnel that are safe from the point of view of sanitary and hygienic regulations, and, when grinding ferroalloys, the fire and explosion safety regulatory requirements.

Paddle-type grinder of the model Pluristadio GR 80 of the Italian Company GUSSEO is presented in Figure 4, and as a part of the grinding installation — in Figure 5. It consists of a lined armored cylindrical body and a rotor — a vertical shaft with two three-tier sections of beaters mounted on it, spaced apart in height. The lower section *1* is equipped with larger beaters and is designed to destroy large fractions. The upper section *2* carries out fine grinding, it is assembled from beaters of a smaller size. In the space between them, screw feeder *3* evenly supplies material to the disk of the lower section of the rotor.

The rotor, made in the form of a centrifugal distributor, on the one hand, directs the material to be grinded into the circumferential gap along the cylindrical surface of the mill body, and, on the other hand, reflects and directs the gas flow pumped by the fan into this gap. Relatively small particles of the material are entrained by the gas flow and directed through the beater of the upper section of the rotor into the separator *4*, in which they are divided into two fractions:

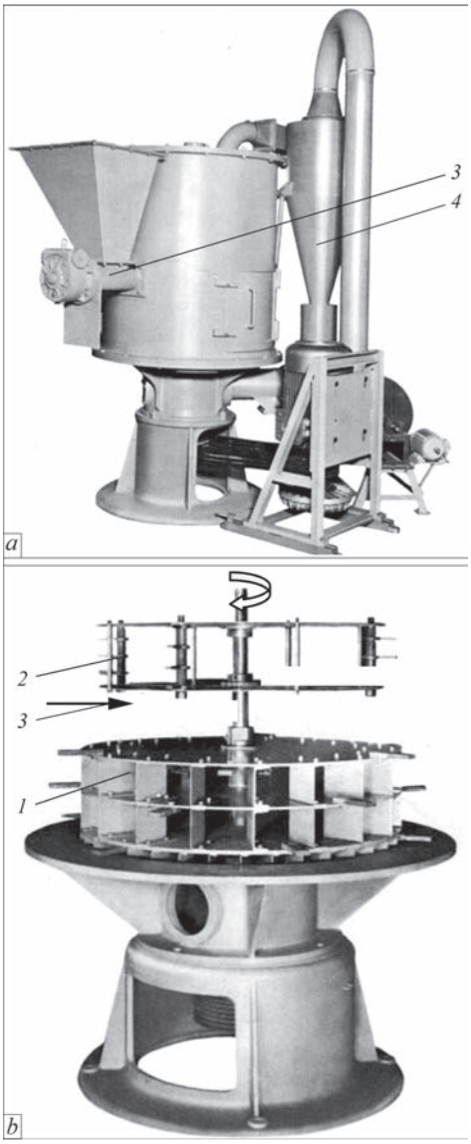

Figure 4. General view (*a*) and grinding rotor (*b*) of paddle-type mill Pluristadio GR 80 (see designations in the text)

the fine (commercial) fraction is carried away and deposited in the cyclone, and a large one is returned to regrinding. Coarser (heavier) particles fall for some time in the circumferential gap of the mill downward, towards the gas flow, get under the beaters of the lower section of the rotor, grinded, and then also carried away upwards, finally grinded by the upper beaters to the end and also directed to the separator *4*.

The scheme of the installation for grinding ferromanganese, ferrotitanium and ferrosilicon based on the paddle-type mill Pluristadio GR 80 is shown in Figure 5.

The granulometric composition of the powder is regulated when the mill is set up by changing the number of beaters suspended on the rotor disks, by the gas flow rate using the separator louvers, and also by changing the rotor speed of the fan impeller. The higher the rate of the gas flow, the coarser particles it picks up and rushes upward under the beaters of the upper section of the rotor. In this case, the integral degree of grinding of the material decreases, and the efficiency of the mill increases. With a decrease in the gas flow rate, the grinding is finer, but the amount of material grinded by the mill decreases.

Since the supplying device is located in the middle part of the mill, i.e., between the upper and lower rotors, and the gas is pumped through the nozzle mount-

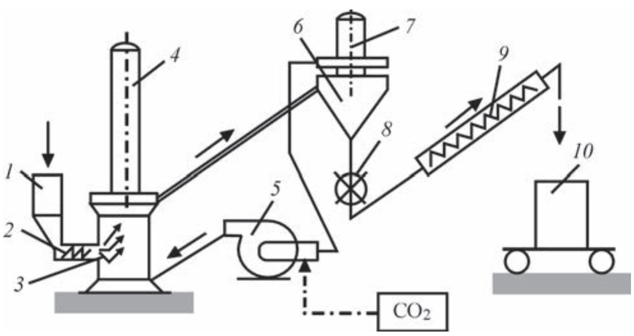

Figure 5. Technological scheme of grinding installation for ferroalloys: *1*, *2* — hopper with screw; *3* — mill; *4*, *7* — inflatable explosion safe valve; *5* — fan; *6* — hopper of cyclone; *8* — stopping valve; *9* — screw; *10* — trolley

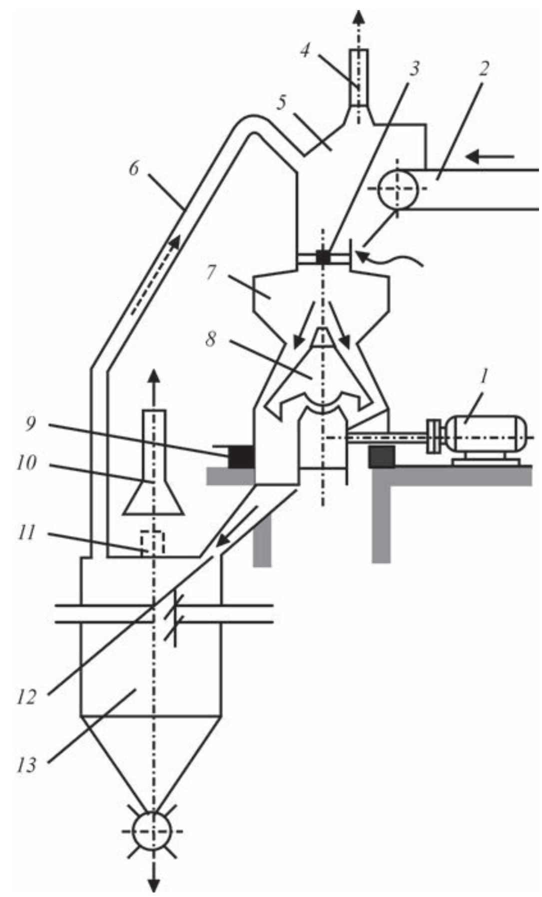

Figure 6. Scheme of aspiration of cone vibration grinder KID-300 [6]: *1* — drive; *2* — supplier; *3–5* — collecting launder, shelter of loading device with aspiration suction; *6* — tapping pipe; *7*, *8* — outer and inner cone of the grinder; *9* — shock absorber; *10*, *11* — funnel and branch-pipe of ejection device (in the variant without a tapping pipe); *12* — discharge launder; *13* — hopper with Kibble for grinded material

ed under the lower grinding disk, overgrinding of the material is excluded.

The system is sealed. CO_2 is supplied to the system, if necessary, with the addition of oxygen, in the amount sufficient to make up losses. The sealing of the system is confirmed by filling the fabric filter bags, with which the mill and the separator are equipped. As a shielding atmosphere, a mixture of nitrogen with oxygen can be used.

The mill Pluristadio GR 80 has a small volume of the working chamber — its diameter is 800 mm, and a height is 1200 mm. It is easily and quickly, within 30 min, cleaned of remnants of the previous material. In terms of efficiency, it meets the requirements for the above-mentioned ferroalloys of the workshop with a capacity of up to 12.5 thou t of electrodes per year, 70 % of which are with rutile and 30 % with low hydrogen coating.

Vibroinertial cone grinder KID-300 [5, 6]. The profile of the grinding chamber of a vibroinertial cone grinder, like that of traditional cone-type vibrogrinders, is formed by the armored surfaces of grinding cones, which mate each other — a stationary outer and a rotating inner one. The outer cone and the spherical support of the inner cone are mounted on the bed of the grinder. The inner cone is driven by electric motor not through the eccentric sleeve, as in a cone grinder of a conventional type, but through the unbalanced vibration exciter. It has a socket of a ball-type profile for the spherical support of the inner cone and is mounted beneath on the driving shaft. As a result of using such a drive, the inner cone, along with the rotation, performs gyrational movements, i.e., the swings characteristic of a conical pendulum.

The resulting force of both centrifugal components, which presses the inner cone to the outer one in a pulsating mode, is the force grinding the material loaded into the milling chamber of the grinder. The working surfaces of grinding bodies act on the grain through the grains surrounding it during cyclic compaction of the layer in the working zone.

During a short time of passing the grinding chamber, the initial material is in a bulk stressed state under the conditions of repeated cycles of compression, bending and unloading. Under such conditions, the material is destroyed mostly according to the laws of fractal kinetics along the weakest surfaces. The coarseness of the powder is regulated by the position of the unbalancing device and the efficiency of the grinder — by changing the size of the unloading slot, i.e., the slot between the linings of the cone and the bowl.

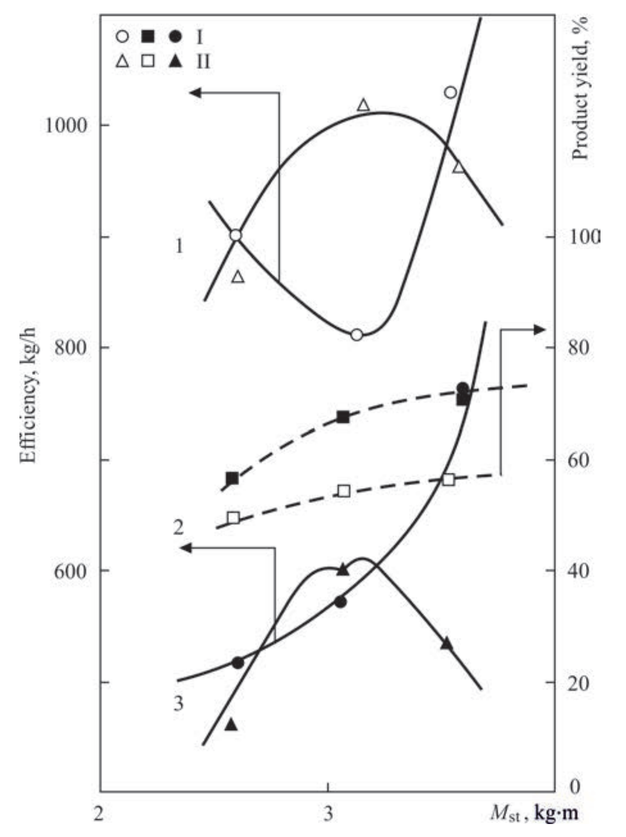

Figure 7. Interdependence of efficiency values of the process of grinding ferrosilicon FS-45 (I) and ferrovanadium FV-35 (II) on static moment of unbalancing in conical inertial of grinder KID-300 (according to data [6])

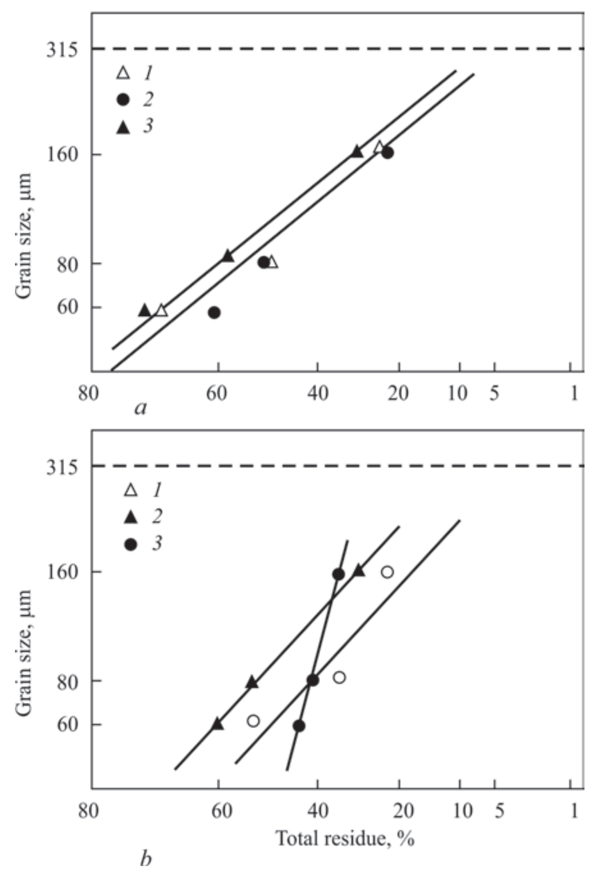

Figure 8. Granulometric composition of powders, produced during grinding ferrosilicon FS-45 (*a*) and ferrovanadium FV-35 (*b*) in installation KID-300 at the values M_{st} equal to 2.52 (*1*), 3.08 (*2*) and 3.48 (*3*) kg·m (according to data [6])

The advantages of inertial grinders such as KID as compared to conventional cone grinders with an eccentric drive include:

● three-... five-time increase in the grinding ratio (up to 15–18, in comparison with the traditional index at the level of 3–5);

● increase in the product yield;

● ability of the grinder to operate under bulk, as well as starting and stopping under the load;

● negligible level of dust above the level of the layer of grinded material in the loading zone.

At the I.M. Frantsevich IPMS of the NAS of Ukraine the grinder KID-300 was tested during grinding a number of ferroalloys, including ferrosilicon of grades FS-45 and ferrovanadium of grades FV-35 with an initial lumps size of 20 mm [6]. The scheme of experimental installation is shown in Figure 6.

Performance indicators of the grinder during the tests are the following:

● rotation speed of unbalanced vibrator $w = 20$ s^{-1};

● static moments of M_{st}, (2.52; 3.08 and 3.48 kg·m);

● width of unloading slot $\Delta = 6$ mm.

The dependences of the performance indicators achieved during this grinding process on the mass of the treated material and the produced target product, kg/h, as well as by the product yield, %, the values of the static moment of unbalancing device, are shown in Figure 7.

The presented data showed that the grinder KID-300 can be used for the preparation of ferroalloy powders that, in terms of grain composition, meet the requirements to the technology of production of low-hydrogen electrodes of general purpose with the aspiration design used in this work, providing a dust concentration in aspirated air not exceeding 1.2 g·m^{-3} with a suction capacity of 900 m^3·h^{-1} [5].

The author appreciates O.D. Nejkov for his meaningful advice and discussion of the materials.

1. Nejkov, O.D., Marchenko, A.E., Nedin, V.V. et al. (1982) On problem of explosion hazard in grinding of ferroalloys. In: *Proc. of All-Union Conf. on Welding Consumables*. Ed. by I.K. Pokhodnya. Kiev, Naukova Dumka 167–172 [in Russian].
2. Vasilieva, G.I., Nejkov, O.D., Chernykh, A.M. et al. (1989) Supply of shielding gas media in installations of ferroalloys grinding. In: *Proc. of 2nd Int. School of Countries-Members of CMEA on Metallurgical and Technological Problems of Basic Electrodes (Sofia, November 1989)*. Kiev, Naukova Dumka, 133–139.
3. Gajrabediyants, E.L., Betchin, V.A., Matveev, N.N. (1977) Technology and equipment of flow-line electrode manufacturing. In: *Technology, organization of manufacturing and management*. NII Informenergo [in Russian].
4. (2009) New frontiers. Grinding mills PALLA–UO in beneficiation. *Gornaya Promyshlennost*, **1** [in Russian].
5. Revkin, V.N., Girshov, V.L., Finkelshtejn, G.A. et al. (1982) Grinding of metal powders and chips. *Poroshk. Metallurgiya*, **4**, 12–17 [in Russian].
6. Denisov, G.A., Ardelyan, A.A., Zarogatsky, L.P. (1989) Technology of grinding of ferroalloys with use of conical inertial crushing machine. In: *Proc. of 2nd Int. School of Countries-Members of CMEA on Metallurgical and Technological Problems of Basic Electrodes (Sofia, November 1989)*. Kiev, Naukova Dumka, 140–146.

Received 24.04.2019

*Calendar of August**

AUGUST 1, 1927 Date of birth of V.F. Grabin (1927–2010), a scientist in the field of metal science and welding, a representative of the Paton school. He made a significant contribution to the development of fundamentals of metal science of metals and alloys, which allowed specifying a number of regulations as to the effect of phase composition on structure and properties of welded joints of metals of different classes and the tendency to crack formation during welding.

AUGUST 2, 1930 Date of birth of S.I. Kuchuk-Yatsenko, a prominent scientist in the field of pressure metal welding, academician, representative of the Paton school. Fundamental research works of the scientist formed the basis for the development of new methods of flash-butt welding using continuous, pulsed and pulsating flashing, patented in many countries of the world. On their basis, S.I. Kuchuk-Yatsenko with a team of specialists from the E.O. Paton Electric Welding Institute developed the technology of welding different products, created control systems and new equipment models, which have no analogues in the world practice.

AUGUST 3, 1934 The engine of tanker «Poughkeepsie Socony» of the American merchant marine was launched. This was one of the most important achievements in the US shipbuilding. The tanker was one of the first to exceed the cost of the shipbuilding program in 5 million USD and was the largest all-welded merchant ship of its time built in the United States and, probably, in the whole world.

AUGUST 4, 2009 British enthusiast and engineer Alan Roy Handley decided to return to the idea of creating metal airship. He called his project Varialift. Alan decided to create a hybrid system capable of combining the advantages of an aircraft, a helicopter and an airship. The first vehicle of the Varialift series, ARH-50, is positioned by A. Handley as an airship for transportation of cargoes weighing 50–55 tons. In 2011 it was successfully tested. The shell of the vehicle was welded from aluminum sheets, the carrier gas was helium, the length of vehicle was 150 m.

AUGUST 5, 1973 From the launching pad of the Baikonur-5 Cosmodrome, the «Mars-6» spacecraft was launched by the «Proton-K» rocket-carrier. In March 1974, the launching vehicle was separated from it. In the manufacture of spacecrafts among other technologies, different welding methods were used to produce permanent joints.

AUGUST 6, 1961 By the rocket-carrier R-7 the spacecraft «Vostok-2» was launched, piloted by the cosmonaut German Stepanovich Titov (1935–2000) on board. The rockets-carriers R-7 opened up the space era for humanity. With their help, among others, the first artificial satellite was launched into orbit, the first satellite with a living being on board was launched into Earth orbit, the first spaceship with a man was launched into Earth orbit. The main methods of welding the rocket structure of aluminum alloys were manual and mechanized welding in an inert gas (argon), as well as resistance spot welding.

AUGUST 7, 1842 Date of birth of N.N. Benardos (1842–1905), engineer, inventor of electric arc welding, author of more than 100 inventions. The invention of electric arc welding and cutting of metals brought him the world fame. The method of Benardos became known all over the world and, thus, it became possible to weld separate metal fragments quite easily. But it took a half of a century until welding became the main technology of joining metals. N.N. Benardos paid a particular attention to arc welding with a carbon electrode, which was called the «Benardos method».

AUGUST 8, 1932 Date of birth of Yu.S. Borisov, representative of the Paton School, a famous scientist in the field of materials science of coatings, including gas-thermal ones, containing amorphous and quasi-crystalline phases. Yu. S. Borisov is an Honoured Worker of Science and Technology of Ukraine, the author of more than 400 articles, monographs, author's certificates and patents.

*The material was prepared by the Steel Work Company (Krivoy Rog, Ukraine) with the participation of the editorial board of the Journal. The Calendar is published every month, starting from the issue of «The Paton Welding Journal» No.1, 2019.

AUGUST 9, 1951 By August 1951, a group of scientists and specialists from the Electric Welding Institute (N.G. Ostapenko, V.K. Lebedev, S.I. Kuchuk-Yatsenko, V.A. Sakharnov and B.A. Galyan) for the first time developed the method of flash-butt welding and appropriate machines for flash-butt welding of rails, pipes and other products. In the future, due to the improvement in the control system, it was possible to create new models of machines, having no analogues in the world.

AUGUST 10, 1943 In August 1943, B.E. Paton and A.M. Makara (Institute of Electric Welding) during the investigation of the submerged arc welding process proved the presence of arc discharge. Later, other researchers determined the dimensions of a gas bubble, measured the voltages between the electrodes, the temperature of the arc column, and other process parameters.

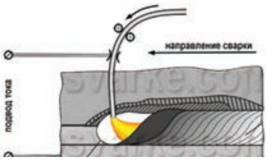

AUGUST 11, 1885 An information was published about the creation of dynamo-machine by E. Thomson. Elihu Thomson (1853–1937) designed a dynamo-machine with self-excitation (power of 18.3 kW, 1800 rpm, weight of 22.5 kg), which provided the welding transformer with alternating current. Namely its three-phase model became the basis for the new arc lighting system, which was developed by Thomson in collaboration with E.J. Houston.

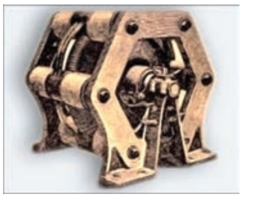

AUGUST 12, 1908 Date of birth of A.E. Asnis (1908–1987), a famous scientist, a representative of the Paton school. He developed many materials for welding and surfacing, unique methods and procedures for investigations the joints and evaluation of their strength under the load conditions. A.E. Asnis was the developer of the scientific fundamentals for the development and selection of steels with a good weldability, which are scarcely-alloyed and insensitive to aging. He participated in the designing of a universal semi-automatic machine with a remote control for welding and cutting at large depths. He is the author of more than 300 scientific works.

AUGUST 13, 1927 The main defence ship of the «Uragan» type was designed, the first Soviet military surface ship in the USSR. Its designing was guided by V. A. Nikitin, a young engineer-shipbuilder. Nikitin was one of the first in the industry who took a risk to apply welding for hull structures to which many shipbuilders and naval sailors were suspicious in those years, preferring a time-tested riveting. «Uragan» entered the history of Soviet shipbuilding as a pioneer ship, from which the construction of the Soviet surface fleet began.

AUGUST 14, 1948 At «Plant No. 402» in Molotovsk, «Ognennyi», a Soviet destroyer ship of the project 30-bis, was laid. The creation of destroyers of this type required a significant increase in the volume of welding. There were not enough specialists, and then girls began to master the difficult profession. The creation of the ship was carried out with the implementing the position-assembly conveyor, large-sized assembly and wide application of electric welding. Since February 12, 1950, the «Ognennyi» was a part of the Northern Fleet.

AUGUST 15, 1947 Independence Day of India is celebrated since 1947. One of the sights of India is an iron (99.722 % F) column in Delhi, over 1500 years old. The researchers found that it was made of separate steel blocks weighing 29–30 kg, joined by means of a forge welding. Its high corrosion resistance is predetermined by an increased phosphorus content (0.114 % P) and a dry climate.

AUGUST 16, 1930 Date of birth of V.S. Gvozdetsky, a representative of the Paton School, a famous scientist in the field of the theory of cathode processes in a welding arc, based on the phenomenon of ion-electron emission of a cathode. These investigations became the basis for the development of new methods of microplasma welding of metals and alloys with a thickness of 0.1–1.0 mm. Due to his works, more than 15,000 apparatuses for different methods of microplasma welding were manufactured and implemented in industry.

AUGUST 17, 1987 The first flight of «Su-33», a Soviet carrier-based fighter of the fourth generation, took place. Many problems caused the need in welding titanium assemblies of large and small thicknesses. Specialized welding equipment was purchased, welding modes and methods for quality control of welds were tested. Among the mastered unique equipment the installation ELU-21 for electron beam welding in vacuum was applied.

AUGUST 18, 1942 The first tanks «Tiger» were manufactured, the German heavy tanks of the World War II period. The roof of the tank turret was joined to the hull sides by welding. The armour plates were abutted using the «dovetail» method and were joined by welding. Much attention was paid to the quality of welds, not only to provide the rigidity of the structure, but also to make it shell-proof. In foreign sources, British and American engineers, as well as Soviet welding scientists criticized both the quality of the filler material of the electrodes used to weld the hulls of Tiger tanks and also the technology of producing welds themselves.

AUGUST 19, 1932 The first flight of the high-speed aircraft AIR-7 took place, designed by the Yakovlev Design Bureau. On November 20, 1932 the pilot Julian Piontkovsky on an AIR-7 aircraft reached a record speed in the USSR of 325 km/h. In the manufacture of aircraft the welding was actively used to save weight. The fuselage is a truss structure, welded from steel pipes with a light frame, which imparts a rounded contour to the linen casing. To the fuselage a small centre wing section of the same welded structure was joined. The main racks of welded steel pipes were joined to the ends of the centre wing section.

AUGUST 20, 1927 The cruiser «Karlsruhe», a German light cruiser was launched, which took part in the World War II. The development of a project of new cruisers, taking into account the limitations of the Versailles Treaty, began in 1924. Three cruisers were built under the project (type «K»): «Konigsberg», «Karlsruhe» and «Cologne». The ship hull was assembled from longitudinal steel frames where welding was used; up to 85 percent of the hull was welded, not riveted as usual. The hull was divided into nineteen watertight compartments, had a double bottom, being 72 % of the length of the ship hull, and joined by welding. On April 9, 1940, the cruiser was sunk by a British submarine «Truant».

AUGUST 21, 1938 In 1938, Dr. Charles Cadwell significantly improved the design of the exothermic welding system of Hans Goldschmidt, who in 1898 patented his method of aluminothermic welding of rails, which was commercially significant. Since that time, its mass application began. The unique use of the process of exothermic welding was used during laying the railway tracks, which were previously joined with the help of cover plates, through holes in the rails.

AUGUST 22, 1972 The prototype of «T-4», a reconnaissance attack bomber-rocket carrier of the Sukhoy Design Bureau, was launched. In the manufacture of aircrafts new technologies were used, many of which had no analogues in the domestic and world aircraft industry. Aircraft glider was made using titanium alloys. The entire production cycle of the «T-4» was automated to maximum (95 % of welding operations). According to the estimates of NIAT, the full transfer of monolithic parts to assembled-welded structures, envisaged in serial production, had to provide a reduction in material consumption by 70 %, labour intensity by 45 % and reduction in production cycles by two to three times.

AUGUST 23, 1382 The defence of Moscow from the invasion of Khan Tokhtamysh began. In the annals of 1382 the successful use of welded artillery shells during the defence was mentioned for the first time. The iron sheet, forged from the bar, was rolled on an iron mandrel into a pipe and welded by a longitudinal weld with an overlap. Then one or two pipes of larger diameter were welded over this pipe, ensuring that the longitudinal welds were located in different places. The pipe billets forged in such a way were short. Therefore, to produce a sufficiently long barrel of guns, several such billets were joined between each other by means of a forge welding.

AUGUST 24, 1939 Date of birth of G.M. Grigorenko, academician, representative of the Paton school. He was directly involved in the development of new methods, equipment and technology of plasma-arc, arc-slag remelting, electroslag technology, induction melting with combined heat sources and in water-cooled sectional moulds. He developed technologies for melting out of high-nitrogen steels, technology for steel alloying with nitrogen from a gas phase. For the first time he analyzed and classified gas exchange processes in electrometallurgy during melting and remelting.

AUGUST 25, 1981 One of the patents of N.N. Rykalin (1903–1985), academician, scientist in the field of welding and metallurgy, was published . During the years of war, N.N. Rykalin carried out investigations on melting of electrodes and penetration of base metal. He is the author of numerous works on thermophysical fundamentals of metal treatment, metal welding, plasma processes in metallurgy. The theory of thermal processes during welding, created by him, served as the basis for the development of technological processes, in which highly-concentrated sources of power like thermal plasma, electron beam, ion fluxes, laser radiation have an effect on a substance.

AUGUST 26, 1934 The submarine «Shch-121» «Zubatka» was launched. It was the first type of medium submarines, built in the USSR. The pipes of the torpedo units were joined with the bulkheads of differential tanks and made a part of the construction of a pressure hull. Six welded bulkheads divided the hull into seven compartments. The beams were fastened to the lining by welding. Successful experiments with welding allowed providing longer service life, as well as reducing the weight of the submarine.

AUGUST 27, 1956 Turner-innovator A.I. Chudikov filed an application and received an authour's certificate No. 106270 for on the «Method of butt welding». Chudikov understood that for the implementation of friction welding it is necessary to keep three basic conditions: to operate at high revolutions of the part, not less than 750–1000 rpm; instantly stop the workpiece treated, so that the metal which transferred into the plastic state does not scroll over the joining area; apply axial force.

AUGUST 28, 1937 Pilot N.P. Shebanov set a world speed record on the aircraft «Steel-7». For its time the aircraft showed excellent characteristics in the range and speed of flight: the average speed on the route Moscow-Sverdlovsk-Sevastopol-Moscow with a length of 5068 km was 405 km/h. Steel pipes and shaped profiles, joined by welding, formed the load-carrying frame of wing and tail units. The aircraft structure with multiple elements turned out to be quite strong.

AUGUST 29, 1932 The main submarine of series VI «Malyutka» was laid. Designer-engineer A.N. Asafov (1886–1933) proposed replacing the riveting of a pressure submarine hull by the electric welding, including the reduction in roughness of the hull and increase in speed.

AUGUST 30, 1940 The monitor of the type «Hassan» (project 1190), the first vessel in a series of Soviet monitors, which served as a part of the Amur military flotilla, was launched. The hull of the ship was riveted, the outer lining and the deck were welded. The height of the side in the middle of the hull was 4 m, the largest length was 88.03 m, the largest width was 11.09 m, and the maximum draft was 2.94 m.

AUGUST 31, 1900 In the early 1900s, almost in several countries, a gas torch (more precisely a cutter) for the purposes of cutting appeared. In 1904, Jottran (Belgium) added a tube with a nozzle to a welding torch for supplying oxygen. In the same year E. Wiss (USA) patented a torch-cutter with concentric nozzles, proposed by E. Smith.